

FINITE ELEMENT ANALYSIS OF SUBREGIONS  
USING A  
SPECIFIED BOUNDARY STIFFNESS/FORCE METHOD ,

by

Cynthia C. Jara-Almonte,

Dissertation submitted to the Faculty of the  
Virginia Polytechnic Institute and State University  
in partial fulfillment of the requirements  
for the degree of

DOCTOR OF PHILOSOPHY

in

Mechanical Engineering

APPROVED:

---

C. E. Knight, Chairman

---

R. A. Comparin

---

S. L. Hendricks

---

H. H. Mabie

---

L. D. Mitchell

November, 1985

Blacksburg, Virginia

FINITE ELEMENT ANALYSIS OF SUBREGIONS  
USING A  
SPECIFIED BOUNDARY STIFFNESS/FORCE METHOD

by

Cynthia C. Jara-Almonte  
Dr. C. E. Knight, Chairman  
Mechanical Engineering Department  
(ABSTRACT)

The accurate finite element analysis of subregions of large structures is difficult to carry out because of uncertainties about how the rest of the structure influences the boundary conditions and loadings of the subregion model. This dissertation describes the theoretical development and computer implementation of a new approach to this problem of modeling subregions. This method, the specified boundary stiffness/force (SBSF) method, results in accurate displacement and stress solutions as the boundary loading and the interaction between the stiffness of the subregion and the rest of the structure are taken into account. This method is computationally efficient because each time that the subregion model is analyzed, only the equations involving the degrees of freedom within the subregion model are solved.

Numerical examples are presented which compare this method to some of the existing methods for subregion analysis on the basis of both accuracy of results and computational efficiency. The SBSF method is shown to be more accurate than another approximate method, the specified boundary displacement (SBD) method and to require approximately the same number of computations for the solution. For one case, the average error in the results of the SBD method was +2.75% while for the SBSF method the average error was -0.3%. The comparisons between the SBSF method and the efficient and exact zooming methods demonstrate that the SBSF method is less accurate

than these methods but is computationally more efficient. In one example, the error for the exact zooming method was -0.9% while for the SBSF method it was -3.7%. Computationally, the exact zooming method requires almost 185% more operations than the SBSF method. Similar results were obtained for the comparison of the efficient zooming method and the SBSF method.

Another use of the SBSF method is in the analysis of design changes which are incorporated into the subregion model but not into the parent model. In one subregion model a circular hole was changed to an elliptical hole. The boundary forces and stiffnesses from the parent model with the circular hole were used in the analysis of the modified subregion model. The results of the analysis of the most refined mesh in this example had an error of only -0.52% when compared to the theoretical result for the modified geometry.

The results of the research presented in this dissertation indicate that the SBSF method is better suited to the analysis of subregions than the other methods documented in the literature. The method is both accurate and computationally efficient as well as easy to use and implement. The SBSF method can also be extended to the accurate analysis of subregion models with design changes which are not incorporated into the parent model.

## ACKNOWLEDGEMENTS

First and foremost, I wish to acknowledge the help and support my husband has given me throughout our years in graduate school. I also wish to thank my son for showing me what is really important in life and my parents, and for their understanding and support throughout my years in school.

Special thanks also go to Dr. C. E. Knight for serving as my advisor for the past four years, for securing funding for me, and for his suggestions and comments throughout this project. Finally, I wish to acknowledge the role that the faculty and staff of the Mechanical Engineering Department has had in my education. I am deeply indebted to them for their contributions of time and effort. In particular, I wish to thank Dr. J. B. Jones for making it possible for me to stay on for my Ph.D., Mr. E. L. Sitler for all the time he has spent making sure that I got paid, Mary Kafura for her help with the computer system, Dr. H. H. Mabie and Dr. L. D. Mitchell for their assistance both in and out of the classroom, and the secretarial staff for their aid.

TABLE OF CONTENTS

Section	page
Abstract . . . . .	ii
Acknowledgements . . . . .	iv
List of Figures. . . . .	vi
List of Tables . . . . .	vii
List of Appendices . . . . .	viii
Introduction . . . . .	1
Literature Review. . . . .	5
Theoretical Development. . . . .	21
Computer Implementation. . . . .	28
Numerical Examples and Additional Studies. . . . .	53
Conclusions. . . . .	94
Recommendations for Future Work. . . . .	97
References . . . . .	99
Appendix A -- Complete Listing of Subroutines Added to MESS/SBSF . . . . .	101
Appendix B -- Finite Element Meshes for Subregion Analysis of. . . . .	114
Example 1.	
Appendix C -- Finite Element Meshes for Direct Analysis of . . . . .	124
Example 1.	
Appendix D -- Finite element Meshes for Subregion Analysis of. . . . .	131
Example 3.	
Vita . . . . .	140

## List of Figures

	Title	page
Figure 1.	Subregion Interface for the Linear Constraint. . . . .	6
Figure 2.	Interior Subdivision to form a Transitive Element. . . . .	8
Figure 3.	Example of the use of a Transitive Element in a Finite . . . . .	9
	Element Mesh	
Figure 4.	Mesh Divisions for the Specified Boundary. . . . .	23
	Stiffness/Force Method	
Figure 5.	Typical Subregion Model for the Specified Boundary . . . . .	25
	Stiffness/Force Method	
Figure 6.	Flow Chart for the Unmodified MESS Program . . . . .	29
Figure 7.	Dynamic Storage of the Stiffness Matrix in the . . . . .	32
	MESS Program	
Figure 8.	Flow Chart for MESS/SBSF Program . . . . .	35
Figure 9.	FORTTRAN Code used to find the Reduced Stiffness. . . . .	37
	Matrix in MESS/SBSF	
Figure 10.	FORTTRAN Code used to Create the NODA Array in. . . . .	40
	MESS/SBSF	
Figure 11.	FORTTRAN Code used to Calculate the Boundary Forces in. . . . .	43
	MESS/SBSF	
Figure 12.	FORTTRAN Code used to Extract the Boundary Stiffnesses. . . . .	45
	$[K_{ab}]$ in MESS/SBSF	
Figure 13.	Example of an Output Boundary Stiffness and Force. . . . .	46
	File from MESS/SBSF	
Figure 14.	Example of a Boundary Stiffness File Modified for. . . . .	49
	use in MESS/SBSF	
Figure 15.	FORTTRAN Code used to Insert the Boundary Stiffnesses . . . . .	50
	into the Global Stiffness Matrix	
Figure 16.	General Plate with Central Hole Problem for Examples 1 . . . . .	54
	through 4	
Figure 17.	Meshes A0 and A1 from Example 1. . . . .	58
Figure 18.	Mesh C1 for Direct Finite Element Analysis of. . . . .	61
	Subregion Model A1	
Figure 19.	Comparison of the $K_t$ values from Example 1 for the . . . . .	64
	Direct and SBSF Methods	
Figure 20.	Mesh A7 from Example 1 . . . . .	68
Figure 21.	Analysis Sequence 1 (A0-A1-A2) from Example 2. . . . .	70
Figure 22.	Analysis Sequence 2 (A0-B1-B2) from Example 2. . . . .	71
Figure 23.	Comparison of the $K_t$ values from Example 2 for the . . . . .	74
	SBD and SBSF Methods	
Figure 24.	Analysis Sequence 1 (A0-A1-A2-A3-A4) for Example 3 . . . . .	76
Figure 25.	Comparison of the $K_t$ values from Example 3 for the . . . . .	80
	Efficient Zooming and SBSF Methods	
Figure 26.	Meshes A0 and A1 from Example 4. . . . .	83
Figure 27.	Mesh A2 from Example 4 . . . . .	84
Figure 28.	Subregion Areas from Example 2 with Reduced Hole . . . . .	88
	Diameter	
Figure 29.	Subregion Area A1 from Example 2 with Elliptical Hole. . . . .	89

## List of Tables

	Title	page
Table 1.	Example Data . . . . .	55
Table 2.	Mesh Characteristics for Example 1 . . . . .	59
Table 3.	Comparison of the SBSF and Direct Methods using the Stress Results of Example 1.	62
Table 4.	Comparison of the SBSF and SBD Methods using the Stress. Results of Example 1.	66
Table 5.	Comparison of the SBSF and SBD Methods using the Stress. Results of Example 2.	72
Table 6.	Mesh Characteristics for Example 3 . . . . .	77
Table 7.	Comparison of the Efficient Zooming and the SBSF Methods using the Stress Results of Example 3.	79
Table 8.	Comparison of the Exact Zooming and the SBSF Methods using the Stress Results of Example 4.	85

## List of Appendices

	Title	page
Appendix A.	Complete Listing of Subroutines Added to MESS/SBSF. . .	101
Appendix B.	Finite Element Meshes for Subregion Analyses of . . . . Example 1.	114
Appendix C.	Finite Element Meshes for Direct Analyses of Example 1.	124
Appendix D.	Finite Element Meshes for Subregion Analyses of . . . . Example 3.	131



## INTRODUCTION

The finite element method has become a widely used tool for stress analysis, especially of large structures such as aircraft, automobiles, and nuclear power plant components. The use of this method is common practice in industry and it is a well developed technology. Instruction in the theory and application of the finite element method is currently available in many undergraduate and graduate engineering curricula. There are also many different finite element codes available, both general purpose codes such as ANSYS or SUPERB for example, as well as an abundance of in-house codes developed at universities or in industry for specific purposes.

The application of the finite element method has allowed engineers to obtain much more information about the stress state in a structure than was previously possible. Many times these structures contain stress concentrators, discontinuities, or other features that the engineer wishes to analyze in more detail. This situation requires a refined mesh so that the stresses will be calculated accurately. The problem of efficiently and accurately analyzing such regions of the structure has not, in general, been well explored.

The simplest and perhaps the most commonly used approaches are to either use a fine mesh throughout the structure or to transition from a fine mesh in the region of interest to a coarser mesh in the rest of the structure. The use of a fine mesh throughout the structure will require a great deal of time both to develop the mesh and to analyze it. Additionally, the results of such an analysis will include more stress and displacement information about the region outside of the area of interest than the analyst needs to accurately assess the conditions in the structure.

Transitioning a finite element mesh can be very effective if done well, but it does require some skill on the part of the analyst to insure that the element sizes do not change abruptly. The use of triangular elements to transition from a fine to coarse mesh may affect the accuracy of the results. If the triangular elements are actually degraded quadrilaterals, the order in which the nodes are specified may skew the stress results for the element by affecting the location of the Gauss integration points. However, both of these methods, an overall fine mesh or local refinement with transitioning to a coarser mesh, have the advantage that neither special finite element codes nor analysis techniques are required.

Some other methods that have been developed to handle this problem are the linear constraint method [1,2,3]<sup>\*</sup>, the specified boundary displacement method [1,4,5], the efficient zooming method [9], and the exact zooming method [10]. All of these methods do require certain capabilities in the finite element code and a familiarity with the finite element theory on the part of the analyst. On the other hand, they do offer the analyst more flexibility in analyzing the structure and allow him to obtain detailed results for only the portion of the structure in which he is interested.

Each of these approaches has its own individual strengths and weaknesses, which would dictate its applicability to a given situation. For example, the linear constraint method uses only a whole structure model with local refinement in the region of interest and constraint equations on the region's interface with the rest of the structure. In contrast, the zooming

---

\* Numbers in square brackets refer to references at the end of this dissertation.

methods and the specified boundary displacement method use both a coarse whole structure model and a separate refined local or subregion model of the area of interest. The boundary conditions for the subregion model are obtained from the analysis of the whole structure model. The specified boundary displacement method requires that the finite element code be capable of imposing non-zero displacement constraints upon nodes while the linear constraint method requires the capability to impose constraint equations upon the relative displacement of nodes. The two zooming methods use a finite element code that has been modified to allow direct manipulation of the stiffness matrix.

The purpose of the work presented in this dissertation was to develop a method for subregion analysis which would fulfill the following criteria: (1) should not be totally dependent upon the displacement solution from the parent model, (2) should accurately transfer the effect of the rest of the structure to the subregion model, (3) should be computationally efficient, and (4) should be easily implemented into an existing finite element code. The approach developed with these expectations in mind is called the specified boundary stiffness/force method. This method uses a coarse whole-structure model with a refined local model. Stiffnesses and forces from the portion of the whole structure model outside of the subregion area are applied to the boundary of the local model. Thus, this method accounts not only for the forces exerted upon the subregion by the rest of the structure but also for the interaction between the stiffnesses of the refined subregion area and those of the part of the structure outside of the subregion area.

The theoretical development of the specified boundary stiffness/force method, including the method of obtaining the boundary stiffnesses and

forces, will be presented. The approach used to implement this method into an existing finite element code will be discussed and the necessary modifications explained. Through the numerical examples included, this new approach will be compared to the specified boundary displacement method and the zooming methods. In addition, a comparison between the results from the specified boundary stiffness/force method and those obtained by a finite element analysis of the whole structure model incorporating the refined subregion area will be made. Examples demonstrating the use of the specified boundary stiffness/force method for the analysis of design changes in the subregion models will also be presented. These comparisons and examples will demonstrate the accuracy and flexibility of this method. Based upon the results of these studies, conclusions about the effectiveness of this method will be made and discussed. Recommendations for future work on the development and application of this method to stress analysis will also be presented.

## LITERATURE REVIEW

As mentioned in the introduction, the finite element stress analysis of large structures often requires the accurate and efficient analysis of local areas such as stress concentrations or fracture sites. Approaches to this problem that have been described in the literature include the linear constraint (LC)<sup>\*</sup> method, the specified boundary displacement (SBD) method, and the zooming methods. Which of these methods would be used for a specific problem depends upon the nature of the problem and the capabilities of the finite element code being used.

The LC method, also referred to as local mesh refinement or mesh grading, requires that the user locally refine the finite element mesh in the region of interest. The transition between the locally refined area and the coarser mesh in the rest of the structure is handled by imposing constraint equations on the extra nodes inserted along the boundary between the local area and the remainder of the structure. The interface between the refined region and the rest of the structure would look like that in Figure 1. Here the extra nodes, those indicated by open circles, would have constraint equations associated with them. These equations would tie the displacements of these nodes to the displacements of the independent nodes, those indicated by solid circles in Figure 1. The specific form of the constraint equation is dependent upon the element formulation but a general form given by Schwartz [1] is:

$$\{u_d\} = [C_i] \{u_i\} \quad (1)$$

In this equation,  $\{u_d\}$  are the displacements of the dependent nodes and  $\{u_i\}$

---

\* Acronyms in parentheses will be used in the remainder of this dissertation to represent the phrase preceding the parentheses.

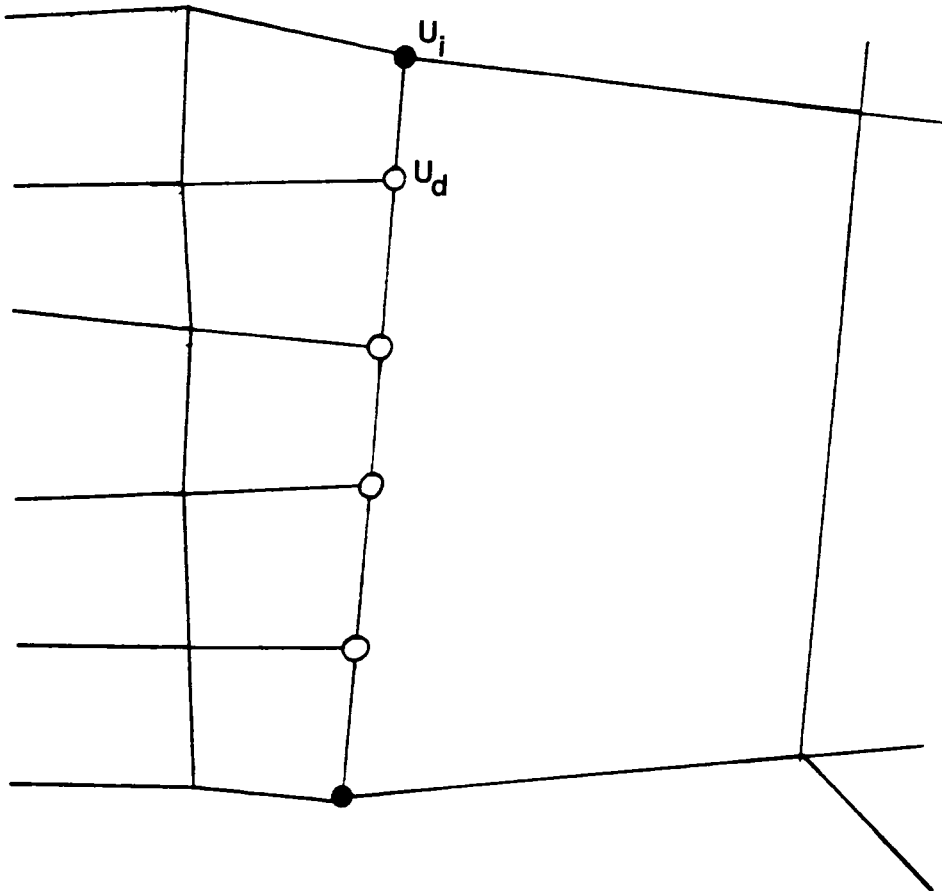


Figure 1. Subregion Interface for the Linear Constraint Method

are the those of the independent nodes. The  $[C_i]$  terms are the constant coefficients which will depend upon the element formulation. For example, Somervaille and Kabaila [2] have developed the necessary equations for both equilibrium and displacement elements.

A special form of the LC method is the transitive element, an element which is designed to be used when transitioning from a coarse mesh to a fine mesh. The most common forms of these elements have an extra midside node on one or more sides of the element. Carey [3] suggests that the use of these elements may result in a solution which does not minimize the energy integral, thus violating the variational principle. The problem with these elements is that the nodal averaging constraint on the extra nodes is applied after the element matrices are assembled. To avoid this difficulty, he presents an element formulation in which the constraints upon the extra nodes are embedded in the element formulation. Carey presents an example which verifies that his element formulation does not violate the variational principle. In that example, the triangular element 1-2-3 in Figure 2 is subdivided into four smaller triangular elements as shown. The element formulation for the new elements includes the constraints on the nodes 4, 5, and 6. When the matrices for the four smaller elements are assembled together, the result is the same as the matrix for the parent element with node sequence 1-2-3. This proves that, if properly incorporated into the element formulation, the constraints should not cause a violation of the variational principle. In Carey's mesh refinement and analysis scheme he uses this type of element formulation for the elements on the boundary of the refined region as shown in Figure 3. Thus, if properly formulated, transitive elements, a variation of the LC method, can be accurately used for subregion analysis.

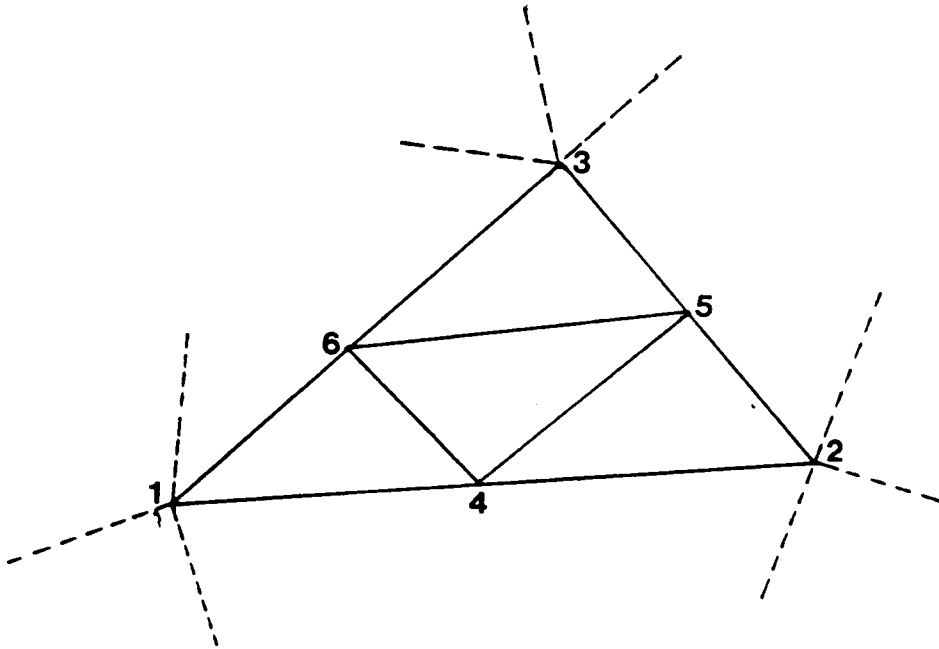


Figure 2. Interior Subdivision to form a Transitive Element



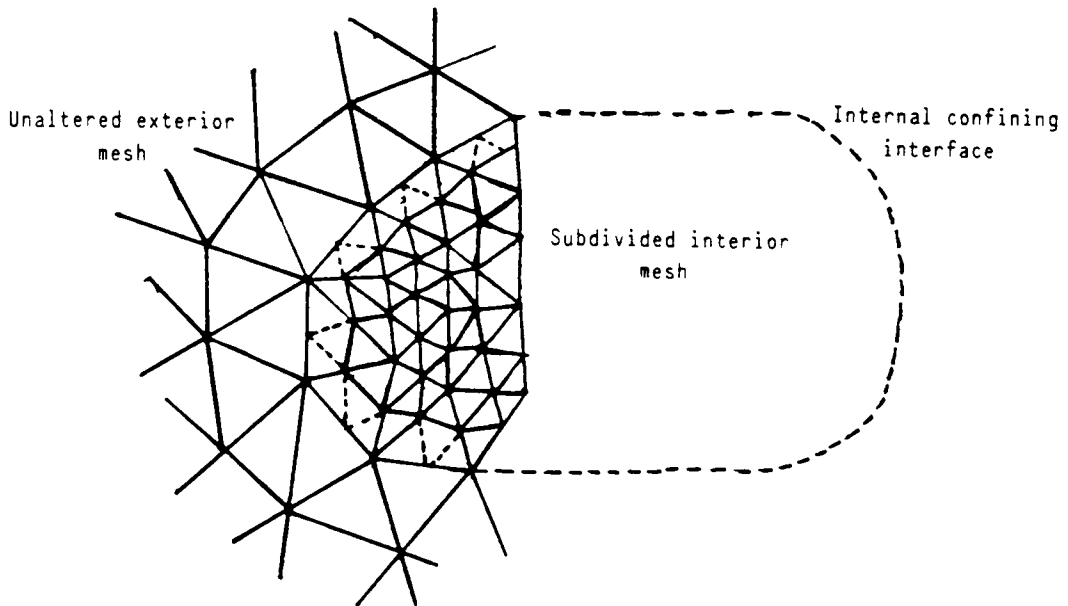


Figure 3. Example of the use of a Transitive Element in a Finite Element Mesh

The advantage of the LC method is that the mesh need only be refined in the specific region of interest. The user does not need to worry about transitioning the mesh to the coarser mesh in the rest of the structure. This type of model should require less computer time than if the whole structure was modeled with a fine mesh. A primary disadvantage of this method is that if the analyst makes any changes in the mesh in the refined area, the whole structure must be reanalyzed. This is not very efficient as small changes in the refined region are unlikely to significantly affect the results in the rest of the structure. As in most methods of subregion analysis, multiple models will be required. Generally, the user will need to analyze a coarse model of the whole structure first so as to identify those regions in which refinement is necessary. Then, the model with local refinement would be developed and analyzed. Also, as described previously, Carey [3] has found that applying constraint equations to nodes when using a standard element formulation may cause the resulting structure formulation to violate the variational principle.

Another method used to handle the problem of analyzing local areas is the SBD method [1,4,5]. In this approach, the entire structure is analyzed using a coarse mesh. A refined subregion model of the local area is then developed. The boundary conditions used for this subregion model are the displacements calculated in the analysis of the whole structure. The displacements of the nodes on the boundary of the subregion which do not coincide with nodes in the whole structure model are interpolated from the displacements of those nodes which do coincide. The interpolation function is dependent upon the element formulation. For a two-dimensional, plane stress, isoparametric element, for example, the displacements of the nodes on the boundary of the subregion can

be generally expressed as

$$\begin{Bmatrix} u_x \\ u_y \end{Bmatrix} = [N_i] \begin{Bmatrix} u_{x_i} \\ u_{y_i} \end{Bmatrix} \quad (2)$$

Here, the vector on the lefthand side is the displacement vector for the new nodes on the boundary of the subregion model, the vector on the righthand side is the displacement vector of the original nodes in the whole structure model, and  $[N_i]$  are the element shape functions.

A comparison of the LC and the SBD methods is presented by Schwartz [1] for two cases of stress concentrators, a central hole and a semi-circular edge notch, in a bar loaded in tension. The results of Schwartz's study demonstrate that under equal conditions, i.e. identical meshes around the stress concentrators, the LC method gives results that are much more accurate than those obtained with the SBD method. Specifically, for the case of a semi-circular edge notch analyzed with eight-noded elements, the results from the LC method have an error of - 3.0% when compared with the theoretically correct value of  $K_t$  from Peterson [6]. In comparison, the percent error for the SBD method was -5.9%. Though the specified displacement method is less accurate, it has several advantages over the LC method. It is relatively easy to use and can be implemented with any finite element code that allows non-zero boundary conditions. This method does not require reanalysis of the entire structure if changes are made in the subregion mesh. The user is also not limited in the arrangement of the nodes on the boundary of the refined area as in the LC method.

As explained by Kelley [4], the user must be cautious when using the SBD method and be aware of potential difficulties. The most important of these is a that a precise displacement field from the whole structure analysis is

required if the results of the subregion analysis are to be accurate. The boundary of the subregion must be far enough away from the region of interest that the displacements obtained from the coarse model analysis of the whole structure are accurate. Unfortunately, it is extremely difficult to define what distance constitutes "far enough away". Kelley [4] states that "the distance away from the discontinuity that the local model must extend is highly dependent upon the coarse model used." He goes on to explain that in some cases it may be more economical to use a very coarse whole structure model and a local model that extends quite a distance away from the detail to be analyzed. At other times, it may be necessary to use a more refined whole structure model and a smaller local model.

Another difficulty with any approach to the finite element analysis of a stress raiser is trying to decide when the finite element mesh is sufficiently refined to give accurate results. Kelley [4] studied this problem using the SBD method to analyze the problem of a flat plate in tension with a central hole. As this problem has a closed-form solution, the values of the stress concentration factors for different ratios of hole size to plate size are readily available [7, 8]. The study used both four-noded and eight-noded, two-dimensional, plane stress isoparametric elements to analyze two different whole structure models and sixteen different local models. It was concluded that for this problem the largest acceptable elements in the local model are approximately nine degrees circumferentially and one-eighth of the hole diameter radially. Additionally, at least two rows of elements in the local model are recommended.

Recent work by Kelley [5] has developed a method of applying the SBD method to a subregion model composed of three-dimensional solid elements

using the results from a parent model of shell elements. This has been developed to handle the problem of analyzing the stress field in the weld at a pipe junction. Previously the approaches used have been (1) the use of formulas such as those from the ASME Boiler and Pressure Vessel Code, (2) use of a very detailed finite element model using three-dimensional solid elements throughout, or (3) the use of a finite element model that combines shell elements with solid elements in the weld area and appropriate constraint equations on the interface. All three of these approaches have drawbacks and may or may not give accurate results depending upon how they are applied to the problem.

The method developed by Kelley uses shell elements for a coarse analysis of the entire structure. The pipe junction is then modeled in more detail with solid elements in a subregion model. The boundary conditions on this 3-D subregion model are the displacements calculated from the results of the whole structure analysis by assuming a linear strain distribution throughout the shell thickness.

The results of the examples in [5] show that this method gives results which are comparable to analyzing the entire structure with solid elements using only 75% of the computer time that would be required for such an analysis. However, to obtain these results, it was necessary for the analyst to modify the shell element thickness at the pipe junction in the whole structure model to reflect the changes due to the weld fillet. It is pointed out that this method is extremely sensitive to minor changes in the whole structure analysis and is not a method to be used by the novice analyst.

Two other methods developed to handle the problem of accurately analyzing local areas are the zooming methods. Hirai describes the

efficient zooming method in [9] and the exact zooming method in [10]. Both approaches allow the user to "zoom" in on the area of interest by developing a separate subregion model of the area. They also allow for multiple levels of zooming, i.e. analyzing a subregion of a subregion. The primary difference in the two methods is the way in which information from the whole structure model is handled during the analysis of the subregion model.

The efficient zooming method [9] uses the techniques of static condensation and reanalysis to develop a solution for the subregion model. This method is termed "exact" because it gives the same solution as the solution from a model of the whole structure with identical refinement in the subregion area. The method requires that the user begin by analyzing a coarse model of the entire structure. The stiffness matrix and its inverse as well as the displacement solution from this analysis are saved for use in the subregion analysis. These terms are saved in partitioned form, broken down into those terms which involve the degrees of freedom which lie outside the subregion area and those which lie inside. After the analysis of the parent model is complete, the user must develop a subregion model. The stiffness terms due to the newly introduced degrees of freedom (dof) in this subregion model will be assembled with the previously stored stiffness matrix from the parent model. The resulting stiffness matrix will be the same as if the whole structure model had been modeled with the same degree of refinement in the subregion area as the subregion model. Thus, this problem formulation would be:

$$\begin{bmatrix} K_{aa}^{(0)} & K_{ab}^{(0)} & 0 \\ K_{ba}^{(0)} & K_{ab}^{(1)} & K_{b1}^{(1)} \\ 0 & K_{1b}^{(1)} & K_{11}^{(1)} \end{bmatrix} \begin{Bmatrix} u_{0a}^{(1)} \\ u_{0b}^{(1)} \\ u_1^{(1)} \end{Bmatrix} = \begin{Bmatrix} F_a^{(0)} \\ F_b^{(0)} \\ 0 \end{Bmatrix} \quad (3)$$

Here, the subscripts are defined as:

- a--the region outside of the subregion model
- b--the original dof in the subregion model
- l--the dof introduced in the subregion model

The superscript 0 refers to terms from the parent model analysis and the superscript 1 refers to terms from the subregion analysis.

Through a series of matrix manipulations, the details of which are presented by Hirai in [9], this system of equations is reduced to a set of equations that only involves the displacements of the original dof in the subregion area, the  $\{u_{0b}\}$  terms. This equation is:

$$\{u_{0b}^{(0)}\} = ([I] - [Y_b]) \{u_{0b}^{(1)}\} \quad (4)$$

where  $[I]$  is the identity matrix and the matrix  $[Y_b]$  results from the application of the exact static reanalysis technique to the problem formulation. To calculate the terms in  $[Y_b]$ , it is necessary to invert the stiffness submatrix  $K_{11}^{(1)}$  from equation 3. The inverse of the parent model stiffness matrix, which was retained from the parent model analysis, is also necessary. The displacement terms on the left hand side of equation 4, the  $\{u_{0b}^{(0)}\}$  terms, were saved from the parent model analysis.

Once the system of equations has been reduced to this point, the matrix  $([I] - [Y_b])$  must be inverted to solve for the unknown displacements  $\{u_{0b}^{(1)}\}$ . The size of this matrix is the same as the number of original dof in the subregion area. These displacements can then be used to find the displacements of the other dof within the subregion model.

A direct solution to the same problem would require the decomposition of a stiffness matrix whose order would be the total number of dof in the model. In [9], it is stated that the efficient zooming method is computationally more efficient than a direct analysis if the total number of dof for the refined

model is much greater than both the number of dof originally within the subregion area and the number introduced into the subregion area from the refinement.

The numerical example presented in [9] is that of a rectangular plate loaded in tension with a central hole. The results are presented for a series of analyses involving multiple levels of zooming. As expected, the efficient zooming methods gives results which are identical to those for a direct analysis with the same degree of refinement but the method is computationally more efficient. No new nodes may be introduced on the boundary of the subregion so that the stiffness matrix for the subregion model can be coupled with the stiffness matrix from the parent model. In addition, at each level of zooming the results, i.e. displacement solution and stiffness terms, from each previous analysis must be retained.

The other zooming method, the exact zooming method, was also developed by Hirai [10]. This approach uses an augmented stiffness matrix and flexibility relations to solve the finite element problem. The flexibility terms are the terms which relate the forces to the displacements and come from the inverted stiffness matrix. This method also begins with an analysis of a parent model. The flexibility terms developed when the stiffness matrix for the parent model is inverted are retained. These terms are written in a partitioned form relating the degrees of freedom within the subregion area to those outside of the subregion area. After the analysis of the parent model, a separate subregion model of the area of interest is developed. The stiffness terms from the subregion model can be combined with the flexibility terms from the parent model analysis to develop a flexibility relationship for the zoomed system. The flexibility formulation for the entire system



would be:

$$\begin{Bmatrix} u_a^{(1)} \\ u_b^{(1)} \end{Bmatrix} = \begin{bmatrix} f_{aa}^{(1)} & f_{ab}^{(1)} \\ f_{ba}^{(1)} & f_{bb}^{(1)} \end{bmatrix} \begin{Bmatrix} F_a^{(1)} \\ F_b^{(1)} \end{Bmatrix} \quad (5)$$

where the subscript a refers to the dof outside of the subregion area and the subscript b to those dof within the subregion area. As the external forces,  $F_a$  and  $F_b$  are known, this system can be solved for the displacements of the dof within the subregion area alone by

$$\{u_b\} = \begin{bmatrix} f_{aa}^{(1)} \end{bmatrix} \{F_a^{(1)}\} + \begin{bmatrix} f_{ab}^{(1)} \end{bmatrix} \{F_b^{(1)}\} \quad (5a)$$

This approach to subregion analysis is exact in the sense that all stiffness, force, and displacement terms are retained and no approximations are made. The displacement solution should be the same as that obtained from the analysis of a whole structure model with the same degree of refinement in the local area as the subregion model. As the flexibility terms are retained from the parent model analysis, only the stiffness submatrices due to the additional dof introduced in the subregion model have to be inverted during the subregion analysis.

The primary advantage that this method has over the efficient zooming method is that only the results of the immediately preceding analysis are required for each subregion analysis. For example, using the nomenclature of [10], a second level zooming analysis would be the analysis of a subregion of a subregion of a parent model. To carry out this second level analysis only the flexibility terms from the first level analysis would be required. The same analysis using the efficient zooming method would require the stiffness terms and displacement values from both the first level analysis and the parent model analysis.

The numerical example presented in [10] is that of a plate loaded in

tension with a central hole. Two analyses sequences are presented, each using a different parent model. The results are compared to the direct analysis approach and to the efficient zooming method. The exact zooming method agrees exactly with the direct approach, as would be expected. Unexpectedly, however, the efficient zooming method and the exact zooming method do not give the same results. Since both methods are essentially exact methods, it seems reasonable to expect the same values. The reason for the differences between these results is clearly explained in [10]. Also, the results of the exact zooming method overestimate the maximum stress in the model as the element size becomes small and they do not show convergence to the theoretically correct results. These observations seem to indicate that there is some problem with this method. Most likely, it is a numerical error due to the amount of truncation error resulting from the large number of numerical operations required the element size becomes smaller and the number of elements greater.

In summary, both zooming methods are essentially ways to solve the exact finite element problem without requiring the inversion of a large stiffness matrix. In this sense, they are both exact methods since no approximations are introduced. As explained previously, the advantage of the exact zooming method over the efficient zooming method is that only the immediate previous zooming level is needed in the exact method. The efficient zooming method requires the stiffnesses and displacements from all previous levels to solve the system of equations for the current level. A disadvantage of both zooming methods is that matrices must be inverted. Matrix inversion is computationally time consuming and inaccuracies can result because of the large number of operations required. Also, the user is not able to introduce

any new nodes on the boundary of the subregion model, a limitation which will affect the arrangement of nodes and elements in the subregion models.

The zooming methods may appear to be another form of substructuring, the technique by which a whole structure model is broken into regions for analysis. In substructuring, the stiffness matrix for each region is assembled and condensed to involve only the degrees of freedom on the boundary of the region. Then, the condensed stiffness matrices from all the regions are joined together to constitute the set of equations for the whole structure analysis. The order of the system is less than it would be if the stiffness matrix had been assembled for the whole structure without condensation. As explained in [8], "a substructure is used in the same way as an individual finite element with internal degrees of freedom that are statically condensed out prior to the element assemblage process".

In this context, substructuring could be used as a method for subregion analysis by defining the subregion model as a substructure of the entire structure model. However, each time that the subregion model was changed the entire structure analysis would have to be redone. In addition, if a second level subregion analysis were to be done, it would be necessary to define two new substructures. The first would be the second level subregion model and the second would be the original first level subregion model with the second level subregion area eliminated. It is clear that for multiple levels of subregion analysis, the number of substructures required would increase rapidly as would the complexity of the modeling.

Based upon this concept of substructure analysis, it may seem that the zooming methods are a substructuring approach to the problem. However, Hirai [9] refutes this idea, stating that the zooming methods are not

substructuring because:

- (1) new nodes and elements are introduced into the original system while substructuring connects existing subsystems to make a total system
- (2) the zooming method considers both the original nodes and the new nodes in the subregion area while the substructuring considers only the new nodes in the substructures to be connected.

It seems that substructuring could be used for the detailed analysis of discontinuities in structures but it is not a convenient method for the repeated reanalysis of a subregion with changing meshes. The necessity to reassemble and solve the entire finite element problem for each analysis also makes it computationally inefficient if the only variables of interest are in the subregion area. In this respect, the zooming methods, which are designed for repeated analyses of a portion of a structure without reassembling all of the equations, are much more efficient. Like substructuring, they are also an exact method of analysis, resulting in the same solution as a direct analysis but computationally more efficient than a direct analysis.

## THEORETICAL DEVELOPMENT

A new approach to subregion analysis by finite element methods is the Specified Boundary Stiffness/Force method (SBSF). In this section the theoretical development of this method will be presented beginning with the formulation of the problem. The approach used to partition the stiffness matrix and the force and displacement vectors makes the derivation of the boundary stiffness terms quite straightforward. However, the calculation of the boundary forces is more complex and two ways of obtaining these terms will be shown. The advantages and disadvantages of each method, along with the basis for choosing the method used will be presented.

The goal of this approach is to be able to isolate the subregion area from the whole structure model and develop a separate, more detailed finite element model of that area. Stiffnesses and forces obtained from the whole structure model after the subregion area has been eliminated will be applied to the boundary of this separate subregion model. This method is similar to the SBD method in that it uses a separate subregion model with boundary conditions obtained from the whole structure analysis. The difference between these two approaches is that the SBD method uses only displacements as the boundary conditions upon the subregion model and does not carry along any of the stiffness interaction between the subregion model and the rest of the structure. The SBSF method is similar to the zooming methods in that both a parent model and a subregion model are used and the stiffness interaction between the different parts of the structure is included. However, the zooming methods allow the response of the entire model (both the subregion area and the rest of the structure) to be recalculated each time a subregion analysis is performed. For both the SBSF and the SBD methods, only the

solution for the dof within the subregion area can be found from the subregion analysis.

The general finite element problem may be written as:

$$[K] \{D\} = \{F\} \quad (6)$$

where  $[K]$  is the structure stiffness matrix,  $\{D\}$  contains the displacements for all of the degrees of freedom in the structure, and  $\{F\}$  is the load vector for the structure. The stiffness matrix will be of the order  $n \times n$  where  $n$  is the total number of degrees of freedom in the structure. For a whole structure or parent model, this general problem may be partitioned as:

$$\begin{bmatrix} [K_a] & [K_{a,ab}] & 0 \\ [K_{ab,a}] & [K_{ab}] & [K_{ab,b}] \\ 0 & [K_{b,ab}] & [K_b] \end{bmatrix} \begin{Bmatrix} D_a \\ D_{ab} \\ D_b \end{Bmatrix} = \begin{Bmatrix} F_a \\ F_{ab} \\ F_b \end{Bmatrix} \quad (7)$$

The subscript definitions are:

a--the region outside the subregion area

b--the region inside the subregion area

ab--the line of nodes that make up the interface between regions a and b

The different parts of the whole structure model are illustrated in Figure 4.

This formulation is convenient for the development of the SBSF method because not only does it divide the structure into the areas outside and inside the subregion area, but it also isolates those dof on the interface to which the boundary stiffnesses and forces will be applied in the subregion model.

Referring to equation 7, the equations dealing with the forces and displacements of the interface and of the subregion area are:

$$[K_{ab,a}] \{D_a\} + [K_{ab}] \{D_{ab}\} + [K_{ab,b}] \{D_b\} = \{F_{ab}\} \quad (8)$$

$$[K_{b,ab}] \{D_{ab}\} + [K_b] \{D_b\} = \{F_b\} \quad (9)$$

These equations can be assembled into matrix form by taking the term involving  $\{D_a\}$  from the solution step for the whole model in equation 8 and moving it to

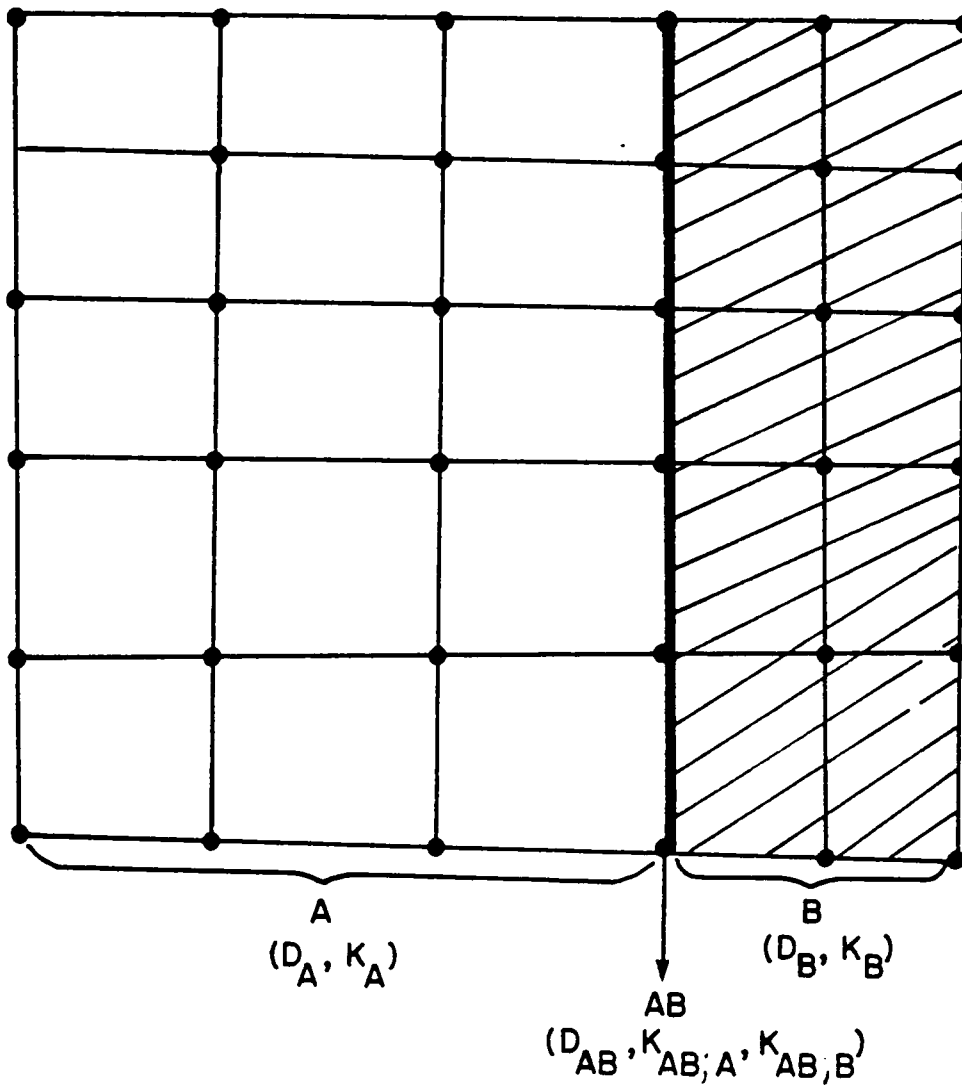


Figure 4. Mesh Divisions for the Specified Boundary Stiffness/Force Method

the righthand side as a force term. The result is the matrix equation:

$$\begin{bmatrix} [K_{ab}] & [K_{ab,b}] \\ [K_{b,ab}] & [K_b] \end{bmatrix} \begin{Bmatrix} D_{ab} \\ D_b \end{Bmatrix} = \begin{Bmatrix} F_{ab} - [K_{ab,a}] \{D_a\} \\ F_b \end{Bmatrix} \quad (10)$$

If the model in Figure 4 is considered to be a whole structure model, than the model shown in Figure 5 would be a typical subregion model from that parent model. The stiffness matrix for the subregion model shown in Figure 5 would include all four stiffness terms shown in equation 10. These terms would be different from the terms in equation 7 because the mesh of the subregion model in Figure 5 is more refined than the mesh in the subregion area of the model in Figure 4. In addition to the stiffness terms from the subregion model, a portion of the  $[K_{ab}]$  submatrix would come from the parent model and would be the stiffness interaction between the subregion area and the rest of the structure. In other words, the  $[K_{ab}]$  submatrix receives contributions from the elements adjacent to the interface, both inside and outside the subregion. When the stiffness matrix for the subregion model is assembled, only the contributions to the  $[K_{ab}]$  submatrix from the elements within the subregion will be summed. The contribution from the elements outside the subregion will be the boundary stiffnesses for the subregion model.

This approach uses the  $-[K_{ab,a}] \{D_a\}$  terms as the boundary forces. Physically, these terms are the forces exerted upon the subregion boundary nodes due to the displacements of the rest of the structure. These boundary forces are applied as external loads upon the subregion model in conjunction with any external loads,  $\{F_{ab}\}$ . Thus, the total load on the nodes on the subregion boundary is  $\{F_{ab}\} - [K_{ab,a}] \{D_a\}$ .

Although it is clear that the term  $[K_{ab,a}] \{D_a\}$  can be considered external force terms, the use of the  $\{D_a\}$  terms to calculate the forces will



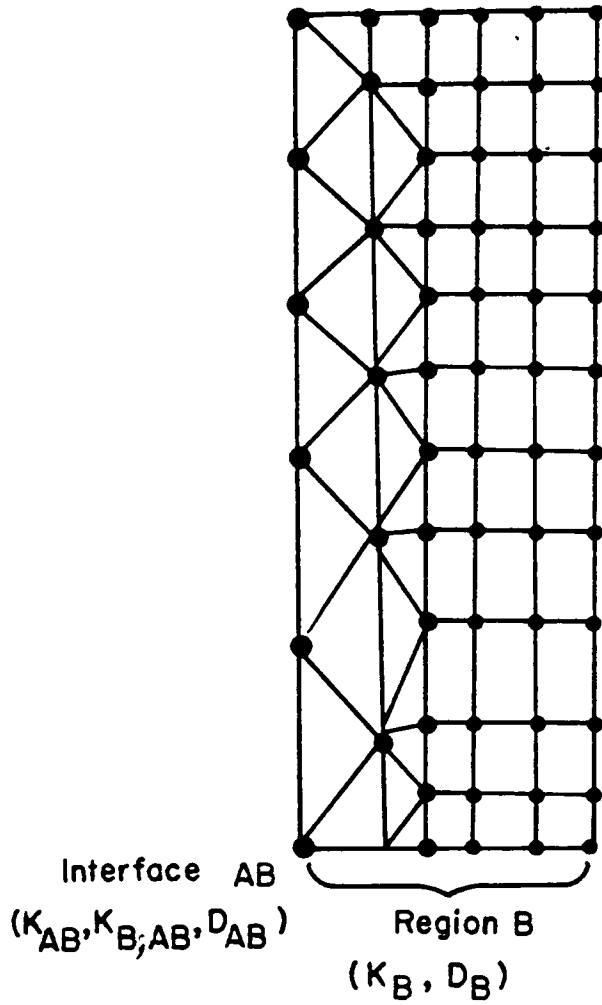


Figure 5. Typical Subregion Model for the Specified Boundary Stiffness/Force Method

introduce some error. These displacement terms are the result of the finite element analysis of a specific whole structure mesh. When the whole structure mesh is changed, different displacement values will result throughout, resulting in some change in the forces upon the interface between the two regions. However, it seems reasonable to expect that if the boundary of the subregion is far enough away from any discontinuity in the structure, changes in the mesh will have only a minor effect upon the displacement values and, subsequently upon the force values. As far as the implementation of the SBSF method is concerned, the advantage of using this approach to find the boundary forces is that the computations involved are simple and would not require a great deal of computer time or involve much numerical error.

In an attempt to avoid using displacement values from the whole structure analysis in the boundary force calculation, alternative methods of calculating the forces were considered. One such approach was to solve the first set of equations in equation 7, the whole structure formulation, for  $\{D_a\}$  and substitute it into the subregion formulation. The equation for  $\{F_a\}$  is:

$$[K_a] \{D_a\} + [K_{a,ab}] \{D_{ab}\} = \{F_a\} \quad (11)$$

Solving for  $\{D_a\}$  this becomes:

$$\{D_a\} = [K_a]^{-1} \{F_a\} - [K_{a,ab}] \{D_{ab}\} \quad (12)$$

When substituted into the subregion formulation the first equation of equation 10 becomes:

$$[K_{ab}] \{D_{ab}\} + [K_{ab,b}] \{D_b\} = \{F_{ab}\} - [K_{ab,a}] [K_a]^{-1} \{F_a\} - [K_{a,ab}] \{D_{ab}\} \quad (13)$$

Then, if the term involving  $\{D_{ab}\}$  is carried over from the righthand side to the lefthand side and the resulting equation combined with the second equation from equation 10, the following subregion analysis formulation is

obtained:

$$\begin{bmatrix} [K_{ab}] - [K_{ab,a}][K_a]^{-1}[K_{a,ab}] & [K_{ab,b}] \\ [K_{b,ab}] & [K_b] \end{bmatrix} \begin{Bmatrix} D_{ab} \\ D_b \end{Bmatrix} = \begin{Bmatrix} F_{ab} - [K_{ab,a}][K_a]^{-1} F_a \\ F_b \end{Bmatrix} \quad (14)$$

The advantage of this formulation is that it avoids the need for precise  $\{D_a\}$  terms by expressing the boundary forces in terms of the unknown displacements  $\{D_{ab}\}$  and the known forces  $\{F_a\}$ . However, from a practical standpoint, this formulation would be difficult to implement efficiently because of the need to invert  $[K_a]$ .

The specified boundary stiffness/force method of subregion analysis uses the formulation presented in equation 10. This approach was chosen over the other method of calculating the boundary forces because it is computationally more efficient. Though there is some error due to the use of the displacement terms in the boundary forces, it should be relatively small. It also seems reasonable to expect that this approach will be more accurate than the specified boundary displacement method. Here, the displacements are only a portion of the information that is being transferred from the parent model to the subregion model. In the SBD method, the only information carried to the subregion model are the displacement terms. Thus, it seems intuitive that inaccuracies in the displacement terms will affect the SBSF solution less than the SBD solution. This will be substantiated by the comparisons of the SBSF, SBD, and direct analysis methods presented in the Numerical Examples section of this dissertation.

## COMPUTER IMPLEMENTATION

The specified boundary stiffness/force method was implemented into an instructional finite element code, MESS, used in the Mechanical Engineering Department at Virginia Polytechnic Institute and State University for static stress analysis. The basis for this program is the program STAP by Bathe [11]. The MESS program has a three element library that includes a two-noded truss element, a four-noded isoparametric plane stress element and a four-noded axisymmetric element. The SBSF method was implemented for the plane stress element only. In this section, an overview of the existing program will be presented followed by an explanation of the modifications made when the SBSF method was implemented into MESS. A detailed explanation of the code additions necessary for the SBSF method will be included. The operation of the modified program, MESS/SBSF, will also be presented along with a description of the steps required to perform a subregion analysis.

MESS uses a dynamic storage system with all problem size dependent data arrays stored in a one-dimensional array. Pointers are used to locate specific arrays within this array. This system is very memory efficient as storage space can be reused as values are no longer needed. Each of the major arrays discussed in the following paragraphs are stored in this single array.

Figure 6, which came from Bathe [11], is a graphical representation of the general flow of the MESS program. The input phase of the program, the first block in Figure 6, begins by reading and storing the nodal point data. From this information, the total number of degrees of freedom (dof) or equations in the model is obtained. The ID\* array, which relates the nodal

---

\* Words in all capitals refer to variable names within the program.

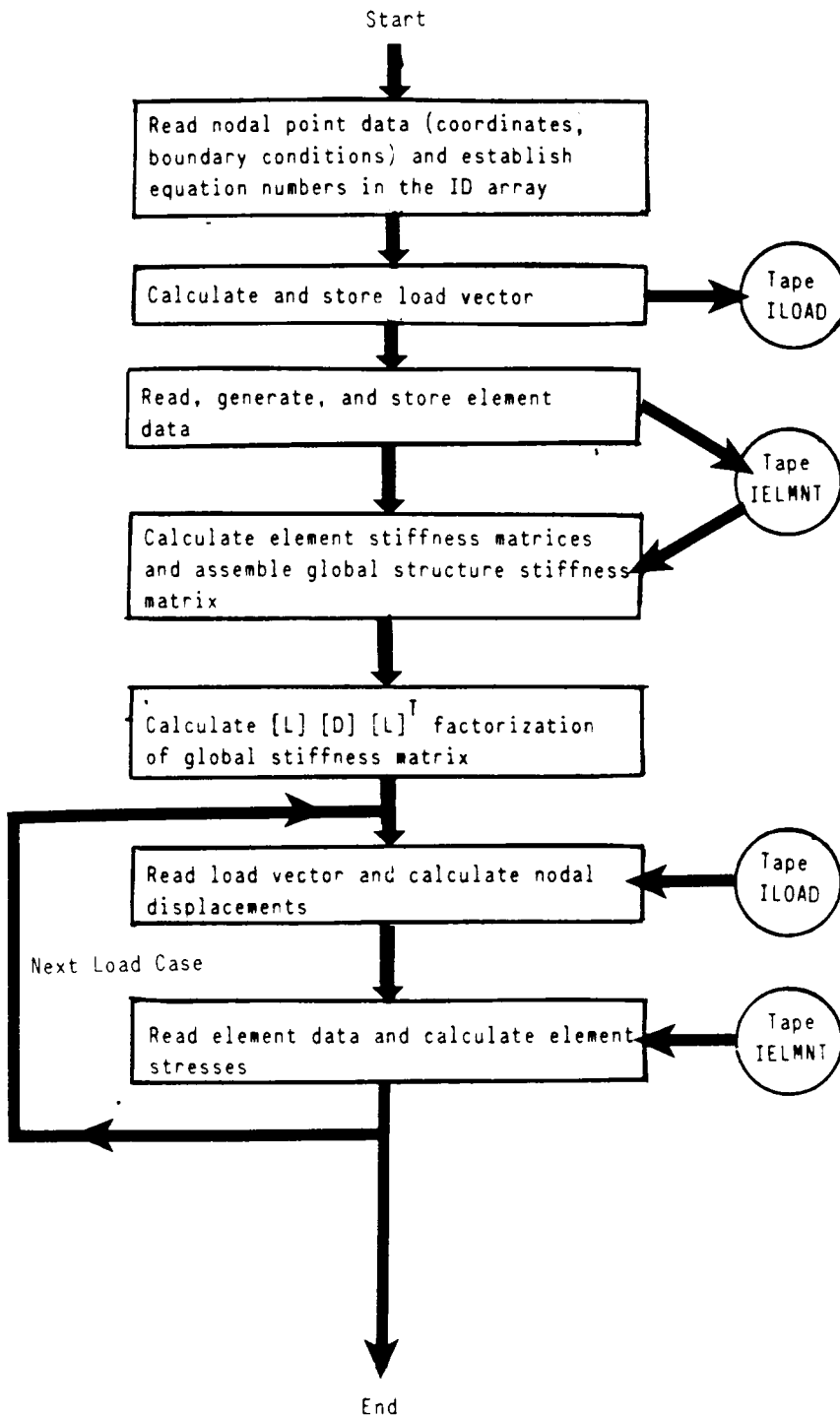


Figure 6. Flow Chart for the Unmodified MESS Program

point dof number to its associated equation number, is constructed. The remainder of the input phase, reading the load information and storing the load vector on tape, is shown in the second block in Figure 6.

In the third task, the element data is read and the connectivity array,  $LM(I,N)$ , constructed. In this array  $I$  ranges from one to the total number of degrees of freedom in an element and  $N$  goes from one to the number of elements. At a specific value of  $I$  and  $N$ ,  $LM$  has the value of the equation number associated with that degree of freedom of the element. Thus, this array relates each element degree of freedom to its associated global degree of freedom. Upon completion of this third task, the input stage of the program is complete and the solution phase begins.

Prior to assembling the stiffness matrix and actually finding the solution for the structure, space must be allocated in the  $A$  array to store the stiffness data. The total number of values to be stored must be calculated before the matrix is assembled to correctly locate the pointers for the global stiffness matrix. The upper half of the symmetric global stiffness matrix will be stored in the  $A$  array in a "skyline" manner. This means that for each column of the stiffness matrix only the terms from the diagonal up to the last non-zero term are stored. All terms above the skyline of the matrix are zero and are not stored. Each of the column heights can be determined from the  $LM$  connectivity array. The total number of entries stored,  $NWK$ , is the sum of all the column heights. Once  $NWK$  has been calculated using the  $LM$  array, the pointers to locate the terms of the stiffness matrix in the  $A$  array can be set.

In order to correctly locate specific terms in the stiffness matrix, one other array must be established. The  $MAXA(N)$  array is the address of the diagonal element of each column  $N$  of the stiffness matrix in the  $A$  matrix. An

example arrangement of the stiffness matrix in the A array along with the corresponding MAXA array is shown in Figure 7. Suppose that the address in A for an arbitrary term (I,J), below the skyline, is desired. This address would be

$$\text{Address} = \text{MAXA}(J) + (J-I) \quad (15)$$

Thus, as each element stiffness matrix is assembled, the LM array will indicate into which row and column of the global stiffness matrix these terms must be inserted. This row and column number in conjunction with the MAXA array will be used to find the specific location in the A array to which the stiffness term is to be added.

Once the storage location for the global stiffness matrix is established, the assemblage of the element stiffness matrices, begins. For the isoparametric elements the stiffness matrix, [K], is of the form

$$[K] = \int [B]^T [C] [B] dV \quad (16)$$

where [B] is the strain-node displacement matrix, [C] is the material property matrix, and dV is a differential of volume. This integral is evaluated numerically using Gauss quadrature for each element at the Gauss points. The quadrilateral isoparametric elements use four Gauss points while the degraded quadrilateral, triangular elements use a single Gauss point.

The development of the element stiffness matrix and the assembly of the global stiffness matrix take place concurrently. As each element stiffness matrix is assembled, the LM and MAXA arrays are used to find the correct location in A for each elemental stiffness term. The value of the stiffness term is then added to the value that is already being stored in that location in A.

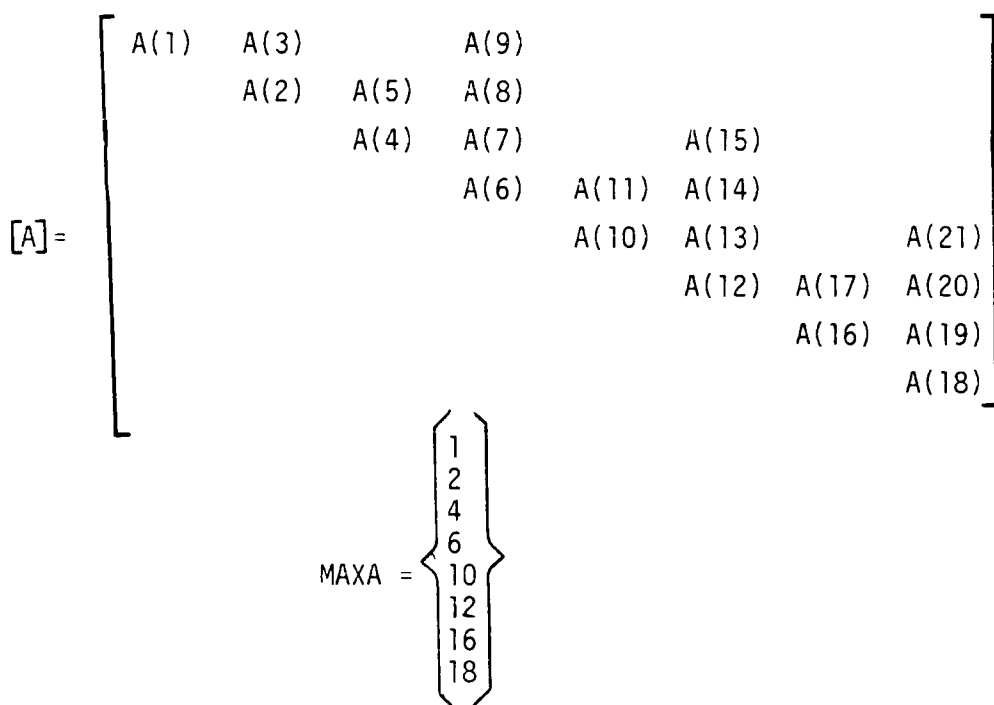


Figure 7. Dynamic Storage of the Stiffness Matrix in the MESS Program



Once the global stiffness matrix is fully assembled, it is upper triangularized, as indicated in the fifth block of Figure 6. Back substitution is then used to find the nodal point displacements. After the displacements are calculated, the stresses are found by using the strain-nodal displacement and stress-strain relationships. In the isoparametric element, the stresses must be evaluated at the Gauss points. These Gauss point stresses are then averaged together to give an average elemental stress for printout. The Gauss point stresses are also extrapolated to the nodes with a least squares surface fit to give the nodal stress values for plotting. As indicated in Figure 6, these last two tasks, solving for the displacements and stresses, are carried out for each load case.

Printed output from the unmodified MESS includes an echo of the input data, the displacement solution for each node, and the averaged stress components at the center of each element. In addition to the primary disk files shown in Figure 6, a number of additional files are created for the post-processing. Graphic post-processing is done by the program MOVIE-BYU [13]. The default graphic output is a mesh plot and an exaggerated deformed shape plot. Contour plots of the X, Y, XY, and Von Mises nodal stress values are optional.

The following paragraphs will explain how the SBSF method was implemented into MESS. The resulting program, MESS/SBSF, can be thought of as operating in two modes. The first mode is the analysis of a parent model and the extraction of stiffness and force data to be used in the subsequent subregion analyses. The second mode is the actual subregion analysis which includes the insertion of the boundary stiffness terms into the global stiffness matrix for the subregion model. Although the two modes of

operation are distinct, it is possible to incorporate both of them into a single analysis. For example, a user could analyze a subregion model using stiffness and force data from a previous model. At the end of this analysis, the subregion model could be redefined as a parent model and a new subregion model defined.

The flow chart for MESS/SBSF is shown in Figure 8. The shaded items are those decisions, tasks, and files that were added in the implementation of the SBSF method. The added disk files are ISTIF, ISSS, and the logical unit 29. The disk file ISTIF contains the LM array and the global stiffness matrix prior to upper triangularization. It was necessary to put this information on a separate tape because these arrays are overwritten during the solution phase. If the user wants to define a subregion of the current model, the original stiffness terms must be used to find the boundary stiffnesses and forces to be applied to the subregion. In disk file ISSS are stored the stiffness values and addresses in the A array for each element's contribution to the global stiffness matrix. This information is needed to calculate the boundary stiffness terms. The unit 29 file contains the boundary stiffnesses and forces. It is an output file from the parent model analysis and an input file for the subregion analysis.

In the first phase of the program, parent model analysis and subregion definition, subroutines SETUP and EXTRACT are used. Subroutine SETUP is called from the main routine after the analysis of the parent model is complete if the user has indicated that he wants to define a subregion of the current model. The major tasks of SETUP are:

- (1) read back into memory the LM array and the global stiffness matrix,

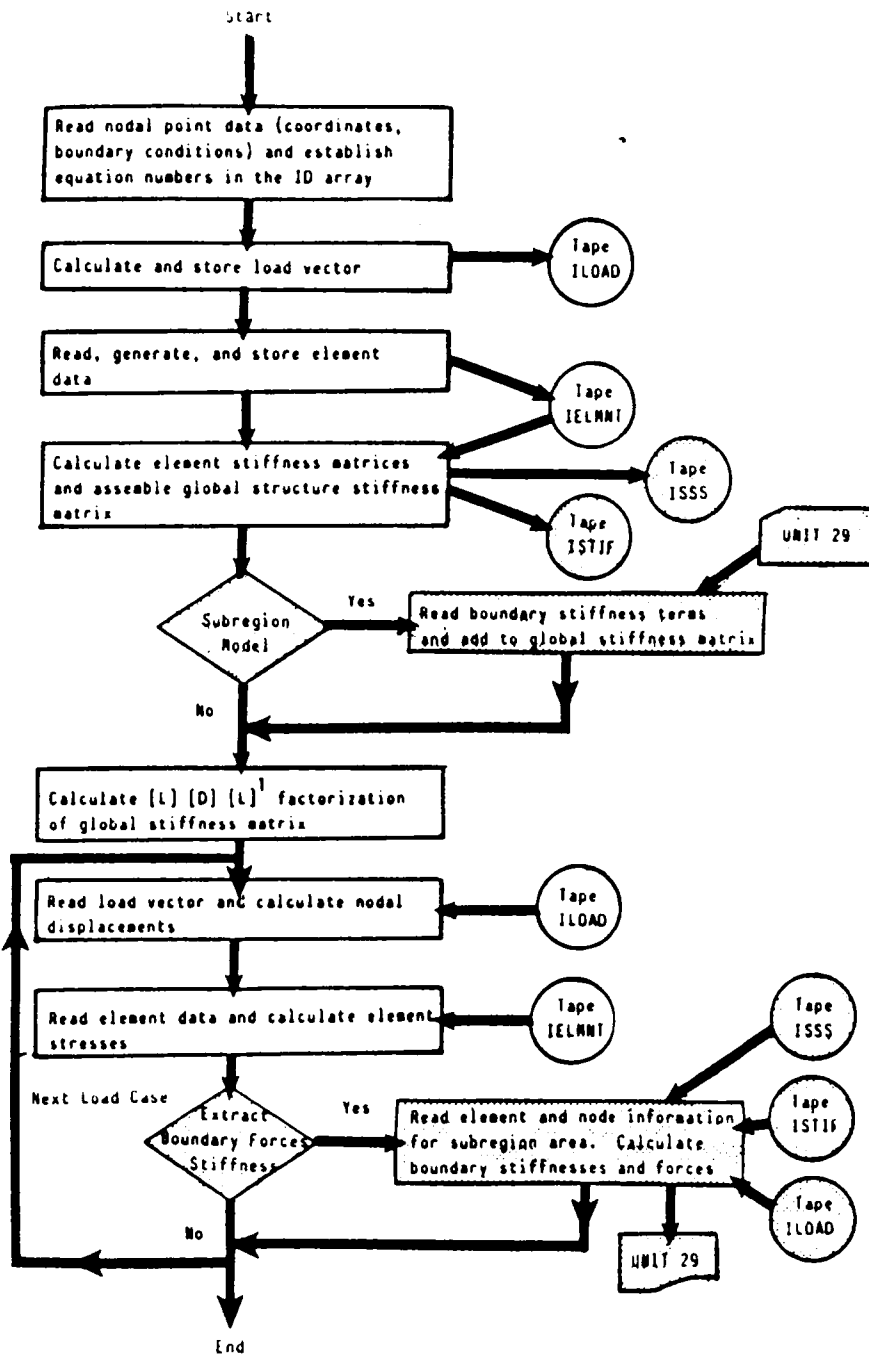


Figure 8. Flow Chart for MESS/SBSF Program

- (2) query the user for the number of original elements in the subregion area of the current model and their element numbers,
- (3) subtract the stiffnesses due to the original elements in the subregion area of the parent model from the global stiffness matrix and zero out the entries in the LM array associated with these elements,
- (4) query the user for the number of nodes on the subregion boundary and their node numbers,
- (5) extract the equation numbers associated with the nodes on the boundary and put them in numerical order,
- (6) retrieve the load vector from tape, and
- (7) extract the equation numbers for the nodes in the structure outside of the subregion and its boundary and put them in numerical order.

Task 1 reads the file ISTIF which was written during the analysis of the model and stores the global stiffness data and the LM connectivity array. The LM array is necessary to find which nodal dof are associated with the elements in the subregion area of the parent model. The global stiffness matrix contains all the stiffness terms for the parent model, including those needed to find the boundary stiffnesses and forces.

Tasks 2 and 3 both have to do with the reduction of the stiffness matrix. The stiffnesses due to the elements in the subregion area of the parent model must be eliminated from the global stiffness matrix prior to the extraction of the boundary stiffness terms. The algorithm used to remove the subregion area stiffness contributions is shown in Figure 9. This code is a portion of subroutine SETUP, the full listing of which is given in Appendix A. File ISSS which was written during the assembly of the global stiffness matrix from the individual element stiffness matrices, contains the element number, the address in the A array of each stiffness term from that element, and the value of that stiffness term. This section of the program first asks the user for

```

C THE USER IS QUERIED FOR THE NUMBER OF ELEMENTS IN THE SUBREGION AREA AND
C THEN INPUTS WHAT THOSE ELEMENTS ARE
C
C ONCE ALL THE ELEMENT NUMBERS ARE READ IN, EACH ENTRY ON TAPE ISSS IS READ
C AND THE ELEMENT NUMBERS IN THE SUBREGION AREA COMPARED WITH THE ELEMENT
C NUMBER FROM ISSS. IF CORRESPONDANCE IS FOUND, THE ASSOCIATED STIFFNESS
C TERM FROM ISSS IS SUBTRACTED FROM THE GLOBAL STIFFNESS MATRIX
C
C AFTER THE STIFFNESS MATRIX IS REDUCED, THE ENTRIES IN THE LM ARRAY FOR THE
C ELEMENTS IN THE SUBREGION AREA ARE ZEROED OUT
C
C   VARIABLES:   NOEL-----NUMBER OF ELEMENTS IN THE SUBREGION AREA
C                IELM(I)--ARRAY OF THE ELEMENT NUMBERS IN THE SUBREGION
C                  AREA
C                II-----ELEMENT NUMBER FROM TAPE ISSS
C                KK-----ADDRESS IN GLOBAL STIFFNESS MATRIX OF STIFFNESS
C                  TERM FROM TAPE ISSS
C                STIF-----ELEMENTAL DOF CONTRIBUTION TO GLOBAL STIFFNESS
C                  MATRIX
C                S(I)-----INITIALLY, GLOBAL STIFFNESS MATRIX; FINALLY,
C                  REDUCED STIFFNESS MATRIX
C                LM(I,J)--ARRAY RELATING ELEMENT DOF TO EQUATION NUMBER
C
C
C   WRITE (OUTPUT,500)
C   READ (IINPUT,*)NOEL
C   DO 15 I=1,NOEL
C     WRITE (OUTPUT,510)
C     READ (IINPUT,*) IELM(I)
15  CONTINUE
C   REWIND (ISSS)
17  READ (ISSS,*,END=25) II,KK,STIF
C   DO 20 I=1,NOEL
C     IF (II.EQ.IELM(I)) S(KK)=S(KK)-STIF
20  CONTINUE
C   GOTO 17
25  DO 27 I=1,NOEL
C     DO 26 J=1,8
C       LM(J,IELM(I))=0
26  CONTINUE
27  CONTINUE

```

Figure 9. FORTRAN Code used to find the Reduced Stiffness Matrix in MESS/SBSF

the number of elements which are in the subregion area of the parent model. In the DO 15 loop the user is asked to enter the element number for each of the elements in the subregion area. These element number are stored in the array IELM. After the file ISSS is rewound, the first line of that file is read at statement 17. The data read from ISSS is the element number (II), the address in the global stiffness matrix (KK), and the stiffness value (STIF) corresponding to the II and KK. In the DO 20 loop, the value of II is checked with each entry in IELM to see if it is one of the elements in the subregion area. If it is, then the stiffness term STIF is subtracted from the global stiffness term at the KK address in the S array. At the conclusion of this DO loop, execution returns to statement 17 and the next line from the disk file ISSS is read. When all of the entries in ISSS have been processed, the execution proceeds to statement 25. There, in the DO 27 loop the LM entries for each of the elements stored in IELM are zeroed out. Thus, at the end of this DO loop, the stiffness matrix stored in the array S will contain only the stiffnesses of the elements outside of the subregion area. Likewise, the LM array will only have nonzero values for those degrees of freedom which are either on the subregion boundary or outside of the subregion area.

Task 4 asks the user for the node numbers which lie on the interface ab between the subregion area and the remainder of the structure. The node numbers on the interface ab may be entered in any order. Then in task 5 the ID array is used to extract the equation numbers associated with these node numbers. The equation numbers are sorted and stored in numerical order in the array NOD. The variable IJ is a counter and will equal the total number of dof on the interface ab. These equation numbers are also the row and column numbers in the stiffness matrix for the stiffness terms associated with these

degrees of freedom. These row and column numbers will be utilized in the extraction of the boundary stiffness submatrix  $[K_{ab}]$  and the stiffness submatrix  $[K_{ab,a}]$  used to calculate the boundary forces.

In task 6, the load vector is read from the file ILOAD, which was part of the original MESS program, and stored in the R array. The load vector will be used in the calculation of the boundary forces.

The last major task in SETUP, task 7, is to create an array NODA which contains all of the equation numbers associated with the nodes outside of the subregion area and its boundary. These equation numbers will be the column numbers needed to extract the  $[K_{ab,a}]$  stiffness submatrix needed to calculate the boundary forces. The section of the program which carries out this task, shown in Figure 10, utilizes the LM array to identify those elements which lie outside of the subregion area. Previously, in task 3, the entries in the LM array associated with the elements in the subregion area were zeroed out. In the DO 50 loop in Figure 10 the values in the LM array are examined for non-zero entries. If a non-zero value is found, then that value is checked to see if it corresponds to a dof on the subregion boundary. This is done in the DO 47 loop by comparing the value from the LM array against the values stored in the NOD array. If a correspondence is found, the execution continues in the DO 50 loop with the next entry in the LM array. However, if no correspondence is found, then the non-zero value from the LM array must be a dof outside of the subregion area, in region a. As a dof can be stored several different times in the LM array, the value from the LM array must be checked to make sure it has not already been stored in the NODA array. This is done in the DO 48 loop. Here, IK is a counter and is equal to the number of values currently stored in the NODA array. If the value has not already been stored, IK is incremented

```

C THIS SETS UP THE NODA ARRAY OF THE EQUATION NUMBERS ASSOCIATED WITH
C THE NODES IN REGION A. THESE EQUATION NUMBERS ARE NOT NECESSARILY
C IN NUMERICAL ORDER. IK WILL BE THE COUNTER FOR THE NUMBER OF
C EQUATIONS IN REGION A
C
C SINCE THE LM ENTRIES ASSOCIATED WITH THE ELEMENTS IN THE SUBREGION
C AREA HAVE BEEN ZEROED OUT, THE DOF OF FREEDOM FOR THE ELEMENTS IN THE
C AREA OUTSIDE THE SUBREGION WILL BE THE NON-ZERO ENTRIES IN THE LM
C ARRAY. THESE DOF CAN THEN BE COMPARED WITH THOSE IN THE NOD ARRAY
C TO ELIMINATE THE DOF ON THE INTERFACE. THE REMAINING DOF WILL BE
C THOSE ASSOCIATED WITH THE NODES IN THE AREA OUTSIDE OF THE SUBREGION
C AREA
C
      IK=0
C      WRITE(OUTPUT,5500) ((LM(I,J),I=1,8),J=1,NUME)
      DO 51 I=1,NUME
        DO 50 J=1,8
          IF (LM(J,I).EQ.0) GOTO 50
          DO 47 K=1,IJ
            IF (LM(J,I).EQ.NOD(K)) GOTO 50
          47 CONTINUE
          C      WRITE(OUTPUT,5200) LM(J,I)
          IF (IK.LT.1) GOTO 49
          DO 48 K=1,IK
            IF (LM(J,I).EQ.NODA(K)) GOTO 50
          48 CONTINUE
          49 IKK=IK+1
            NODA(IK)=LM(J,I)
          C      WRITE(OUTPUT,5600)IK
          C      WRITE(OUTPUT,5700)NODA(IK)
          50 CONTINUE
          51 CONTINUE
C      WRITE(OUTPUT,5200) IK

```

Figure 10. FORTRAN Code used to Create the NODA Array in MESS/SBSF



by one and the value stored in the NODA array. If it has been stored, then the program execution continues back at the DO 50 loop with the next entry in the LM array. Once the entire LM array has been examined, the NODA array will contain all of the dof in region a and IK will be the number of entries stored in NODA.

Thus, after the completion of tasks 1 thorough 7 in subroutine SETUP, the global stiffness matrix contains only the stiffness terms due to the elements outside of the subregion area. Also, the set of equation numbers for both interface ab and region a have been isolated. These equation numbers will be the row and column numbers used to locate the boundary stiffness submatrix  $[K_{ab}]$  and the stiffness submatrix  $[K_{ab,a}]$  needed to calculate the boundary forces. In addition, the external load vector R has been retrieved from disk file to be used in finding the boundary forces.

At this point in the program, subroutine EXTRACT is called. This subroutine will do the actual extraction of the boundary stiffness terms and calculation of the boundary force terms. The major tasks in this subroutine are:

- (1) calculation of the boundary force terms,
- (2) extraction of the fraction of the  $[K_{ab}]$  stiffness terms due to the model outside of region b, and
- (3) writing the boundary stiffnesses and forces to the output file.

Task 1, the calculation of the boundary force terms,  $\{F_i\}$ , uses the equation:

$$\{F_i\} = \{F_{ab}\} - [K_{ab,a}] \{D_a\} \quad (17)$$

Here,  $\{F_{ab}\}$  are the existing external loads on the nodes on the subregion boundary,  $[K_{ab,a}]$  is the stiffness submatrix relating the dof on the

interface ab to the dof in region a, and  $\{D_a\}$  is the displacement vector for the nodes in region a. The code used to find these terms and to do the calculations is shown in Figure 11. The full listing of subroutine EXTRACT is in Appendix A. The stiffness terms are found by using the NOD array terms for the row numbers and the NODA array terms for the column numbers. Thus, the DO 500 loop will loop over the rows with indices 1 to IJ, the total number of entries in the NOD array. Likewise, the DO 250 loop will be used to find the column numbers and the indices are from 1 to IK, the total number of entries in the NODA array. First, a row number will be established using the indices on the DO 500 loop. Then, for this row number, in the DO 250 loop the stiffness term for each column number will be extracted.

The extraction of the stiffness terms uses the algorithm presented in equation 15. Referring to Figure 11, II will be the row number and NN will be the column number. These values will be compared to make sure that NN is greater than II. If it is not greater, then the values will be interchanged. Then, at statement 225 the difference between the column and the row number, DEL, will be computed. The sum of this term and the address of the diagonal element of the NN column number is the desired address KK. The stiffness term is then the value in the stiffness matrix, S, at the location KK, unless KK is greater than or equal to the address of the diagonal element of the next column (MAXA(NN+1)). In this case, the desired stiffness term will be zero. This is a result of the skyline storage method used for the stiffness matrix as explained in conjunction with Figure 7. The extracted stiffness term is then multiplied by the displacement from the parent model solution associated term with that column number dof. As each product is computed, it will be summed with all previous products for the row number. After all of the

```

C THE BOUNDARY FORCES ARE FOUND BY MULTIPLYING EACH ROW OF THE Kab-a MATRIX
C BY THE DISPLACEMENT VECTOR FOR THE DOF IN REGION A. THE PRODUCT IS THEN
C SUBTRACTED FROM ANY EXTERNAL FORCES ON THE ASSOCIATED NODE ON THE
C INTERFACE.
C
C THE NUMBER OF ROWS IN Kab,a IS IJ, THE NUMBER OF DOF ON THE SUBREGION
C INTERFACE. THE NUMBER OF COLUMNS IS IK, THE NUMBER OF DOF IN REGION A OF
C THE STRUCTURE.
C
C TO LOCATE THE STIFFNESS TERMS, THE DIFFERENCE BETWEEN THE COLUMN AND THE
C ROW NUMBER IS ADDED TO THE ADDRESS OF THE DIAGONAL ENTRY ASSOCIATED WITH
C THE COLUMN NUMBER. IF THIS VALUE IS GREATER THAN OR EQUAL TO THE DIAGONAL
C ADDRESS FOR THE NEXT COLUMN, THE STIFFNESS TERM IS ZERO. OTHERWISE, THE
C STIFFNESS TERM IS THE ENTRY IN THE S ARRAY AT THE CALCULATED ADDRESS.
C
      DO 500 I=1,IJ
          NEWT=0.00
          DO 250 N=1,IK
              II=NOD(I)
              NN=NODA(N)
              IF (NN.GE.II) GOTO 225
                  II=NN
                  NN=NOD(I)
225          DEL=NN-II
              KK=DEL+MAXA(NN)
              TERM=S(KK)
              IF (KK.GE.MAXA(NN+1)) TERM=0.00
              NEWT=NEWT+TERM*DISP(NODA(N))
250          CONTINUE
          F(NOD(I))=R(NOD(I))-NEWT
500      CONTINUE

```

Figure 11. FORTRAN Code used to Calculate the Boundary Forces in MESS/SBSF

multiplications for each row are completed, the cumulative sum of all the operations is subtracted from any external loads associated with that row number. The result will be the boundary force for the row number dof.

Task 2, the extraction of the boundary stiffness terms, uses the code shown in Figure 12. This section of the program uses the equation numbers in the NOD array as the row and column numbers and extracts the stiffness terms associated with them. The indices on the outer loop, the DO 2000 loop, are used to specify the row number and range from one to IJ, the total number of entries in the NOD array. The inner loop, the DO 1500 loop, will be used to find the column number. As the numbers in the NOD array are stored in numerical order, the indices on the inner loop range from the current row number to the last column number. This will insure that the column number is always greater than the row number and there will be no need to check this in the code. The actual boundary stiffness terms are extracted from the reduced stiffness matrix the same way as described for Figure 11.

Finally, in task 3, the boundary stiffnesses and forces are written out to the unit 29 file for the user to use in the analysis of the subregion. In the output file the terms are all referenced to the equation numbers of the current model. Thus, as can be seen from the output file listing shown in Figure 13, the stiffness terms are listed first with row and column designations which correspond to the equation numbers in the parent model. The force terms follow the stiffness terms and are also referenced to a specific equation number from the parent model. These equation numbers are those for the nodes on the interface between the subregion and the rest of the model.

After the parent model analysis has been completed and the boundary

```

C THIS LOOP LOCATES THE Kab TERMS IN THE REDUCED STIFFNESS MATRIX
C
C THE Kab MATRIX IS SIZE IJ X IJ. THE TERMS ARE FOUND BY ADDING THE
C DIFFERENCE BETWEEN THE COLUMN AND ROW NUMBER TO THE ENTRY IN THE MAXA
C ARRAY FOR THE COLUMN. THIS SUM IS THEN COMPARED TO THE VALUE IN MAXA FOR
C THE NEXT COLUMN. IF IT IS GREATER THAN OR EQUAL TO THIS VALUE, THE
C STIFFNESS TERM IS ZERO. OTHERWISE, THE STIFFNESS TERM IS THE ENTRY IN THE
C S ARRAY AT THE CALCULATED ADDRESS.
C
C AS EACH TERM IN Kab IS FOUND, IT IS WRITTEN OUT TO THE UNIT 29 FILE ALONG
C WITH ITS ROW AND COLUMN DESIGNATION ASSOCIATED WITH THE CURRENT MODEL
C
      DO 2000 I=1,IJ
        DO 1500 J=I,IJ
          II=NOD(I)
          JJ=NOD(J)
          DEL=JJ-II
          KK=MAXA(JJ)+DEL
          TERM=S(KK)
          IF (KK.GE.MAXA(JJ+1)) TERM=0.DO
          IF (TERM.NE.0.DO) WRITE(29,6000) II,JJ,TERM
1500      CONTINUE
2000      CONTINUE

```

Figure 12. FORTRAN Code used to Extract the Boundary Stiffnesses  $[K_{ab}]$  in MESS/SBSF

```
STIFF( 9, 9)= 15195907.5355578265
STIFF( 9, 10)= 2082978.0914680619
STIFF( 9, 11)= 1201908.1243653211
STIFF( 10, 10)= 29542080.6805931479
STIFF( 10, 11)= -6298236.2773453863
STIFF( 10, 12)= -9828355.7486562259
STIFF( 10, 13)= 4215703.5766237774
STIFF( 11, 11)= 35268027.9329920821
STIFF( 11, 12)= 5232303.5766237776
STIFF( 11, 13)= -3672896.9486710122
STIFF( 12, 12)= 57908248.0882868953
STIFF( 12, 13)= -20041214.2143346174
STIFF( 12, 14)= -3672896.9486710129
STIFF( 12, 15)= 4215703.5766237776
STIFF( 13, 13)= 57908248.0882868953
STIFF( 13, 14)= 5232303.5766237776
STIFF( 13, 15)= -9828355.7486562268
STIFF( 14, 14)= 35268027.9329920821
STIFF( 14, 15)= -6298236.2773453863
STIFF( 14, 16)= 1201908.1243653211
STIFF( 15, 15)= 29542080.6805931479
STIFF( 15, 16)= 2082978.0914680619
STIFF( 16, 16)= 15195907.5355578265
FORCE( 9)= -348.3961854054
FORCE( 10)= 367.2494569363
FORCE( 11)= -660.6359076939
FORCE( 12)= 4257.5498353703
FORCE( 13)= -1912.4292785143
FORCE( 14)= 3537.8615226697
FORCE( 15)= -156.8066657571
FORCE( 16)= 1799.4683161585
```

Figure 13. Example of an Output Boundary Stiffness and Force File from MESS/SBSF

stiffness and force terms have been extracted for the specified subregion area, the user must create the subregion model to be used in the second mode of operation. The geometrical boundaries of the subregion model must be the same as the boundaries of the subregion area defined during the parent model analysis. The nodes that were on the interface ab in the parent model must be in the same locations in the subregion model. In addition, in the subregion model, no new nodes may be introduced on the interface ab. However, on all the other edges and in the interior of the subregion model as many new nodes as desired may be added.

Once the geometry of the subregion model is defined, the boundary stiffness and force data from the whole structure analysis must be adapted to the particular subregion model. The boundary forces are applied as external loads to the subregion model and the values are entered into the input file to MESS/SBSF. The boundary stiffness data must be referenced to the equation numbers of the subregion model instead of to the equation numbers of the parent model. In general, the equation numbers for the nodes on the cut boundary of the subregion model will not be the same as the equation numbers on the interface ab in the parent model. The subregion model will have a different number of nodes and a different numbering pattern than was used in the subregion area of the parent model. The user must develop the correlation between the equation number from the parent model and the equation number in the subregion model. This is most easily accomplished by creating the subregion model and running a geometry check on it with MESS/SBSF. Part of the output from the geometry check will be a listing of the equation numbers associated with each node number. The user can then create a table listing the interface node number in the parent model,

associated equation number in the parent model, corresponding cut boundary node number in the subregion model, and corresponding equation number in the subregion model. A boundary stiffness file ready for use in a subregion analysis will resemble that shown in Figure 14. The addresses of the stiffness terms in the file shown in Figure 14 are those for a specific subregion model. The stiffness terms, though, are the same as those in the file shown in Figure 13. Once a subregion area of a parent model has been defined and the boundary stiffness terms extracted, those terms can be used for different subregion models provided that the addresses are those for the specific subregion model. Either commas or spaces can be used as delimiters in this file as the data is free format.

During the subregion analysis, the boundary stiffness file will be interpreted by the subroutine IMPLEMENT. The algorithm for this routine is shown in Figure 15 and a complete listing of the subroutine is in Appendix A. Its function is to insert the boundary stiffness terms into the global stiffness matrix of the subregion model. It is called from the plane stress element routine after the global stiffness matrix has been assembled. Referring to Figure 15, at statement 10, the row equation number, the column equation number, and the stiffness value are read from disk file unit 29, the boundary stiffness file. As explained earlier, the equation numbers must correspond to the subregion model. In the statements between 10 and 15 in Figure 15, the row and column number are checked to make sure the column number is greater than the row number. Then, at statement 15, DEL, the difference between the column and row number is calculated. This value is then added to the address from the MAXA array for the diagonal element corresponding to the specified column number. The sum, KK, is the address in the global stiffness



```
61, 61, 15195907.5355578265
61, 62, 2082978.0914680619
61, 63, 1201908.1243653211
62, 62, 29542080.6805931479
62, 63, -6298236.2773453863
62, 64, -9828355.7486562259
62, 65, 4215703.5766237774
63, 63, 35268027.9329920821
63, 64, 5232303.5766237776
63, 65, -3672896.9486710122
64, 64, 57908248.0882868953
64, 65, -20041214.2143346174
64, 66, -3672896.9486710129
64, 67, 4215703.5766237776
65, 65, 57908248.0882868953
65, 66, 5232303.5766237776
65, 67, -9828355.7486562268
66, 66, 35268027.9329920821
66, 67, -6298236.2773453863
66, 68, 1201908.1243653211
67, 67, 29542080.6805931479
67, 68, 2082978.0914680618
68, 68, 15195907.5355578265
```

Figure 14. Example of a Boundary Stiffness File Modified for use in MESS/SBSF

```
C THIS SUBROUTINE READS IN THE ROW AND COLUMN NUMBER AND BOUNDARY STIFFNESS
C TERM FROM THE UNIT 29 FILE. IT THEN USES THE ROW AND COLUMN NUMBER AND
C THE MAXA ARRAY TO FIND THE CORRECT ADDRESS IN THE A ARRAY FOR THE
C STIFFNESS TERM. ONCE THE ADDRESS IS FOUND, THE BOUNDARY STIFFNESS TERM
C IS ADDED TO THE EXISTING TERMS IN THAT LOCATION
C
10 READ(29,*,END=30) I,J,S
C
    II=I
    JJ=J
    IF (I.LE.J) GOTO 15
    JJ=I
    II=J
15 DEL=JJ-II
    KK=MAXA(JJ)+DEL
    A(KK)=A(KK)+S
    GOTO 10
30 CONTINUE
```

Figure 15. FORTRAN Code used to Insert the Boundary Stiffnesses into the Global Stiffness Matrix

matrix for the boundary stiffness term. The boundary stiffness term from the unit 29 file is then added to the value already stored at the specified address. This procedure is repeated for each line of data in the unit 29 file. After all of the boundary stiffness file has been, execution returns to the plane stress element routine and the solution proceeds in the usual manner.

Thus, in summary, the MESS/SBSF program operates in two modes. The general analysis path is:

A. Mode 1 Operation

- (1) create the parent model,
- (2) analyze the parent model,
- (3) define the subregion area after the parent model analysis is complete,

B. Mode 2 Operation

- (1) create the subregion model,
- (2) run a geometry check and use the equation number listing to develop a correlation between equation numbers in the parent model and those in the subregion model,
- (3) modify the addresses of the boundary stiffness terms to the corresponding equation numbers for the subregion model,
- (4) apply the boundary forces as external loads to the subregion model, and,
- (5) analyze the subregion model incorporating the boundary stiffnesses into the global stiffness matrix.

As noted previously, it is possible to return to mode 1 at the end of the second mode analysis if a subregion of a subregion is to be defined.

It should be noted that the definition of the subregion area takes place after the results from the parent model are available. Thus, the size of the subregion area can be based upon the spacing of the stress contours or the

stress values, for example. This is an advantage over the substructuring or linear constraint approaches, both of which require the creation of the subregion model without access to the results of the whole structure analysis.

As mentioned above, the complete listing of each of the new subroutines in the MESS/SBSF program can be found in Appendix A. A user's guide and a complete listing of the MESS/SBSF program can be found in [14].

## NUMERICAL EXAMPLES AND ADDITIONAL STUDIES

In this section four numerical examples will be used to compare the specified boundary stiffness/force method to the direct approach, the specified boundary displacement method, and the zooming methods. For the comparisons of the SBSF method to both the direct approach and the SBD method, MESS/SBSF was used to analyze two parent models and seven subregion models. These models were very similar to those analyzed by Kelley [2]. For the direct analysis, whole structure models were developed where the elements in the subregion area of the parent model were replaced by the separate subregion models. The comparison of the results of the SBSF analyses with those of the direct analyses is used to evaluate the sensitivity of the SBSF method to the approximations introduced in the calculation of the boundary forces.

The results of these SBSF analyses were also compared to the results of the SBD analysis of similar models presented by Kelley [2]. Another comparison between the SBSF and SBD methods was done by analyzing a problem using both MESS/SBSF and SUPERB [15]. Because SUPERB allows for non-zero displacement boundary conditions it is possible to use it for an SBD analysis. These comparisons between the SBD and SBSF methods are important because both of these methods have some inherent error due to the approximations made in the boundary conditions on the subregion model. Comparing these two methods will allow an assessment of the relative accuracy of each method and the sensitivity of each method to the displacement field from the parent model.

The SBSF method was compared to the zooming methods by duplicating the meshes from Hirai's work [9,10] and analyzing them with MESS/SBSF. The results from the SBSF analysis were compared to the published results for the efficient and exact zooming methods. The comparisons of the zooming

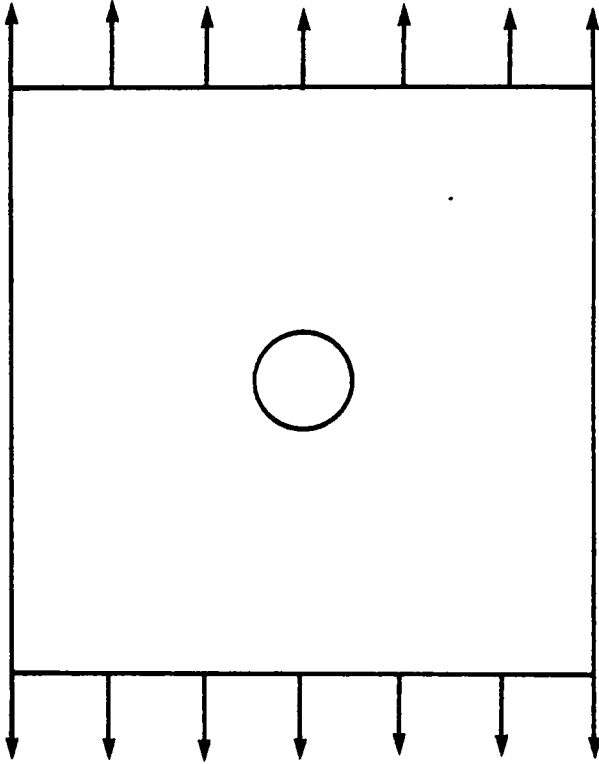


Figure 16. General Plate with Central Hole Problem for Examples 1 through 4

Table 1  
Example Data

	Example 1	Example 2	Example 3	Example 4
Plate Size (L x W x T)	1016 x 1016 x 25.4 (mm)	152.4 x 152.4 x 12.7 (mm)	400 x 200 x 1 (mm)	40 x 20 x 1 (mm)
Hole Diameter	50.8 mm	25.4 mm	50 mm	4 mm
Total Load	170,316 N	111,205 N	1961 N	196.1 N
$\sigma^*$ $\sigma_{\max}$	19.66 Mpa	177.4 Mpa	31.77 Mpa	30.79 Mpa
$K_t^*$	2.852	2.573	2.430	2.512

---

\* From Roark and Young [7]

methods, which are exact methods, with the SBSF method, an approximate method, will be another means of evaluating the error introduced into the subregion analysis by the inaccuracies in the boundary forces.

For all of the examples presented, the problem considered is that of a flat plate in tension with a center hole. The general geometry is shown in Figure 16 and the specifications; i.e. plate size, hole size, total load,  $\sigma_{\max}$ , and  $K_t$ , for each example, are tabulated in Table 1. The theoretical values of  $\sigma_{\max}$  and  $K_t$  were obtained from Roark and Young [7].

Finally, the results of two additional studies involving the SBSF method will be presented. The first of these is the result of an analysis of a design change in the subregion model. Specifically, this will involve the analysis of plate with a central hole where the hole size is different in the subregion model than it is in the parent model. This problem will be analyzed with the SBSF method and the results compared to the theoretical results for the modified geometry.

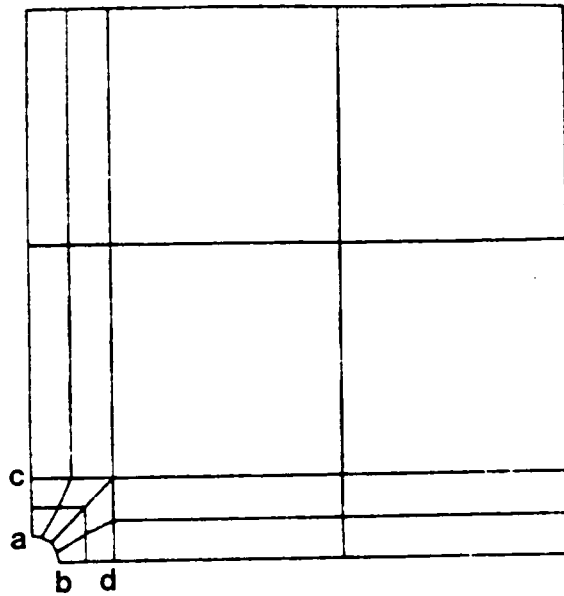
The second study is a comparison of the computational requirements of each of the methods of subregion analysis. By using approximations to the number of multiplications and divisions required to upper triangularize, back substitute, and invert a matrix, the approximate number of computations required for a solution using each method can be calculated. These numbers will be compared to determine which method requires the least number of operations and would be the most economical to use. The methods considered are the direct analysis, the linear constraint method, the SBD method, the SBSF method, the exact zooming method, and the efficient zooming method. Of course, the final choice of a method is based upon a combination of the computational efficiency and the relative accuracy.



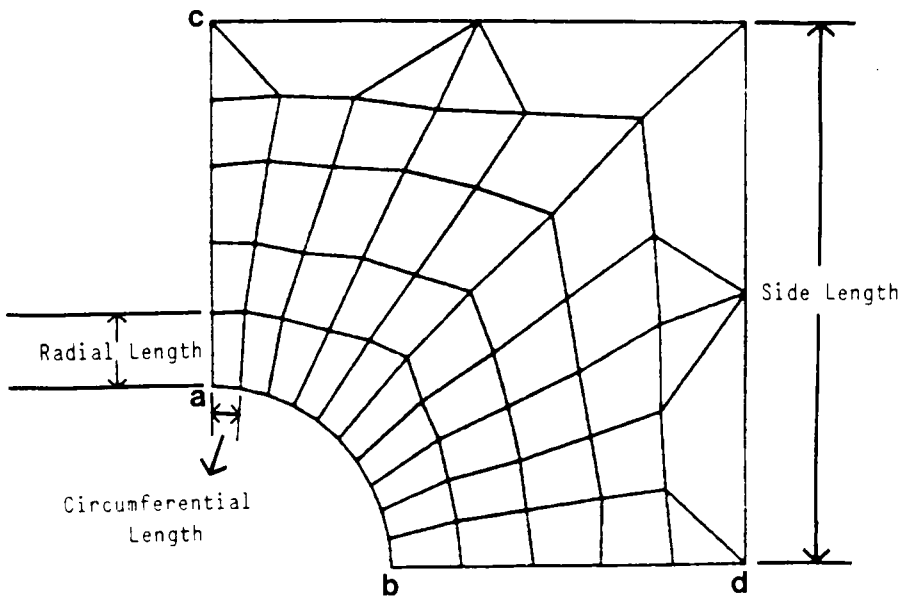
### A. Example 1

This example is the analysis of a square plate, 101.6 mm by 101.6 mm by 25.4 mm thick, loaded in tension with a 50.8 mm diameter central hole. In this example, the results of SBSF analyses of this problem will be compared to both direct analyses and analyses using the SBD method. Because of symmetry, only a quarter section of the plate was modeled. For this example two parent models and seven subregion models were developed. The first parent model and the subregion meshes are duplicates of those analyzed by Kelley [2]. Figure 17a illustrates the parent model A $\emptyset$ . The other parent model, B $\emptyset$ , is similar to this model except that the elements around the edge of the hole have a smaller radial length. The parent models, duplicated from [2], have several modeling flaws. The transition from the small elements around the hole to the larger elements in the rest of the model is too abrupt and could cause inaccuracies in the solution. Also, the ratio of the side lengths of several of the elements is bad. Ideally, a quadrilateral isoparametric finite element should be as close as possible to a square. In other words, the ratio of adjacent sides of a four-noded element should be close to one. Several of the elements in the parent model used in [2] have side length ratios of five. These long, thin elements will introduce some error into the solution. Despite these flaws, this model was used so that the results presented in [2] from the SBD method could be compared to the results of the SBSF method.

The subregion mesh A1, shown in Figure 17b, illustrates the general relationship between a parent model and a subregion model. The parameters side length, radial size, and circumferential size are tabulated in Table 2 for each of the models used in this example. The various subregion models



a. Whole Structure Model A0



b. Subregion Model A1

Figure 17. Meshes A0 and A1 from Example 1

Table 2  
Mesh Characteristics for Example 1

Mesh	Side Length	Radial Divisions	Element Size Radially*	Circumferential Divisions	Element Size Circumferentially*	Aspect Ratio**
A $\emptyset$ <sup>†</sup>	---	---	1.00	4	0.393	2.545
A1	3.0	5	0.40	10	0.157	2.548
A2	3.0	4	0.50	6	0.262	1.908
A3	3.0	5	0.40	4	0.393	1.017
A4	3.0	5	0.40	6	0.262	1.527
A5	3.0	5	0.40	8	0.196	2.041
A6	2.0	3	0.33	10	0.157	2.121
B $\emptyset$ <sup>†</sup>	---	---	0.50	4	0.393	1.272
B1	1.5	2	0.25	10	0.157	1.592

\* Element sizes refer to the smallest dimensions of the elements at the edge of the hole.

\*\* Ratio of radial size to circumferential size.

† Parent Models; side length and radial divisions not applicable.

differ in both the overall size of the subregion as well as the number and size of the elements within the subregion. As indicated in Table 2, the first five subregions which are designated A1 through A5 come from parent model A $\emptyset$ . These all have a side length of 3.0 and encompass two rows of elements around the hole in the parent model. The sixth subregion model, A6 also comes from the parent model A $\emptyset$  but it has a side length of 2.0 and only covers one row of elements around the hole in the parent model. The last subregion model, B1, is taken from the second parent model, B $\emptyset$ . It too encompasses one row of elements around the hole in the subregion model but its side length is 1.5. The parent model B $\emptyset$  and all of the subregion models are shown in Appendix B.

These subregion meshes were analyzed using the SBSF method with the boundary stiffnesses and forces coming from the appropriate parent model. A direct analysis was also done for each subregion model. The models used for the direct analyses were whole structure models with the same degree of refinement in the subregion area as the subregion models. For example, the mesh shown in Figure 18 is that used for the direct analysis of the subregion model A1 shown in Figure 17b. This mesh is essentially the mesh of Figure 17b inserted into the whole structure model in Figure 17a. Whole structure models of this type were developed for all of the subregion models and are illustrated in Appendix C.

The results of a comparison between the SBSF method and the direct finite element method are presented in Table 3. For each method, the stress concentration factor,  $K_t$ , based upon both the maximum element stress and the maximum nodal stress from each model is tabulated. Also included is the percent difference between these values for each method. The theoretical value of  $K_t$  is not included because this comparison is intended only to be an

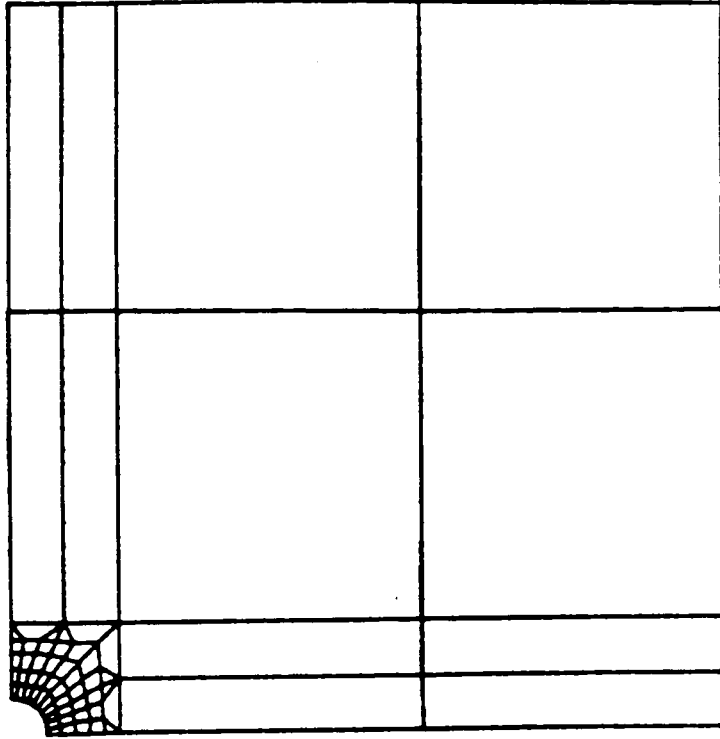


Figure 18. Mesh C1 for Direct Finite Element Analysis of Subregion Model A1

Table 3

Comparison of the SBSF and Direct Methods  
using the  
Stress Concentration Factor,  $K_t$ , from Example 1

Mesh	SBSF Max. Element Stress $K_t$	Direct Max. Element Stress $K_t$	%diff	SBSF Max. Nodal <sup>+</sup> Stress $K_t$	Direct Max. Nodal <sup>+</sup> Stress $K_t$	%diff
A0**	1.520	-----	-----	2.130	-----	-----
A1	1.986	1.993	-0.35	2.650	2.661	-0.41
A2	1.849	1.854	-0.27	2.542	2.550	-0.31
A3	1.917	1.923	-0.31	2.613	2.620	-0.27
A4	1.939	1.945	-0.31	2.639	2.648	-0.34
A5	2.011	2.019	-0.40	2.668	2.679	-0.41
A6	2.016	2.046	-1.5	2.648	2.688	-1.5
B0**	1.731	-----	-----	2.400	-----	-----
B1	2.110	2.133	-1.1	2.695	2.726	-1.1

-----

\* Located at element centroid

+ Theoretical Value = 2.852

\*\* Parent Models

evaluation of the sensitivity of the SBSF method to inaccuracies in the boundary forces.

As can be seen from Table 3, the SBSF method and the direct finite element analysis give similar results for all of the models. The low percent differences between the two methods indicates that the boundary forces are relatively insensitive to inaccuracies in the displacements used to calculate them. As shown in the theoretical development of the SBSF method, the boundary forces are calculated as  $\{F_{ab}\} = [K_{ab,a}] \{D_a\}$ , where the  $\{D_a\}$  terms come from the displacement solution of the parent model. The values of these displacement terms are dependent upon the mesh used in the parent model and will vary as the parent model is changed. However, the low percent difference between the results of the two approaches indicates that the error in the boundary force terms does not greatly affect the results of the subregion analysis.

The subregion models which only covered one row of elements around the hole, A6 and B1, have the highest percent errors, 1.5% and 1.1% respectively. The displacements used to calculate the forces used in these subregion models are from the nodes in the parent model close to the edge of the hole. In this area, the displacement field is changing rapidly and is very dependent upon the arrangement of the nodes and elements. It would, therefore, be expected that the boundary forces for these models would be more inaccurate. As a result, these models would have greater differences between the SBSF and the direct methods than those subregion models which encompass a larger portion of the parent model.

The  $K_t$  values based upon the maximum nodal stress values from these analyses are plotted in Figure 19. In this figure the vertical axis is the

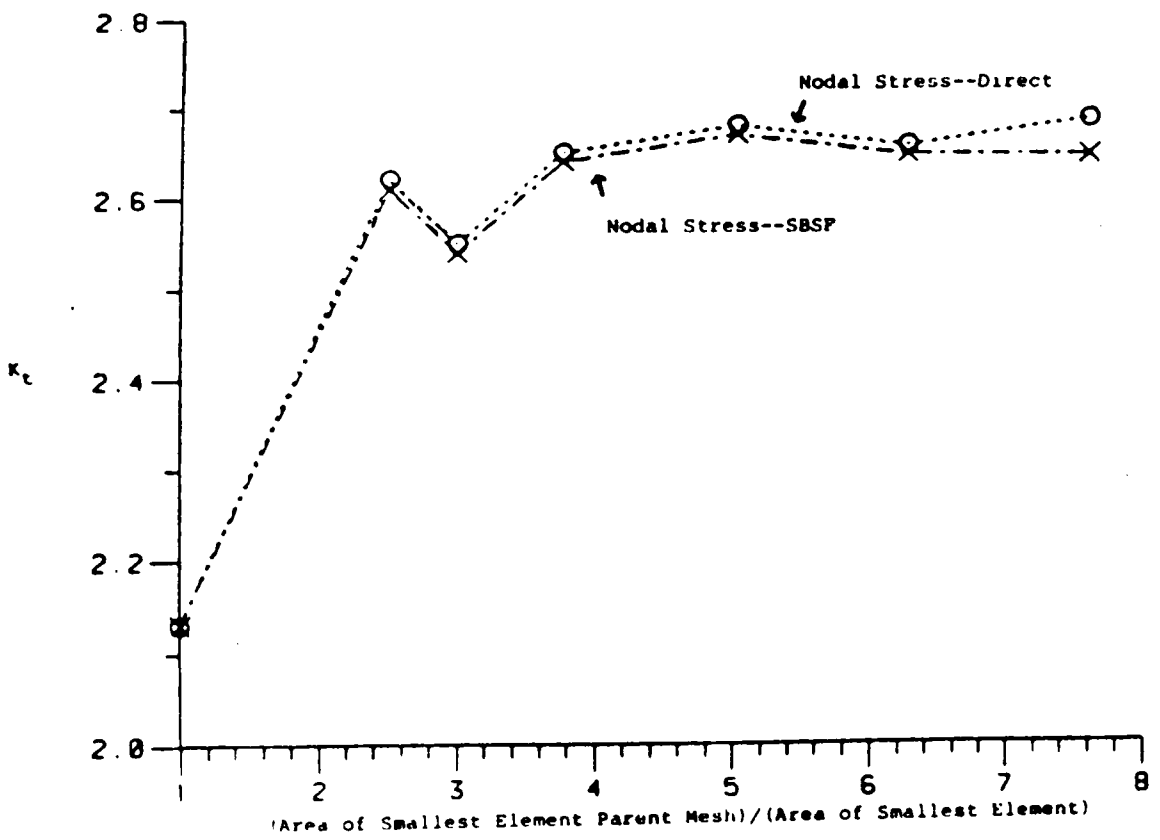


Figure 19. Comparison of the  $K_t$  values from Example 1 for the Direct and SBSF Methods



value of  $K_t$  and the horizontal axis is a measure of the refinement of each model. The values plotted on the horizontal axis are the area of the smallest element in mesh A divided by the area of the smallest element in the subregion or refined meshes. This figure shows that there is very little difference in the values of  $K_t$  from the SBSF approach and the direct analysis approach. Also, this plot shows that these values of  $K_t$  do not monotonically converge as the mesh is refined. Both the SBSF analyses and the direct approach analyses show this oscillation, indicating that this is not a result of the SBSF approach. The approach used to extrapolate the nodal stress values from the Gauss point stresses is a least squares fit as described by Hinton and Campbell [15]. In the derivation and explanation of this method, Hinton and Campbell suggest that the extrapolated values may be inaccurate if there is a steep stress gradient across the element. In the problem being considered in this comparison, the steep stress gradient across the corner element may be the cause of the oscillations in the  $K_t$  values plotted.

The results of the SBSF analyses were also compared to the results of Kelley's [2] analyses of the same meshes using the SBD approach. In Table 4 are listed the value of  $K_t$  calculated from the maximum nodal stress from MESS/SBSF, the percent error between these results and the theoretical value of  $K_t$ , and the percent error from [2] for the same models analyzed with ANSYS using the SBD method. The  $K_t$  values obtained with the SBD method are not included in Table 4 because these values were not presented in [2]. Also, Kelley does not give a theoretical value of  $K_t$  for the problem he analyzes. He simply states that it approaches three and references Seely [8]. For the geometry he presents, the value of  $K_t$  from Roark and Young [7] is 2.85. Because both the calculated and theoretical  $K_t$  values are omitted from the

Table 4

Comparison of SBSF and SBD Methods  
using the  
Stress Results of Example 1

	SBD $K_t^*$	SBD % Error <sup>**</sup>	SBSF $K_t^+$	SBSF % Error <sup>++</sup>
A0 <sup>+++</sup>		-22.8	2.129	-25.3
A1		- 4.6	2.650	- 7.1
A2		- 8.9	2.541	-10.9
A3		-11.4	2.612	- 8.5
A4		- 7.0	2.639	- 7.5
A5		- 5.4	2.668	- 6.4
A6		- 4.3	2.648	- 7.1
A7		-----	2.723	- 4.5
B0 <sup>+++</sup>		-----	2.399	-15.9
B1		- 1.6	2.695	- 5.4

-----  
\* No values given in [2]

\*\* From [2]; No theoretical value given

+ Based upon maximum nodal stress

++ Theoretical Value 2.852

+++ Parent Models

results presented in [2], comparing the percent error from the SBSF analyses to those from the SBD analyses may not be valid.

The percent errors from the SBSF analyses of the parent models AØ and BØ are 25.3% and 15.9%, respectively. As pointed out earlier, these parent models are poor models and can not be expected to give accurate results. The percent error for the subregion analyses range from 5.4% to 10.9% for the SBSF method and 1.6% to 11.4% for the SBD method. It must be taken into consideration though, that the analyses done with the SBD method were done with ANSYS, using the STIF42 element. This element uses a nine point Gauss integration to evaluate the stiffness matrix and the stresses [12]. There is no option to lower the integration order. The SBSF analyses were done using the plane stress element in MESS/SBSF which uses a four point Gauss integration. Thus, for the same meshes, the analyses using ANSYS will give more accurate stress results because of the higher number of Gauss points.

Also included in Table 4 are the results of the analysis of mesh A7. This mesh, illustrated in Figure 20, is not from [2]. It was developed to investigate the effect of further refinement upon the results of the SBSF analysis. This model is mesh A1 with the elements around the hole divided in half radially. The value of  $K_t$  based upon the nodal stress is 2.72, an error of -4.6% when compared to the theoretical value from [7]. This result indicates that the SBSF method is comparable in accuracy to the SBD analyses done with ANSYS if the mesh is sufficiently refined.

In summary, the results of this first example show that the SBSF method is relatively insensitive to errors in the boundary force terms. The maximum error between an SBSF analysis and a direct analysis, for the meshes considered, was 1.5%. The uncertainties associated with the results of the

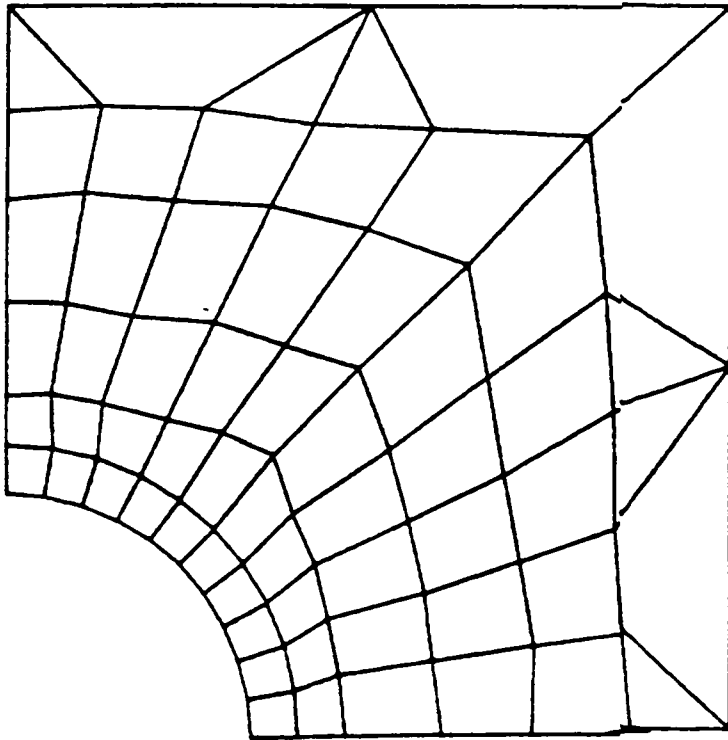


Figure 20. Mesh A7 from Example 1

SBD analyses presented in [2] along with the differences in the element formulations used, make it difficult to draw absolute conclusions about the relative accuracies of each method. A better comparison between the SBSF and SBD methods is presented in the next example.

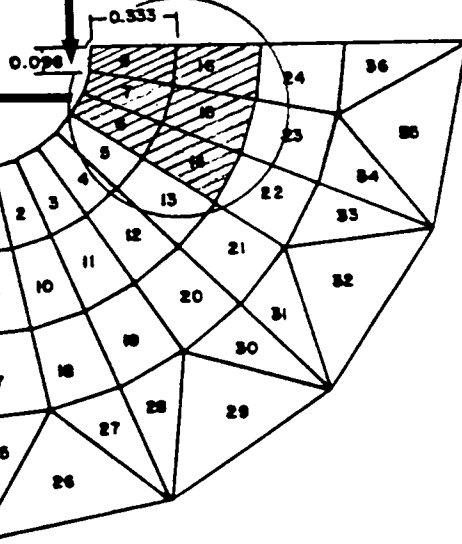
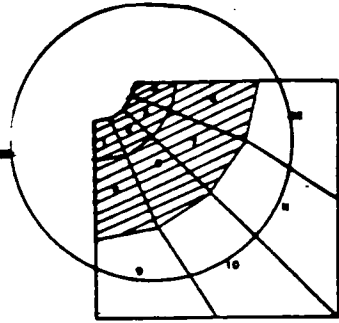
#### B. Example 2

The purpose of the second example is to compare the SBSF and SBD methods on a more fair basis than was possible in the first example. The plane stress element in SUPERB uses a four point Gauss integration as does the plane stress element in MESS/SBSF. SUPERB also allows non-zero displacement boundary conditions which enables it to be used for a SBD subregion analysis. In this example, the same models will be analyzed using the SBSF method with MESS/SBSF and the SBD method with SUPERB. The comparison of the results of these analyses will be a more valid measure of the relative accuracies of these methods than the comparison presented in Example 1.

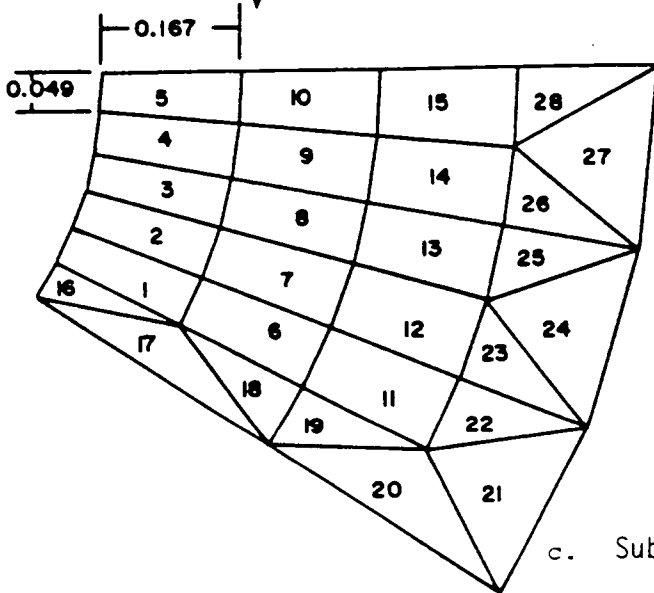
This example uses one parent model and four subregion models to find the maximum stress in a 152.4 by 152.4 by 12.7 millimeter plate with a 25.4 millimeter diameter circular hole loaded in tension. The first analysis sequence, meshes A --A1--A2, is shown in Figure 21. The meshes for the second analysis sequence, A --B1--B2 are illustrated in Figure 22. The primary difference in the analysis sequences is that subregion model A1 encompasses two rows of elements from the parent model A while subregion model B1 only covers one row of elements.

These meshes were analyzed using both the SBSF method as implemented in MESS and the SBD method, using the SUPERB finite element code. The stress concentration factor,  $K_t$ , calculated from the maximum nodal stress values for the each subregion model is tabulated in Table 5 for both approaches. Also

a. Whole Structure Model A $\emptyset$



b. Subregion Model A1



c. Subregion Model A2

Figure 21. Analysis Sequence 1 (A $\emptyset$ -A1-A2) from Example 2

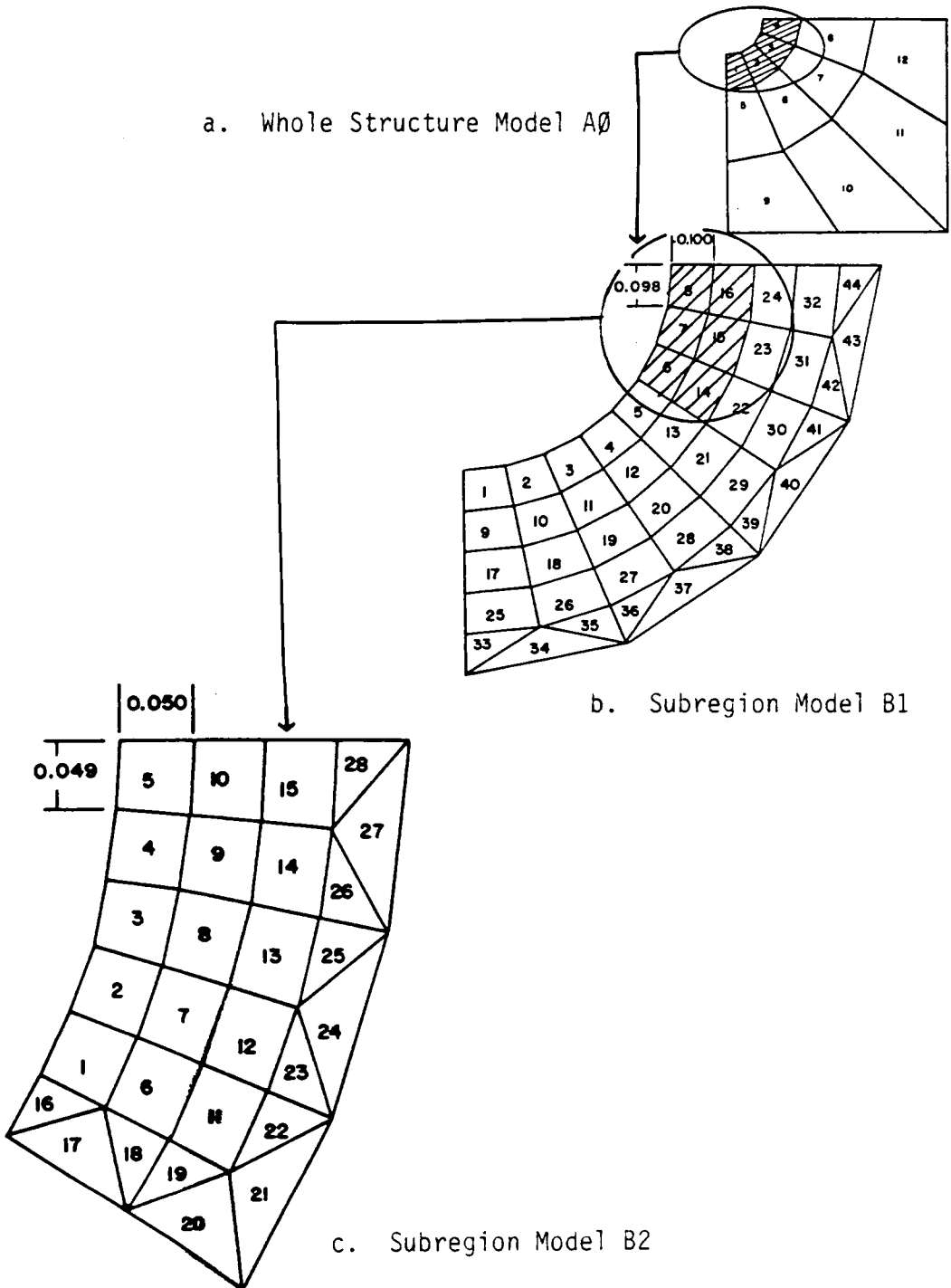


Figure 22. Analysis Sequence 2 (A $\emptyset$ -B1-B2) from Example 2

Table 5

Comparison of the SBSF and the SBD Methods  
using the  
Stress Results of Example 2

Mesh	SBSF		SBD	
	Max. Nodal Stress $K_t$	% Error	Max. Nodal Stress $K_t$	% Error
A1	2.34	- 9.2	2.32	- 9.7
A2	2.57	- 0.3	2.52	- 1.9
B1	2.52	- 2.0	2.75	+ 7.0
B2	2.57	- 0.3	2.76	+ 7.4

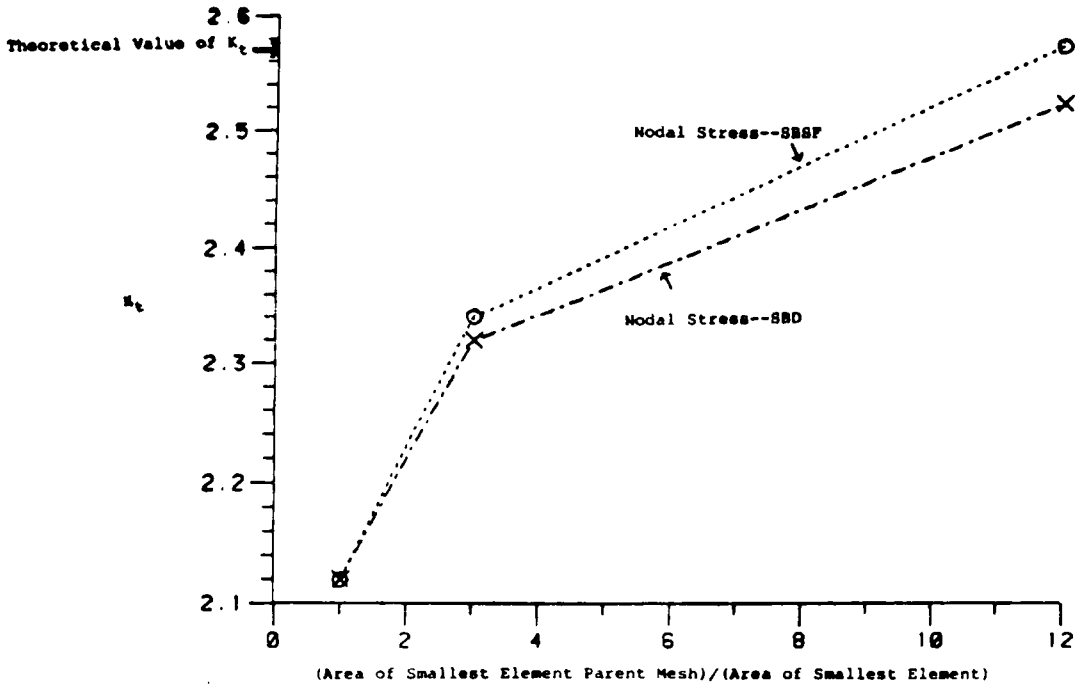
-----  
\* Theoretical Value = 2.57



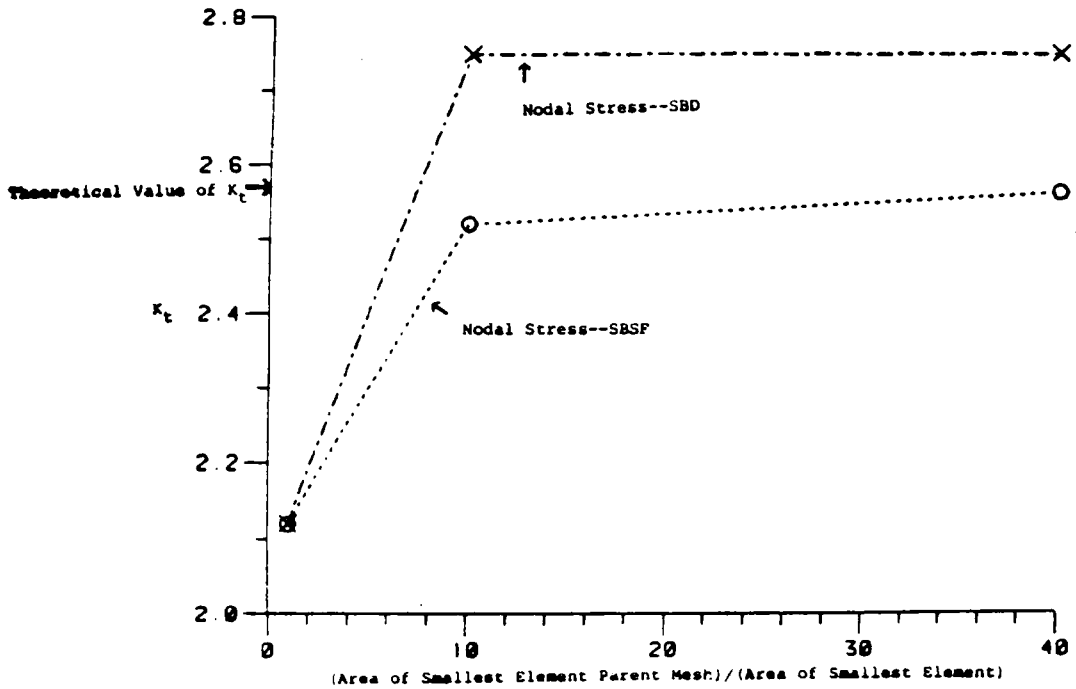
included are the percent errors between these calculated values and the theoretical value of 2.57. As can be seen from these results, the SBSF method monotonically converges upon the theoretical value of maximum stress for both analysis sequences. The results of the SBD analysis are more inaccurate and one sequence converges upon the theoretical value from below, while the other sequence overestimates the maximum stress and diverges slightly. The results for the sequence which converges, the A1 and A2 subregion models, show that both the SBSF and the SBD methods converged to the theoretical value of the maximum stress. This was expected as the boundary of these subregion models is far enough away from the hole that the displacement field should be fairly stable. The SBSF method was able to predict the maximum stress level in the structure more accurately than the SBD method. The percent error for mesh A2 was -0.31% for the SBSF method and -1.9% for the SBD method.

The results of the other sequence came from the analysis of the subregion models B1 and B2. These models are from an area in the parent model in which the displacement field is changing rapidly. As expected, this causes problems for the SBD analysis, demonstrated by the fact that these analyses overestimate the maximum stress in the structure. The SBSF method, which is relatively insensitive to a rapidly changing displacement field, was able to give good results for the second sequence. The smallest percent errors in this sequence were -0.27% for the SBSF method and +7.4% for the SBD method.

Figures 23a and 23b show the results of the SBSF analyses of these meshes in graphical form. In these figures the vertical axis is the value of  $K_t$ . The theoretical value of  $K_t$  for this example is 2.57 as indicated on the plots. The horizontal axis is a measure of the refinement of the model. Figure 23a shows the results of the first analysis sequence for both the SBSF and the SBD



a. Sequence 1 (A0-A1-A2)



b. Sequence 2 (A0-B1-B2)

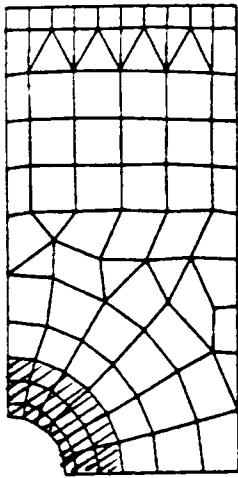
Figure 23. Comparison of the  $K_t$  values from Example 2 for the SBD and SBSF Methods

method while Figure 23b illustrates the results of the second analysis sequence for both methods. These plots clearly illustrate that the SBSF method is more accurate than the SBD method.

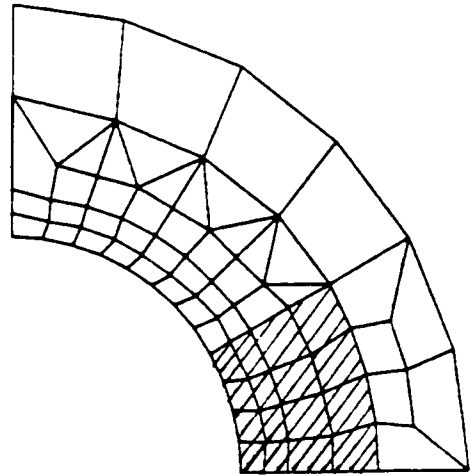
In summary, this example shows that when the SBSF and SBD methods are compared using elements with a similar formulation and the same number of Gauss integration points, the SBSF method is more accurate than the SBD method. For subregions which extend far enough away from the edge of the hole, both methods give good results. However, if the boundary of the subregion model is in an area of the parent model where the displacement field is changing rapidly, the SBSF method gives better results.

### C. Example 3

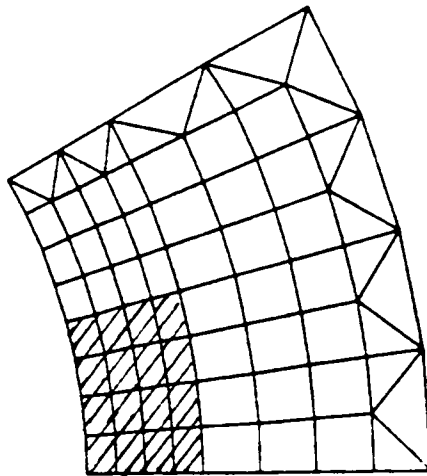
The purpose of the third example is to compare the SBSF method, which is an approximate method, to the efficient zooming method, an exact method. This example replicated Hirai's numerical example [9]. The problem is a 400 by 200 by 1 millimeter flat plate with a 50 millimeter diameter central hole loaded in tension. One parent model and six subregion models were developed for this problem. Four different analysis sequences were used. In these sequences, each model after the parent model is a subregion of the previous model. Using the mesh designations from [9], the first sequence is A $\emptyset$ -A1-A2-A3-A4. These meshes, as used with MESS/SBSF, are shown in Figure 24. The meshes for the other analyses sequences, (A $\emptyset$ -C1-A2-A3-A4, A $\emptyset$ -D1-A2-A3-A4, and A $\emptyset$ -D1-A2-H3) are in Appendix D. The details of all of the meshes are tabulated in Table 6. The meshes shown in Figure 24 are not all to the same scale so it is difficult to see the differences in element size from mesh A $\emptyset$  to mesh A4. However, from the information in Table 6, it can be seen that the area of the smallest element in mesh A $\emptyset$  is two hundred fifty six time the



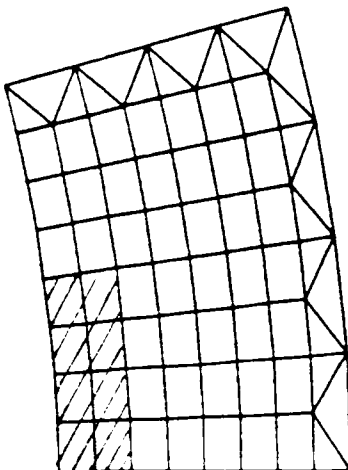
a. Whole Structure  
Model A0



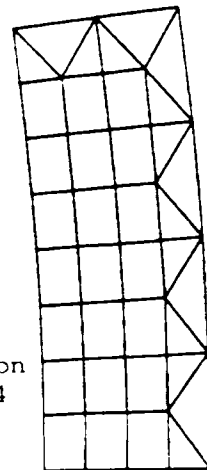
b. Subregion Model A1



c. Subregion Model A2



d. Subregion  
Model A3



e. Subregion  
Model A4

Figure 24. Analysis Sequence 1 (A0-A1-A2-A3-A4) from Example 3  
(Shaded regions indicate area encompassed by subsequent subregion model)

Table 6

## Mesh Characteristics for Example 3

Mesh	Side Length	Element Size Radially*	Element Size Circumferentially*	Aspect** Ratio
AØ <sup>+</sup>	-----	5.000	6.545	0.764
A1	25.00	2.500	3.273	0.764
A2	15.00	1.250	1.636	0.764
A3	5.00	0.625	0.818	0.764
A4	1.25	0.313	0.409	0.764
C1	25.00	2.500	3.273	0.764
D1	40.00	2.500	3.273	0.764
H3	7.50	0.750	0.818	0.917

---

\* Element sizes refer to the smallest dimension of the elements at the edge of the hole.

\*\* Ratio of radial size to circumferential size.

+ Parent Model

area of the smallest element in mesh A4. This means that the element side lengths of the smallest element in mesh A4 are one-sixteenth of the element side lengths of the smallest element in mesh AØ. It can also be seen from Table 6 that, with the exception of mesh H3, the corner elements all have the same aspect ratio.

The major difference between the meshes shown in Figure 24 and those in [9] is that Hirai used only triangular elements in his work. When the meshes from [9] were duplicated for use with MESS/SBSF, the triangular elements were combined to make quadrilaterals. The resulting meshes, as shown in Figure 24 and Appendix D, have the same number of nodal points as those in [9] but fewer number of elements.

The meshes in each analysis sequence were analyzed with MESS/SBSF. The results of these analyses are tabulated in Table 7. Included there are the calculated values of  $K_t$  from the SBSF analysis based upon both the maximum element center stress and the maximum extrapolated nodal stress, the percent error in these values, the values of  $K_t$  from [9] for the efficient zooming method analysis, and the percent error in the values from [9]. Except for subregion A4, the values of  $K_t$  for the efficient zooming method were taken from a plot in [9] and are approximate. The values of  $K_t$  for subregion A4 were the only tabulated values of  $K_t$  in [9]. It is not clear from [9] whether the values of  $K_t$  reported are from nodal stress values or element center stress values.

Figure 25 is a plot of the results of the first analysis sequence, AØ-A1-A2-A3-A4. As in Figure 19, the value of  $K_t$  is plotted on the vertical axis. The horizontal axis in Figure 25 is a measure of the refinement of the model. On this graph are plotted the calculated values of  $K_t$  based upon both the

Table 7

Comparison of the Efficient Zooming and the SBSF Methods  
using the  
Stress Results of Example 3

Mesh	SBSF Max. Elem. Str. $K_t$	% Error*	SBSF Max. Nodal Str. $K_t$	% Error*	Efficient Zooming** $K_t$	% Error*
AØ	1.89	-22.0	2.36	-2.9	2.18	-10.3
A1	2.12	-12.4	2.42	-0.4	2.33	- 4.1
A2	2.25	- 7.0	2.41	-0.8	2.37	- 2.5
A3	2.32	- 4.2	2.40	-1.2	2.38	- 2.1
A4	2.35	- 2.8	2.40	-1.2	2.39	- 1.6
AØ	1.89	-22.0	2.36	-2.9	2.18	-10.3
C1	2.11	-12.7	2.41	-0.8	2.33	- 4.1
A2	2.25	- 7.0	2.41	-0.8	2.37	- 2.5
A3	2.32	- 4.3	2.40	-1.2	2.39	- 1.6
A4	2.37	- 2.1	2.42	-0.4	2.38	- 2.1
AØ	1.89	-22.0	2.36	-2.9	2.18	-10.3
D1	2.13	-12.3	2.42	-0.4	2.35	- 3.3
A2	2.29	- 5.9	2.45	+0.8	2.40	- 1.2
A3	2.35	- 3.1	2.44	+0.4	2.41	- 0.8
A4	2.39	- 1.7	2.43	0.0	2.41	- 0.8
AØ	1.89	-22.0	2.36	-2.9	2.18	-10.3
D1	2.13	-12.3	2.42	-0.4	2.35	- 3.3
A2	2.29	- 5.9	2.45	+0.8	2.40	- 1.2
H3	2.31	- 4.8	2.41	-0.8	2.42	- 0.4

\* Theoretical Value = 2.43

\*\* From [9]

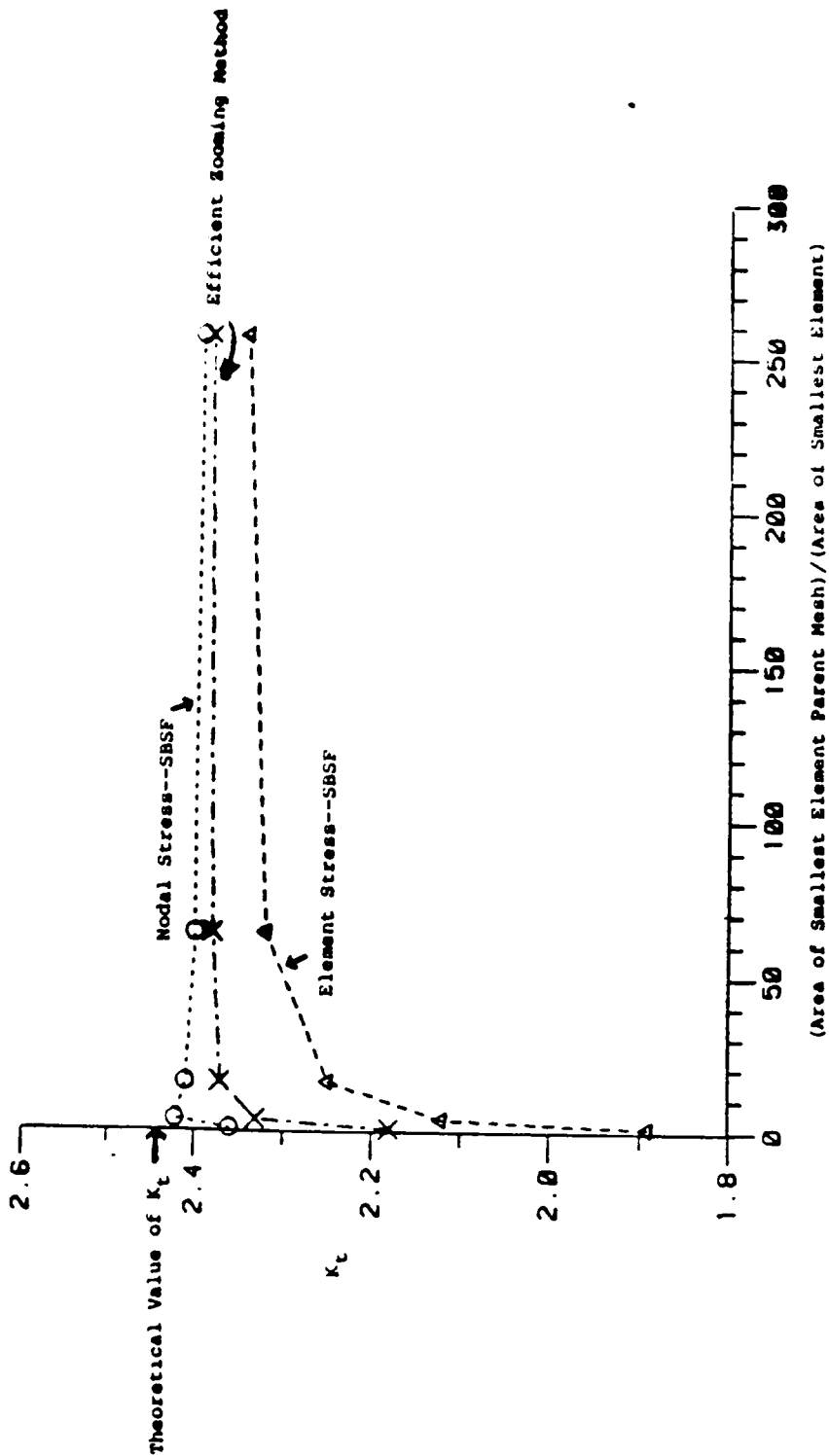


Figure 25. Comparison of the  $K_t$  values from Example 3 for the Efficient Zooming and SBSF Methods



element center stress and the maximum nodal stress along with the values of  $K_t$  reported by Hirai [9] for the efficient zooming method. It can be seen from this figure that for the SBSF results, the element values monotonically converge while the nodal values show some oscillation. As explained in conjunction with Figure 19, this is probably due to the extrapolation technique used.

Since the nodal stress and element center stress values of  $K_t$  from the SBSF analyses bracket the values reported by Hirai [9] for the efficient zooming method, it appears that the two methods give comparable results. No details are given in [9] about the type of element used, the integration order, or which stress values are used to compute  $K_t$ . The efficient zooming method should be more accurate than the SBSF because it is an exact method, in the sense that all stiffness terms are retained and no approximations are made. It has already been shown that the SBSF method is relatively insensitive to errors in the boundary forces and gives results only slightly different than those obtained from a direct analysis. As the efficient zooming method is really a computationally more efficient manner of carrying out a direct analysis, it seems reasonable that, if the element formulations were the same, the SBSF method should be only slightly less accurate than the efficient zooming method.

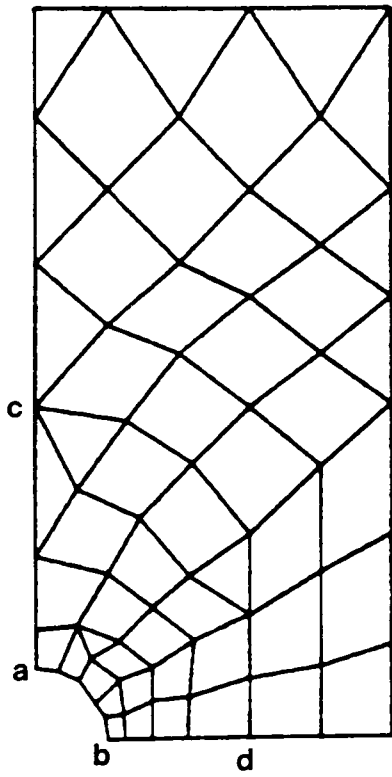
#### C. Example 4

The fourth example is a duplication of an example using the exact zooming method from Hirai [10]. The problem is a 40 by 20 by 1 millimeter plate with a 4 millimeter diameter central hole with a tensile load as shown in Figure 16. The purpose of this example is to compare the SBSF method with the exact zooming method. For this comparison a parent model and a subregion

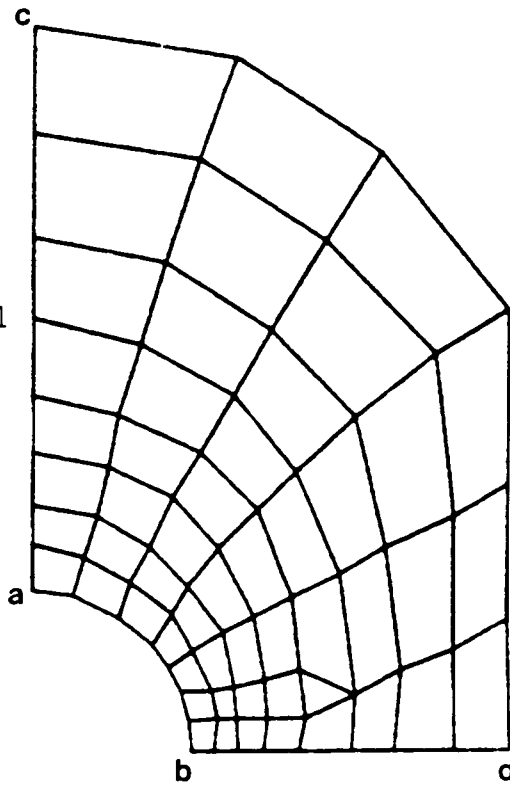
model, meshes A0 and A1 respectively, were duplicated from [10]. The meshes used for the SBSF analyses are shown in Figure 26. As was the case in example 3, the primary difference between these meshes and those used for the exact zooming analysis in [10] is that Hirai used only triangular elements in his work. One additional subregion model, designated mesh A2 and shown in Figure 27, was also developed for this example. In mesh A2 the corner element from mesh A1 is divided into three smaller elements. The side lengths of the smallest element in mesh A2 are one-fourth of the side lengths of the smallest element in A0. The purpose of this additional subregion model was to see what effect the additional refinement would have upon the accuracy of the results from the SBSF method. As this model has no corresponding model in Hirai's work [10], the results can not be compared to those from the exact zooming method.

The results of the SBSF analyses of the parent model and the subregion models are presented in Table 8, along with the results of the exact zooming analyses of the corresponding models from [10]. The results for the SBSF analyses include the calculated values of  $K_t$ , both from the element center stress values and the extrapolated nodal stress values, and the percent error in these values of  $K_t$ . For the exact zooming analyses, the values of  $K_t$  from [10] as well as the percent error in these values are listed. It is not clear from [10] whether these values of  $K_t$  are based upon nodal stress or element center stress.

Again, the values of  $K_t$  calculated from the nodal stress values for the SBSF analyses show some oscillation. As explained previously, it is felt that this oscillation is a result of the method used to extrapolate the Gauss point stresses to the nodal points and not of the SBSF method. Comparing the



a. Whole Structure Model  $A_0$



b. Subregion Model  $A_1$

Figure 26. Meshes from Example 4

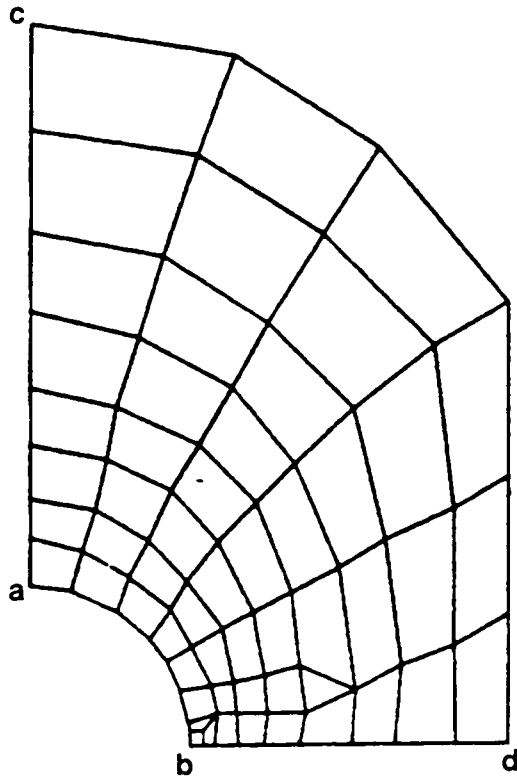


Figure 27. Subregion Model A2 from Example 4

Table 8

Comparison of the Exact Zooming and the SBSF Methods  
using the  
Stress Results of Example 4

Mesh	SBSF Max. Elem. Str. K <sub>t</sub>	% Error*	SBSF Max. Nodal Str. K <sub>t</sub>	% Error*	Exact Zooming K <sub>t</sub> **	% Error*
A0	1.90	-24.4	2.46	-2.1	2.41	- 4.1
A1	2.02	-19.6	2.42	-3.7	2.49	- 0.9
A2 <sup>†</sup>	2.25	-10.4	2.48	-1.3	-----	-----

\* -----  
Theoretical Value = 2.51

\*\* From [10]

† No comparable model in [10]

values from the SBSF analyses to those from the exact zooming analysis, it can be seen that the two methods give comparable results. As expected, the exact zooming method is, in general, more accurate. The lowest percent error for the exact zooming method is  $-0.9\%$  for the subregion model A1. The SBSF analysis of this subregion model had an error of  $-3.7\%$ . The lowest percent error for the SBSF method was  $-1.3\%$  for the subregion model A2. These differences in accuracy are small and are reasonable because the zooming method is an exact method. The SBSF method is an approximate method and, as shown in example 1, gives results which are slightly less accurate than a direct analysis. The additional refinement in the subregion model A2 decreased the error in the SBSF analysis by about half ( $-3.7\%$  to  $-1.3\%$ ).

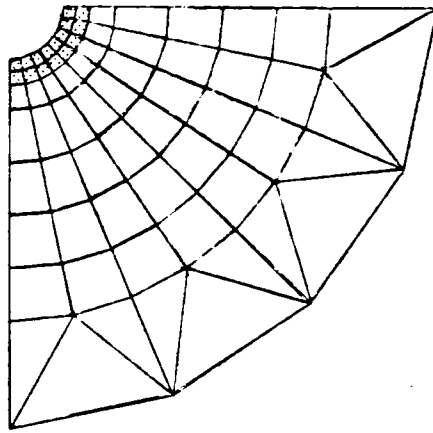
#### E. Additional Studies

##### 1. Subregion Redesign

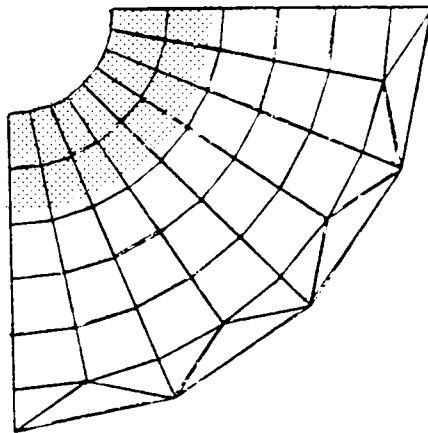
In this section the effect of geometry change in the subregion model will be studied. Many times, if an initial analysis indicates that the stresses are too high, it is desirable to evaluate design changes. For the other methods of subregion modeling (SBD, LC, and zooming methods), the best way of accurately assessing the effect of a design change is to go back to the parent model and incorporate the design change into that model. Then, that model would be analyzed, the necessary information for the subregion analysis extracted, the subregion model modified to incorporate the design change, and the subregion model analyzed. The use of the SBSF method allows this procedure to be streamlined because it is only necessary to modify and analyze the subregion model. The examples presented in this section illustrate the application of the SBSF method to the analysis of a design modification in the subregion model.

The two subregion areas, A1 and B1, from example 2 were used in this study. In the first case, the diameter of the hole in those subregion models was changed from 25.4 millimeters to 12.7 units. Several subregion meshes were developed with the smaller hole geometry. The most refined of these meshes for each of the subregion areas are shown in Figure 28. The shaded region in these meshes is the added area from the reduction in the hole diameter. The theoretical value of  $K_t$  for the modified geometry is 2.76 [7]. All of the meshes developed were analyzed using MESS/SBSF with the boundary stiffnesses and forces obtained from the unmodified parent model for the subregion area. The values of  $K_t$  calculated from the nodal stress results of the most refined models are 2.71 and 2.72 for the subregions corresponding to the original meshes A1 and B1, respectively. The percent errors are -1.8% for mesh A1 and -1.4% for mesh B1. This seems to indicate that the SBSF method will give accurate results for the analysis of design changes which are only incorporated into the subregion model.

As further verification of this use of the SBSF method, the hole in the subregion A1 was changed to an elliptical hole. The major axis of the ellipse is 25.4 millimeters and the minor axis is 12.7 millimeters. The major axis of the ellipse is perpendicular to the applied load on the plate. For this geometry, the theoretical value of  $K_t$  from Roark and Young [7] is 4.24. A series of meshes were developed for this geometry and analyzed using MESS/SBSF. The most refined of these meshes is shown in Figure 29. For the mesh shown in Figure 29, the value of  $K_t$  based upon the maximum nodal stress, is 4.22. This result is 0.47% less than theoretical result of 4.24. This result again indicates that the SBSF method can be used for the analysis of geometry changes of the subregion model.



a. Subregion Area A1



b. Subregion Area B1

Figure 28. Subregion Areas from Example 2 with Reduced Hole Diameter



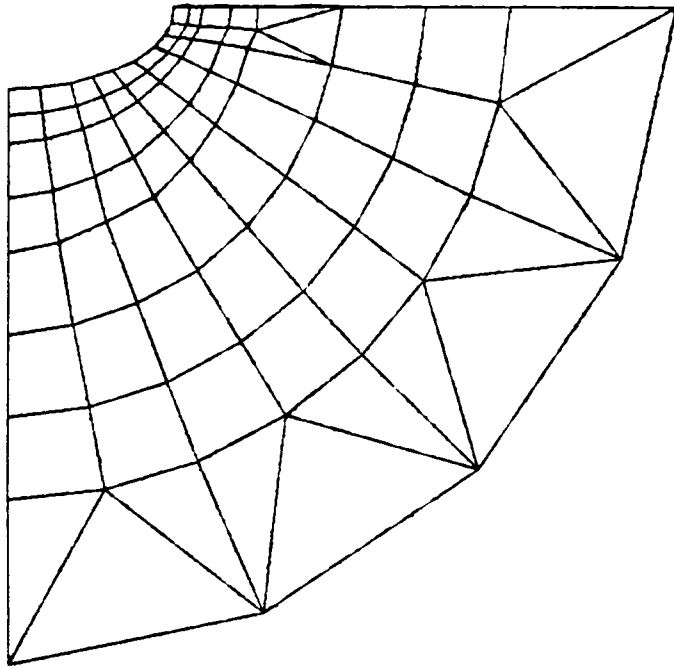


Figure 29. Subregion Area A1 from Example 2 with Elliptical Hole

## 2. Comparison of Computational Efficiency

Often times the choice of a method for subregion analysis is dictated not only by availability and accuracy but also by computational efficiency. A very accurate method which is computationally expensive may not always be the best choice for every problem. At times, a less accurate but cheaper and less time consuming method may be preferable. Thus, in addition to the comparisons based upon the results of the various methods, a comparison was also made of the computational effort required by each of the methods for subregion analysis. As there was not a code available which had all of these methods implemented, these comparisons are not based upon actual computational time but, rather, upon the approximate number of multiplications and divisions required for a solution by each method. Only the operations required to manipulate the stiffness matrix to find the complete displacement solution are considered.

The approximations to the number of operations required came from Riess [16] and Cook [17]. Riess [16] states that the number of operations required to upper triangularize a matrix of size  $n \times n$  is approximately  $n^3/3$  while the number of operations to back substitute is approximately  $n(n+1)/2$ . Cook [17] estimates that inverting a matrix requires three times as many operations as upper triangularizing it would. These estimates were used to calculate the approximate number of operations required for the solution of the first subregion model, A1, from example 2. The methods considered were the direct method or linear constraint method, the SBSF or SBD method, the exact zooming method, and the efficient zooming method. For this problem, the parent model has 8 dof outside the subregion area and 24 dof within the subregion area. In the subregion model, 48 additional dof were introduced.

For either the direct method or the linear constraint method, the stiffness matrix is of the order 80 by 80. Approximately 174,000 operations (multiplications or divisions) are required to find the displacement solution for this system using either of these approaches. For the SBD and SBSF methods, there are two systems of equations to be solved. From the parent model there are 32 equations and the subregion model has 72 equations. These methods would require a total of 138,500 operations to find the complete displacement solution.

The number of operations required to solve this problem using either of the zooming methods is more difficult to compute. For the efficient zooming method, to find the displacement solution for the original dof within the subregion area, two matrices (size 32 by 32 and 24 by 24) must be decomposed and a 48 by 48 matrix must be inverted. This portion of the analysis would require a total of 130,500 operations. To complete the displacement solution for the dof within the subregion, two matrices (size 48 by 48 and 48 by 24) and a vector 24 by 1 are all multiplied together. The number of operations needed to complete the displacement solution for this problem is 56,400. Thus, the total number of operations required to solve this problem using the efficient zooming method is 186,900.

The exact zooming method requires the inversion of three matrices and some additional matrix multiplications to solve this problem. The matrices to be inverted are of sizes 8 by 8, 24 by 24, and 72 by 72. Approximately 387,500 multiplications or divisions would be needed to carry out these inversions. The additional multiplications required to solve for the displacements would require approximately 7400 operations for a total of 394,900 multiplications or divisions.

For the problem being considered in this comparison, the number of multiplications and divisions required for a complete displacement solution from each method is:

Exact zooming method	394,900
Efficient zooming method	186,900
Direct method or linear constraint	173,900
SBD or SBSF methods	138,500

These results indicate that the SBD and SBSF methods are computationally the most efficient methods. The efficient zooming method requires a few more operations than the direct or linear constraint or the approximate methods. The exact zooming method requires more than twice as many multiplications and divisions than the direct method.

It must be noted that the approximations used in the preceding paragraphs assume that the matrices to be operated on are full matrices, that is, they are not banded or sparse matrices. If these conditions exist, fewer operations would be required to triangularize or invert the matrix. Bathe [11] estimates that upper triangularizing a banded matrix requires  $nm_k^2/2$  operations where  $n$  is the number of dof and  $m_k$  is the maximum half bandwidth. Likewise, he estimates that back substitution would require an additional  $2nm_k$  operations. For the direct analysis of the subregion model A1 from example 2, the model would have 80 dof and a half bandwidth of 20. Based upon the approximations from [11], 19,200 multiplications and divisions would be required to find the displacement solution for this model. For the SBD and SBSF methods the parent model would have 32 dof and a half bandwidth of 11. The subregion model, A1, has 72 dof and a half bandwidth of 19. Thus, for the SBD or SBSF methods, approximately 18,372 multiplications would be

required.

Comparing the number of operations required if the stiffness matrix is banded to the number required for a full matrix shows that the use of a banded matrix greatly reduces the number of operations. For the direct method, the banded stiffness matrix requires only 11% of the number of operations required for a full matrix. For the SBSF and SBD methods, the solution with banded matrices requires 13% of the number of operations for a full matrix. Even with banded matrices, the SBSF and the SBD methods are computationally more efficient than the direct approach.

It is difficult to make similar estimates for the zooming methods because of uncertainties about how the stiffness matrix bandwidth is affected by the matrix operations required by these methods. Also, because of the approach used in the zooming methods to partition the stiffness matrix and the displacement and load vectors, it would be difficult to construct a subregion model with a very narrow bandwidth. It can be assumed that the use of banded stiffness matrices in the zooming methods will have some effect upon the number of operations required for a displacement solution. However, because of the approach used to partition the problem and the many matrix operations required to reach a solution, it is unlikely that the reduction in the number of operations will be as great as that for the other methods considered. Thus, the SBD or SBSF methods will still require the fewest number of operations to reach a displacement solution.

## CONCLUSIONS

The results of the examples presented in the previous section show that the specified boundary stiffness/force method is a viable approach to finite element subregion analysis. It is an approximate method because the boundary force terms are dependent upon the displacements from the parent model analysis. However, the loss of accuracy due to this approximation is small. As shown in example 1, the maximum difference in the stress results between a subregion analysis and a direct analysis of a whole structure model incorporating the subregion model is 1.5%. This small percent difference shows that the inaccuracies in the displacement terms used to calculate the boundary forces do not have a large effect upon the accuracy of the results obtained.

As demonstrated by the results of example 2, the SBSF method is more accurate than the other approximate method, the SBD method. For the most refined meshes in example 2, the average error was -0.3% for the SBSF method and +2.75% for the SBD method. This example also indicates that the SBSF method is able to give much better results than the SBD method for the cases where the subregion boundary is close to a discontinuity and the displacement field is rapidly changing.

The results from the SBSF method are not as accurate as those obtained from analyses utilizing either of the zooming methods. This is not surprising though, as in these methods all of the stiffness terms are retained and no additional approximations are made. However, both of the zooming methods require more computational effort than the SBSF method. There is a greater potential for errors due to roundoff or numerical precision in the zooming methods simply because of the large number of mathematical operations

required.

The SBSF method is also computationally more efficient than the linear constraint method or the direct approach. The SBD and SBSF methods require approximately the same number of operations to solve for the displacements of the nodes in the subregion model.

The SBSF method can also be used to analyze the effect of design changes in the subregion model. As explained in the previous section, the geometry of a subregion model can be modified and the resulting mesh analyzed without having to reanalyze the parent model. This capability would be very useful in the preliminary evaluation of the effect of a design change to a subregion area. The examples which demonstrated this use of the SBSF method showed good convergence to the theoretically correct results for the modified geometry. For the case in which the diameter of a hole in the subregion model was reduced, the most refined mesh had an error of -1.4%. In the analysis where a circular hole was changed to an elliptical hole in the subregion model, the results from the most refined mesh were in error by -0.47%. These examples indicate that the SBSF method is an accurate approach to the analysis of design changes which are only incorporated into the subregion model.

In summary, the SBSF method is more accurate than the SBD method because it is less sensitive to inaccuracies in the displacement field from the parent model. Computationally, the two methods require approximately the same number of operations. The SBSF method is less accurate than the zooming methods or the direct approach but it is computationally more efficient than any of these methods. An advantage of the SBSF method over the linear constraint method or the direct approach is that the subregion area for the

SBSF method is defined after the results from the parent model are available. Also, changes in the subregion model do not require reanalysis of the entire structure as is the case for either the linear constraint or the direct approaches. The SBSF method can also be used to analyze design modifications in the subregion model without reanalyzing the parent model. Overall, when compared to the other methods, the SBSF method seems to be a better approach to the problem of subregion analysis. This new method is accurate, computationally efficient, easily implemented into existing finite element codes, and easily applied to a wide range of problems.



## RECOMMENDATIONS FOR FUTURE WORK

This dissertation presents the initial work done in the development and implementation of the specified boundary stiffness/force method for finite element subregion analysis. Additional work on the implementation and usage of this method remains to be done. Two areas that should be investigated are presented in the following paragraphs.

First, the task of adapting the output boundary stiffnesses and forces from the parent model to the input boundary terms for the subregion model needs to be made more "user-friendly". One potential way of accomplishing this would be to have the MESS/SBSF program retain the coordinates and equation numbers of the nodal points on the interface ab from the parent model. Then, when a subregion analysis is performed, the coordinates of all the nodal points in the subregion model could be compared to the stored coordinates from the parent model. As correspondences are found, a correlation table could be developed between the equation numbers for the nodal points on the interface ab in the parent model and those for the corresponding nodal points on the boundary of the subregion model. This correlation table could then be used to automatically determine the correct equation numbers for the boundary stiffnesses and forces from the parent model. This approach would not require the user to take any part in determining the correct addresses for the stiffness terms or in entering the nodal point loads for the subregion model.

Additional comparisons between this method and other methods for subregion analysis are also needed. These other methods include the zooming methods, the specified boundary displacement method, the linear constraint method, substructuring, and the direct analysis approach. The comparisons

between the SBSF method and these other approaches should examine both accuracy of results and computational requirements. These comparisons also need to be done on a more equal basis than those presented in this dissertation. Not only should the meshes used for each method be identical but also the same element formulation should be used for all of the analyses. It would also be beneficial to carry out these comparisons for models with many degrees of freedom, where the differences in the computational efficiencies of the various methods would be more evident.

## REFERENCES

1. Schwartz, D. J., "Practical Analysis of Stress Raisers in Solid Structures", Proceedings of the 4th International Conferences on Vehicle Structural Mechanics, Society of Automotive Engineers, Warrendale, PA, 15096, November 1981.
2. Somervaille, I. J., Kabaila, A. P., "Mesh Grading Techniques for Compatible and Equilibrium Elements", Finite Element Methods in Engineering, The University of New South Wales, 1974, pp. 257-269.
3. Carey, G. F., "A Mesh-Refinement Scheme for Finite Element Computations", Computer Methods in Applied Mechanics and Engineering, Vol. 7, 1976, pp. 93-105.
4. Kelley, F. S., "Mesh Requirements for the Analysis of a Stress Concentration by the Specified Boundary Displacement Method", Proceedings of the Second International Computer Engineering Conference, Computer Engineering Division, ASME, August 1982.
5. Kelley, F. S., "Simplified Finite Element Analysis of Stress Discontinuities in Shell Structures", ASME 84-PVP-86.
6. Peterson, R. E., Stress Concentration Factors, Wiley-International, New York, 1974.
7. Roark, R. J., and Young, W. C., Formulas for Stress and Strain, 5th edition, McGraw-Hill Co., 1975.
8. Seely, F. B., Advanced Mechanics of Materials, John Wiley and Sons, New York, 1960.
9. Hirai, I., Wang, B. P., and Pilkey, W. D., "An Efficient Zooming Method for Finite Element Analysis", International Journal of Numerical Methods in Engineering, Vol. 20, 1984, pp. 1671-1683.
10. Hirai, I., et.al., "An Exact Zooming Method", Finite Elements in Analysis and Design, Vol. 1, 1985, pp. 61-69.
11. Bathe, K., Finite Element Procedures in Engineering Analysis, Prentice-Hall, Englewood Cliffs, New Jersey, 1982.
12. ANSYS User's Manual, Swanson Analysis Systems, Inc., Houston, PA., Revision 4-1, March 1983.
13. Brigham Young University, MOVIE.BYU -- A General Purpose Computer Graphics System, Brigham Young University Computer Science Department, Provo, Utah, 1981.

14. Virginia Polytechnic Institute and State University, User's Guide and Program Listing for MESS/SBSF, Virginia Polytechnic Institute and State University, Mechanical Engineering Department, Blacksburg, Virginia, 1985.
15. Hinton, E., and Campbell, J. S., "Local and Global Smoothing of Discontinuous Finite Element Functions Using Least Squares Method", International Journal of Numerical Methods in Engineering, Vol. 8, 1979, pp. 461-480.
16. Riess, R. D., and Johnson, L. W., Numerical Analysis, Addison-Wesley Publishing Co., Reading, Massachusetts, 1982.
17. Cook, R. D., Concepts and Applications of Finite Element Analysis, John Wiley and Sons, New York, 1974.

APPENDIX A

```

C*****
C
C          SUBROUTINE SETUP
C
C PROGRAMMER: C. JARA-ALMONTE
C DATE:      July 1984
C LOCATION:  MECHANICAL ENGINEERING DEPARTMENT
C            V.P.I. AND STATE UNIVERSITY
C            BLACKSBURG, VIRGINIA 24060
C*****
C
C SUBROUTINE PURPOSE:
* THIS SUBROUTINE QUERIES THE USER FOR INFORMATION ABOUT THE PART OF
* THE WHOLE STRUCTURE MODEL THAT WILL BE MODELED AS A SUBREGION AND
* SETS UP THE ARRAYS CONTAINING THE EQUATION NUMBERS FOR THE REGIONS
* OF THE MODEL, FINDS THE REDUCED STIFFNESS MATRIX, AND READS IN THE
* LOAD VECTOR.
C*****
C
C
C*****
C SUBROUTINE CALLED BY:  MAIN
C
C
C
C SUBROUTINE CALLS:  EXTRACT
C
C
C*****
C
C SPECIAL NOTES: ONLY CALLED IF USER ANSWERS Y(es) WHEN ASKED IN
C                THE MAIN PROGRAM IF HE IS GOING TO DO SUBREGION
C                MODELING
C
C VARIABLES:      LM(I,J)--RELATES EQUATION NUMBER TO ELEMENTAL DOF
C                ID(I,J)--RELATES EQUATION NUMBER TO NODE POINT NUMBER
C                S(I)-----INITIALLY, THE GLOBAL STIFFNESS MATRIX BEFORE
C                TRIANGULARIZATION, FINALLY, THE REDUCED
C                STIFFNESS MATRIX
C                IJ-----NUMBER OF DOF ON INTERFACE AB
C                NOD(I)---ARRAY CONTAINING EQUATION NUMBERS OF NODES
C                ON INTERFACE AB
C                IK-----NUMBER OF DOF IN AREA OUTSIDE OF SUBREGION
C                NODA(I)--ARRAY CONTAINING EQUATION NUMBERS OF NODES
C                OUTSIDE SUBREGION AREA
C                IELM(I)--ARRAY CONTAINING ELEMENT NUMBERS IN THE
C                SUBREGION AREA

```

```

C          NWK-----TOTAL NUMBER OF ENTRIES IN STIFFNESS MATRIX  *
C          NEQ-----TOTAL NUMBER OF EQUATIONS                    *
C          MAXA(I)--ARRAY CONTAINING THE ADDRESSES OF THE         *
C                   DIAGONAL ENTRIES IN THE STIFFNESS MATRIX     *
C          R(I)-----LOAD VECTOR                                  *
C
C TAPES:    ISTIF----STIFFNESS MATRIX PRIOR TO TRIANGULARIZATION *
C          ISSS-----CONTRIBUTION FROM EACH ELEMENT DOF TO GLOBAL *
C                   STIFFNESS MATRIX                             *
C          ILOAD----CONTAINS LOAD VECTOR                          *
C          UNIT 29--OUTPUT TAPE WITH BOUNDARY STIFFNESS AND FORCE *
C                   DATA                                         *
C*****
C
C                   MODIFICATION HISTORY                          *
C
C   DATE      PROGRAMMER      MODIFICATION                    *
C
C
C
C*****
C          SUBROUTINE SETUP(ID,MAXA,S,DISP,LM,R,NOD,F,NODA,IELM)
C          IMPLICIT REAL*8(A-H,O-Z)
C          INTEGER OUTPUT, DEL
C          CHARACTER*15 FN
C          CHARACTER*1 Q
C          LOGICAL LLL
C
C          COMMON/SOL/NUMNP,NEQ,NUBC,NWK,NUMEST,MIDEST,MAXEST,MK
C          COMMON/TAPES/IELMNT,ILOAD,IIN,IOUT,MGEOM,MDISP,MSTR1,MSTR2,MSTR3,
* MSTR4,MOVIET,MENGY,JENGY,LENGY,KENGY,IENGY,INBC,ISTIF,ISSS
C          COMMON/EL/IND,NPAR(10),NUMEG,MTOT,NFIRST,NLAST,ITWO
C          COMMON/DEVI/IINPUT,OUTPUT
C
C          EQUIVALENCE (NPAR(2),NUME)
C          DIMENSION S(NWK),MAXA(NEQ),ID(3,NUMNP),NOD(NEQ),LM(8,NUME)
C          DIMENSION F(NEQ),R(NEQ),NPT(200),NODA(NEQ),NHOLD(200),DISP(NEQ)
C          DIMENSION IELM(NUME)
C
C THIS SECTION OF CODE ASKS THE USER FOR THE NAME OF THE FILE IN WHICH
C TO PUT THE BOUNDARY STIFFNESS AND FORCE DATA. IT THEN CHECKS TO
C SEE IF THIS FILE EXISTS. IF IT DOES, THE USER IS ASKED IF HE WANTS
C TO CREATE A NEW VERSION OR NOT. IF IT DOES NOT EXIST, THE FILE IS
C OPENED ON UNIT 29 FOR WRITE.
C
C          WRITE(OUTPUT,999) 538976285,538976283,538976268,738976280,
1538976282
5          WRITE(OUTPUT,1000)
          READ(IINPUT,1015)FN
          INQUIRE(FILE=FN, EXIST=LLL)

```

```

        IF (.NOT.LLL) GOTO 10
        WRITE(OUTPUT,1010)
        READ(IINPUT,1020) Q
        IF (Q.EQ.'N') GOTO 5
10      OPEN(UNIT=29,NAME=FN,TYPE='NEW')
C
C ALL WRITE STATEMENTS PRECEDED BY "C" WERE USED DURING DEBUGING AND
C ARE NOT ESSENTIAL TO THE PROGRAM OPERATION
C
C      WRITE(OUTPUT,5000)
C ISTIF IS THE TAPE WRITTEN DURING THE ANALYSIS PROCESS. IT CONTAINS
C THE LM ARRAY AND THE GLOBAL STIFFNESS MATRIX PRIOR TO UPPER
C TRIANGULARIZATION
C
C      REWIND (ISTIF)
C      *      READ(ISTIF)((LM(1,J),LM(2,J),LM(3,J),LM(4,J),LM(5,J)
C              ,LM(6,J),LM(7,J),LM(8,J)),J=1,NUME)
C
C      WRITE(OUTPUT,5500) ((LM(I,J),I=1,8),J=1,NUME)
C      WRITE(OUTPUT,5010)
C
C      READ(ISTIF) (S(I),I=1,NWK)
C
C      WRITE(OUTPUT,5100)
C
C THE USER IS QUERIED FOR THE NUMBER OF ELEMENTS IN THE SUBREGION AREA
C AND THEN INPUTS WHAT THOSE ELEMENTS ARE
C ONCE ALL THE ELEMENT NUMBERS ARE READ IN AND STORED IN IELM, THE
C STIFFNESSES DUE TO EACH OF THOSE ELEMENTS ARE SUBTRACTED FROM THE
C GLOBAL STIFFNESS TERMS IN THE S ARRAY
C
C      WRITE(OUTPUT,500)
C      READ(IINPUT,*)NOEL
C      DO 15 I=1,NOEL
C          WRITE(OUTPUT,510)
C          READ(IINPUT,*)IELM(I)
15     CONTINUE
C      REWIND (ISSS)
17     READ(ISSS,*,END=25)II,KK,STIF
C      DO 20 I=1,NOEL
C          IF (II.EQ.IELM(I)) S(KK)=S(KK)-STIF
20     CONTINUE
C      GOTO 17
25     DO 27 I=1,NOEL
C          DO 26 J=1,8
C              LM(J,IELM(I))=0
26     CONTINUE
27     CONTINUE
C
C THIS LOOP WILL GET THE EQUATION NUMBERS FOR THE NODES ON THE
C INTERFACE AND WILL SORT THEM AND STORE THEM IN NUMERICAL ORDER

```



C GETTING RID OF ZEROS.  
 C THE NHOLD ARRAY IS ONLY USED HERE TO HOLD VALUES WHILE THE SORTING  
 C IS BEING DONE

```

C
  WRITE(OUTPUT,520)
  READ(IINPUT,*)NNOD
  DO 40 I=1,NNOD
    WRITE(OUTPUT,530)
    READ(IINPUT,*)N
    NOD(2*I-1)=ID(1,N)
    NOD(2*I)=ID(2,N)
40  CONTINUE
    IJ=0
    DO 41 I=1,NNOD*2
      IF (NOD(I).EQ.0) GOTO 41
      IJ=IJ+1
      NHOLD(IJ)=NOD(I)
      NPT(IJ)=IJ
41  CONTINUE
C  WRITE(OUTPUT,5200) IJ
    DO 42 I=1,IJ
      NOD(I)=NHOLD(I)
      NHOLD(I)=0
42  CONTINUE
    DO 44 I=1,IJ-1
      I1=I
      LEAST=NOD(NPT(I))
      DO 43 J=I+1,IJ
        IF (NOD(NPT(J)).LT.LEAST)THEN
          I1=J
          LEAST=NOD(NPT(J))
        END IF
43  CONTINUE
      IF (I1.NE.I) THEN
        NTEMP=NPT(I)
        NPT(I)=NPT(I1)
        NPT(I1)=NTEMP
      END IF
44  CONTINUE
    DO 45 I=1,IJ
      NHOLD(I)=NOD(NPT(I))
45  CONTINUE
    DO 46 I=1,IJ
      NOD(I)=NHOLD(I)
      NHOLD(I)=0
      NPT(I)=0
46  CONTINUE
C  WRITE(OUTPUT,5200) (NOD(I),I=1,IJ)
C
C THIS GETS THE LOAD VECTOR OFF TAPE ILOAD
C

```

```

        REWIND(ILOAD)
        READ(ILOAD) R
C
C        WRITE(OUTPUT,5300)
C
C THIS SETS UP THE NODA ARRAY OF THE EQUATION NUMBERS ASSOCIATED WITH
C THE NODES IN REGION A. THESE EQUATION NUMBERS ARE NOT NECESSARILY
C IN NUMERICAL ORDER. IK WILL BE THE COUNTER FOR THE NUMBER OF
C EQUATIONS IN REGION A
C
        IK=0
C        WRITE(OUTPUT,5500) ((LM(I,J),I=1,8),J=1,NUME)
        DO 51 I=1,NUME
            DO 50 J=1,8
                IF (LM(J,I).EQ.0) GOTO 50
                DO 47 K=1,IJ
                    IF (LM(J,I).EQ.NOD(K)) GOTO 50
47                CONTINUE
C                WRITE(OUTPUT,5200) LM(J,I)
                IF (IK.LT.1) GOTO 49
                DO 48 K=1,IK
                    IF (LM(J,I).EQ.NODA(K)) GOTO 50
48                CONTINUE
49                IK=IK+1
                NODA(IK)=LM(J,I)
C                WRITE(OUTPUT,5600)IK
C                WRITE(OUTPUT,5700)NODA(IK)
50                CONTINUE
51                CONTINUE
C                WRITE(OUTPUT,5200) IK
C
C THE ARRAY NPT WILL BE USED IN THE SORTING ROUTINE TO ARRANGE
C THE NODA ARRAY IN ASCENDING NUMERICAL ORDER
C
        DO 60 I=1,IK
            NPT(I)=I
60        CONTINUE
C THESE LOOPS WILL SORT THE NODA ARRAY AND PUT THE EQUATION
C NUMBERS IN NUMERICAL ORDER.
C
        DO 80 I=1,IK-1
            I1=I
            LEAST=NODA(NPT(I))
            DO 70 J=I+1,IK
                IF (NODA(NPT(J)).LT.LEAST)THEN
                    I1=J
                    LEAST=NODA(NPT(J))
            END IF
70        CONTINUE
            IF (I1.NE.I) THEN
                NTEMP=NPT(I)

```

```

        NPT(I)=NPT(I1)
        NPT(I1)=NTEMP
    END IF
80    CONTINUE
    DO 85 I=1,IK
        NHOLD(I)=NODA(NPT(I))
85    CONTINUE
    DO 90 I=1,IK
        NODA(I)=NHOLD(I)
90    CONTINUE
C    WRITE(OUTPUT,5200) (NODA(I),I=1,IK)
C
C SUBROUTINE EXTRACT CALCULATES THE BOUNDARY FORCES AND EXTRACTS
C THE KAB STIFFNESS TERMS FROM THE REDUCED STIFFNESS MATRIX S
C
    CALL EXTRACT(S,MAXA,NODA,R,NOD,DISP,F,IK,IJ)
C
500    FORMAT(1X,'HOW MANY ELEMENTS LIE IN THE SUBREGION AREA
* ? ',,$)
510    FORMAT(1X,'ENTER THE ELEMENT NUMBERS WHICH LIE IN THE SUB
* REGION AREA ',,$)
520    FORMAT(1X,'HOW MANY NODES WILL LIE ON THE SUBREGION BOUNDARY
* ',,$)
530    FORMAT(1X,'ENTER THE NODE NUMBERS ON THE SUBREGION BOUNDARY
* ',,$)
1000   FORMAT(1X,'ENTER THE FILE SPEC FOR THE STIFFNESS AND FORCE
* DATA OUTPUT ',,$)
1010   FORMAT(1X,'THE FILE SPEC YOU SPECIFIED ALREADY EXISTS. DO
* YOU WANT TO CREATE A NEW VERSION (Y or N)? ',,$)
1015   FORMAT(A15)
1020   FORMAT(A1)
5000   FORMAT(1X,'IN SETUP')
5010   FORMAT(1X,'LM VALUES READ IN')
5100   FORMAT(1X,'STIFFNESS VALUES READ IN')
5200   FORMAT(I7)
5300   FORMAT(1X,'FORCE VALUES READ IN')
5500   FORMAT(8I7)
5600   FORMAT(1X,'IK EQUALS',I7)
5700   FORMAT(1X,'NODA(IK) EQUALS', I7)

RETURN
END

```

```

C*****
C
C          SUBROUTINE EXTRACT
C
C PROGRAMMER: C. JARA-ALMONTE
C DATE:       JULY 1984
C LOCATION:   MECHANICAL ENGINEERING DEPARTMENT
C             V.P.I. AND STATE UNIVERSITY
C             BLACKSBURG, VIRGINIA 24060
C*****
C
C SUBROUTINE PURPOSE:
C   THIS SUBROUTINE TAKES THE REDUCED STIFFNESS MATRIX FROM
C   SETUP, THE LOAD VECTOR, AND THE DISPLACEMENT VECTOR AND
C   FINDS THE BOUNDARY FORCES. IT ALSO EXTRACTS THE KAB TERMS
C   FROM THE REDUCED STIFFNESS MATRIX
C*****
C
C SUBROUTINE CALLED BY:  SETUP
C
C
C
C SUBROUTINE CALLS:
C
C
C*****
C
C SPECIAL NOTES:
C
C VARIABLES:   S(I)-----REDUCED STIFFNESS MATRIX FROM SETUP
C              NOD(I)---EQUATION NUMBERS FOR INTERFACE NODES
C              NODA(I)--EQUATION NUMBERS FOR NODES OUTSIDE OF
C                      SUBREGION
C              DISP(I)--DISPLACEMENTS FOR EACH DOF FROM FINITE
C                      ELEMENT SOLUTION
C              R(I)-----LOAD VECTOR
C              F(I)-----CALCULATED BOUNDARY FORCES
C              TERM-----VALUE EXTRACTED FROM STIFFNESS MATRIX
C*****
C
C          MODIFICATION HISTORY
C
C DATE      PROGRAMMER      MODIFICATION
C
C
C
C
C

```

```

C*****
C      SUBROUTINE EXTRACT(S,MAXA,NODA,R,NOD,DISP,F,IK,IJ)
C
C      IMPLICIT REAL*8 (A-H,O-Z)
C      REAL*8 NEWT
C      INTEGER DEL,OUTPUT
C
C      COMMON/SOL/NUMNP,NEQ,NUBC,NWK,NUMEST,MIDEST,MAXEST,MK
C      COMMON/TAPES/IELMNT,ILOAD,IIN,IOUT,MGEOM,MDISP,MSTR1,MSTR2,MSTR3
C      * ,MSTR4,MOVIET,MENGY,JENGY,LENGY,KENGY,IENGY,INBC,ISTIF,ISSS
C      COMMON/DEVI/IINPUT,OUTPUT
C      COMMON/EL/IND,NPAR(10),NUMEG,MTOT,NFIRST,NLAST,ITWO
C
C      DIMENSION S(NWK),MAXA(NEQ),NODA(NEQ),DISP(NEQ)
C      DIMENSION F(NEQ),R(NEQ),NOD(NEQ)
C
C      THIS LOOP CALCULATES THE BOUNDARY FORCES BY FINDING THE PRODUCT OF
C      Kab-a AND Da AND SUBTRACTING IT FROM THE LOAD VECTOR R
C
C      DO 500 I=1,IJ
C          NEWT=0.DO
C          DO 250 N=1,IK
C              II=NOD(I)
C              NN=NODA(N)
C              IF (NN.GE.II) GOTO 225
C              II=NN
C              NN=NOD(I)
C          225          DEL=NN-II
C              KK=DEL+MAXA(NN)
C              TERM=S(KK)
C              IF (KK.GE.MAXA(NN+1))TERM=0.DO
C              NEWT=NEWT+TERM*DISP(NODA(N))
C          250          CONTINUE
C              F(NOD(I))=R(NOD(I))-NEWT
C          500          CONTINUE
C
C      THIS LOOP LOCATES THE Kab TERMS IN THE REDUCED STIFFNESS MATRIX
C
C      DO 2000 I=1,IJ
C          DO 1500 J=I,IJ
C              II=NOD(I)
C              JJ=NOD(J)
C              DEL=JJ-II
C              KK=MAXA(JJ)+DEL
C              TERM=S(KK)
C              IF (KK.GE.MAXA(JJ+1))TERM=0.DO
C
C      THE EXTRACTED STIFFNESS TERMS ARE WRITTEN OUT TO UNIT 29 WHICH THE
C      USER GAVE A FILE NAME TO IN SUBROUTINE SETUP
C
C          IF (TERM.NE.0.DO) WRITE(29,6000) II,JJ,TERM

```

```
1500          CONTINUE
2000          CONTINUE
C
C THIS WRITES THE BOUNDARY FORCES TO THE UNIT 29 TAPE
C
      WRITE(29,5000) (NOD(I),F(NOD(I)),I=1,IJ)
C
5000  FORMAT(1X,'FORCE(',I5,') =',F20.10)
6000  FORMAT(1X,'STIFF(',I5,',',I5,')=',F20.10)
      RETURN
      END
```

```

C*****
C
C          SUBROUTINE IMPLEMENT
C
C PROGRAMMER: C. JARA-ALMONTE
C DATE:      July 1984
C LOCATION:  MECHANICAL ENGINEERING DEPARTMENT
C            V.P.I. AND STATE UNIVERSITY
C            BLACKSBURG, VIRGINIA 24060
C
C*****
C
C SUBROUTINE PURPOSE:
C THIS SUBROUTINE TAKES THE BOUNDARY STIFFNESSES FROM THE USER
C SPECIFIED FILE AND INSERTS THEM IN THE PROPER POSITION IN THE
C GLOBAL STIFFNESS MATRIX.
C
C*****
C
C
C
C*****
C
C SUBROUTINE CALLED BY:  ISOPARAMETERIC
C
C
C
C SUBROUTINE CALLS:
C
C
C*****
C
C SPECIAL NOTES: ONLY CALLED IF USER ANSWERS Y(es) WHEN ASKED IN
C                ISOPARAMETERIC IF THE ANALYSIS IS A SUBREGION
C                ANALYSIS
C
C
C VARIABLES:  A(I)-----THE GLOBAL STIFFNESS MATRIX
C             MAXA(I)--ARRAY CONTAINING THE ADDRESSES OF THE
C                   DIAGONAL ENTRIES IN THE STIFFNESS MATRIX
C             I-----ROW ADDRESS OF BOUNDARY STIFFNESS TERM
C             J-----COLUMN ADDRESS OF BOUNDARY STIFFNESS TERM
C             S-----BOUNDARY STIFFNESS TERM
C             DEL-----DIFFERENCE BETWEEN COLUMN AND ROW NUMBER
C             KK-----ADDRESS IN A MATRIX FOR STIFFNESS TERM
C
C TAPES:      UNIT 29--INPUT TAPE WITH BOUNDARY STIFFNESS DATA
C
C*****
C
C          MODIFICATION HISTORY
C

```

```

C
C DATE PROGRAMMER MODIFICATION
C
C
C
C
C *****
C
C SUBROUTINE IMPLEMENT(MAXA,A)
C
C IMPLICIT REAL*8 (A-H,O-Z)
C INTEGER OUTPUT, DEL
C CHARACTER*15 FN
C CHARACTER*1 Q
C LOGICAL LLL
C
C COMMON/TAPES/IELMNT,ILOAD,IIN,IOUT,MGEOM,MSTR1,MSTR2,MSTR3,
* MSTR4,MOVIET,MENGY,JENGY,KENGY,IENGY,INBC,ISTIF,ISSS
C COMMON/DEVI/IINPUT,OUTPUT
C COMMON/SOL/NUMNP,NEQ,NUBC,NWK,NUMEST,MIDEST,MAXEST,MK
C
C DIMENSION A(NWK),MAXA(NEQ)
C
C THESE STATEMENTS ASK THE USER FOR THE NAME OF THE FILE CONTAINING THE *
C BOUNDARY STIFFNESS DATA. THE PROGRAM THEN CHECKS TO MAKE SURE THE *
C FILE EXISTS. IF IT DOES, IT IS OPENED ON UNIT 29 FOR READING *
C
C 1 WRITE(OUTPUT,1000)
C READ(IINPUT,1010)FN
C INQUIRE(FILE=FN,EXIST=LLL,NUMBER=N)
C IF (LLL) GOTO 5
C WRITE(OUTPUT,1020)
C READ(IINPUT,1030)Q
C IF (Q.EQ.'Y') GOTO 1
C STOP
C
C 5 IF (N.EQ.29) CLOSE(UNIT=29)
C OPEN(UNIT=29,NAME=FN,TYPE='OLD')
C
C THIS READS THE ADDRESS (ROW AND COLUMN) AND THE STIFFNESS VALUE FROM
C THE FILE ASSIGNED TO UNIT 29
C
C 10 READ(29,*,END=30) I,J,S
C
C THE NEXT FEW STATEMENTS LOCATE THE POSITION IN THE A ARRAY FOR THIS
C STIFFNESS TERM USING THE ROW AND COLUMN DESIGNATIONS AND THE MAXA
C ARRAY TO FIND THE POSITION
C
C II=I
C JJ=J
C IF (I.LE.J) GOTO 15

```



```
      JJ=I
      II=J
15     DEL=JJ-II
      KK=MAXA(JJ)+DEL
      A(KK)=A(KK)+S
      GOTO 10
30     CONTINUE
C
1000   FORMAT(/,17H ENTER FILE NAME ,/,14H WITH BOUNDARY ,/,
      *15H STIFFNESS DATA,/,/2H ¶,$)
1010   FORMAT(A80)
1020   FORMAT(15H THIS FILE DOES ,/,15H NOT EXIST. DO ,/,/
      *16H YOU WISH TO TRY ,/,14H AGAIN? (Y/N)¶,$)
1030   FORMAT(A1)
      RETURN
      END
```

APPENDIX B

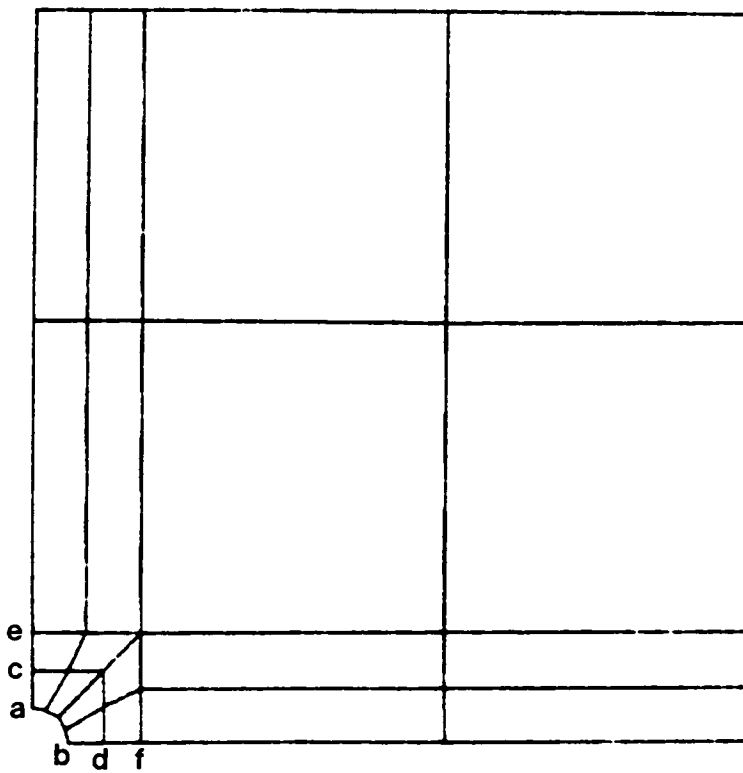


Figure B1. Whole Structure Model A0

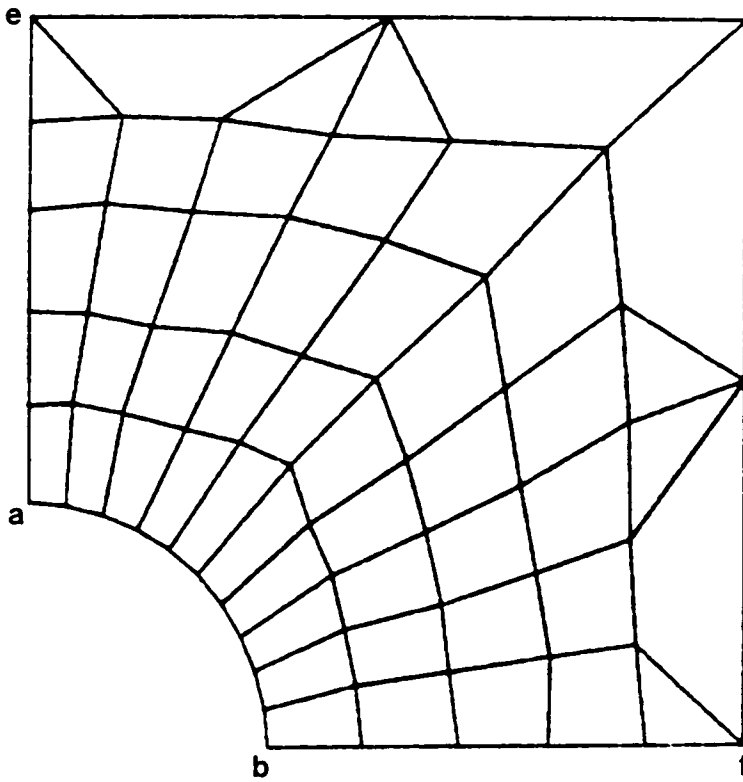


Figure B2. Subregion Model A1

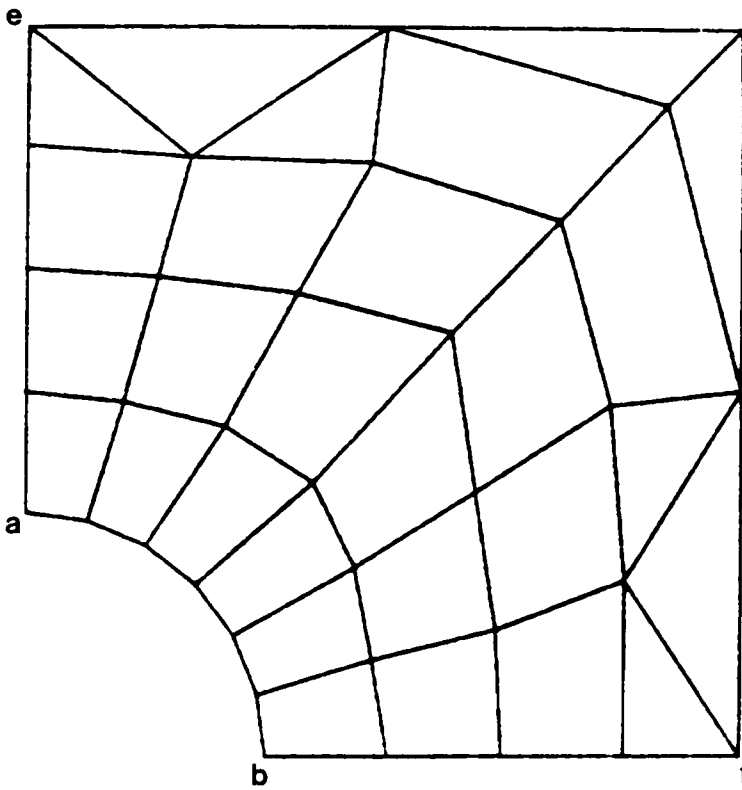


Figure B3. Subregion Model A2

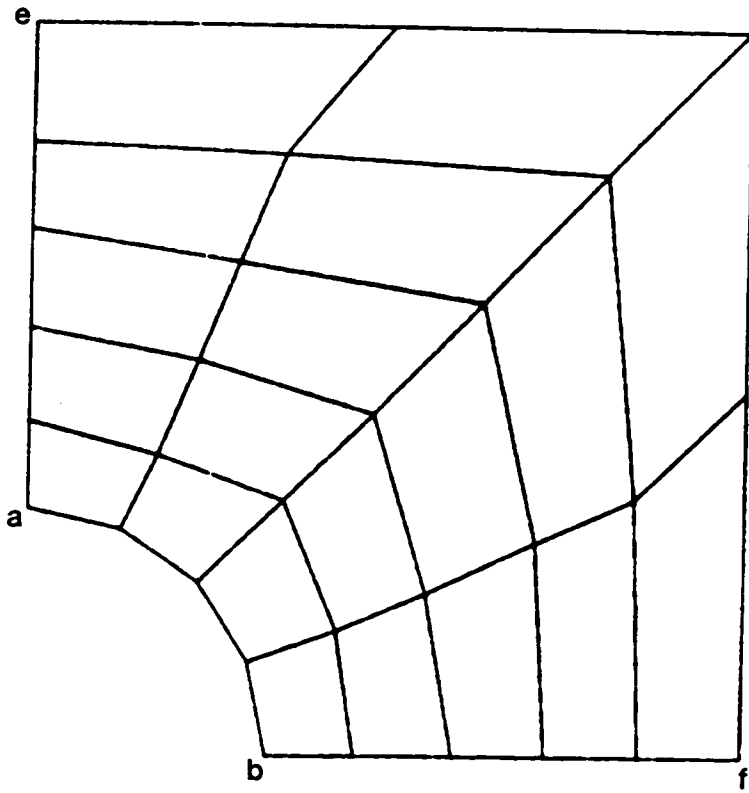


Figure B4. Subregion Model A3

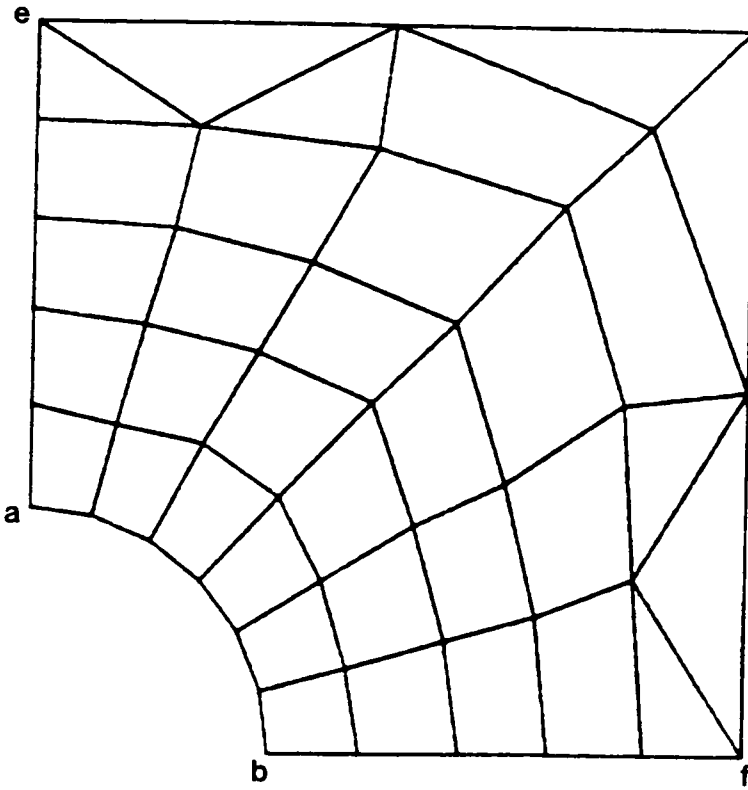


Figure B5. Subregion Model A4

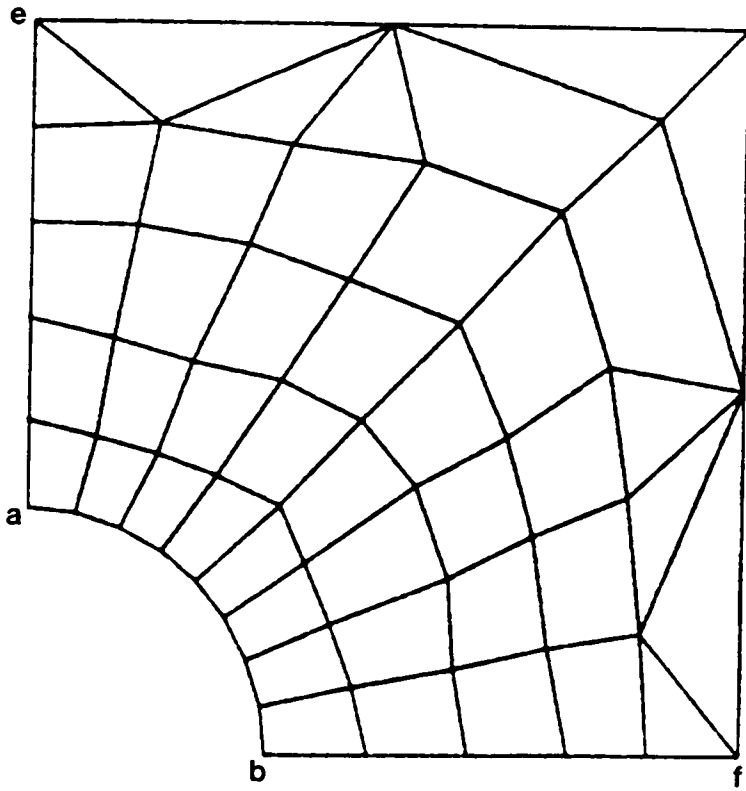


Figure B6. Subregion Model A5



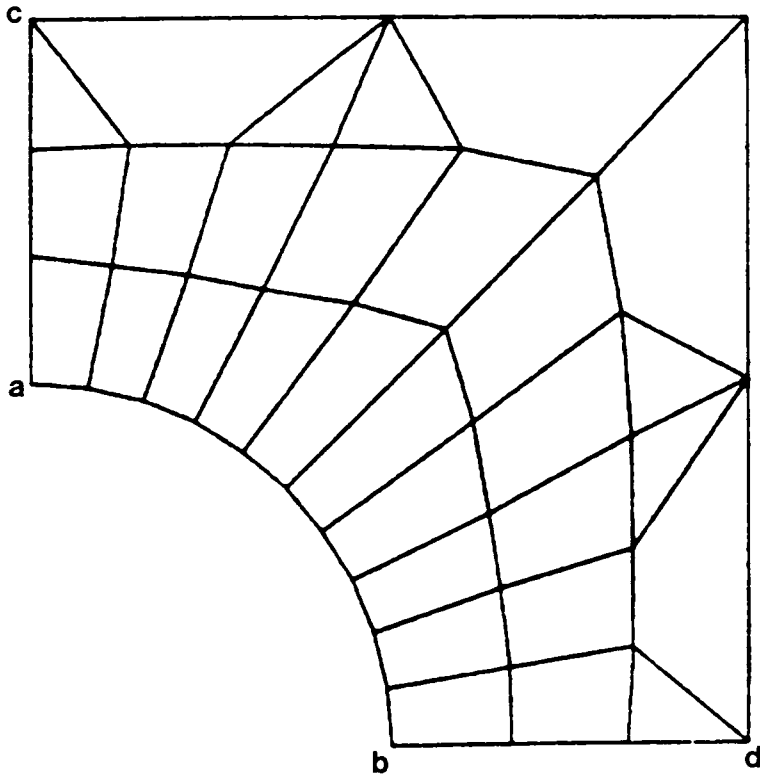


Figure B7. Subregion Model A6

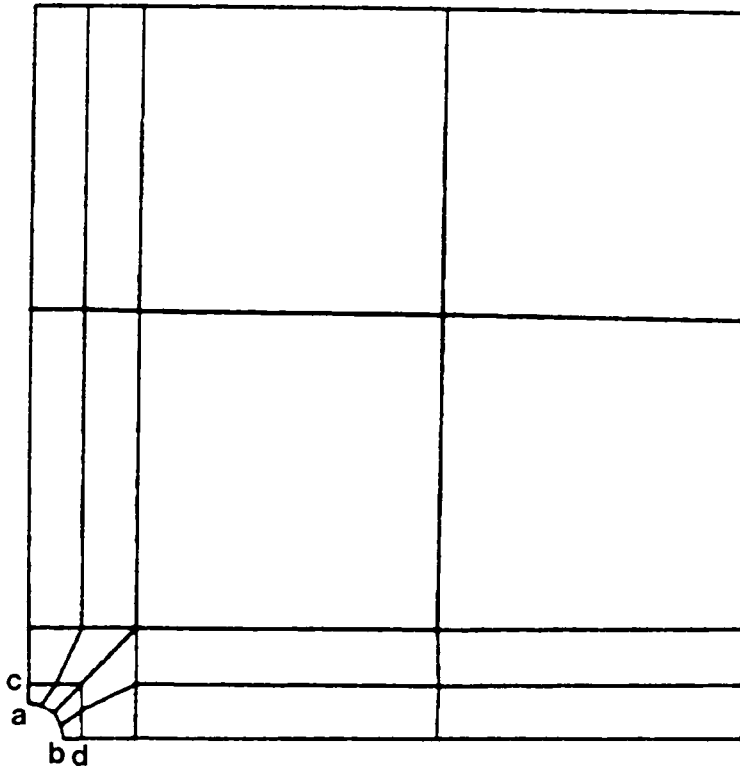


Figure B8. Whole Structure Model BØ

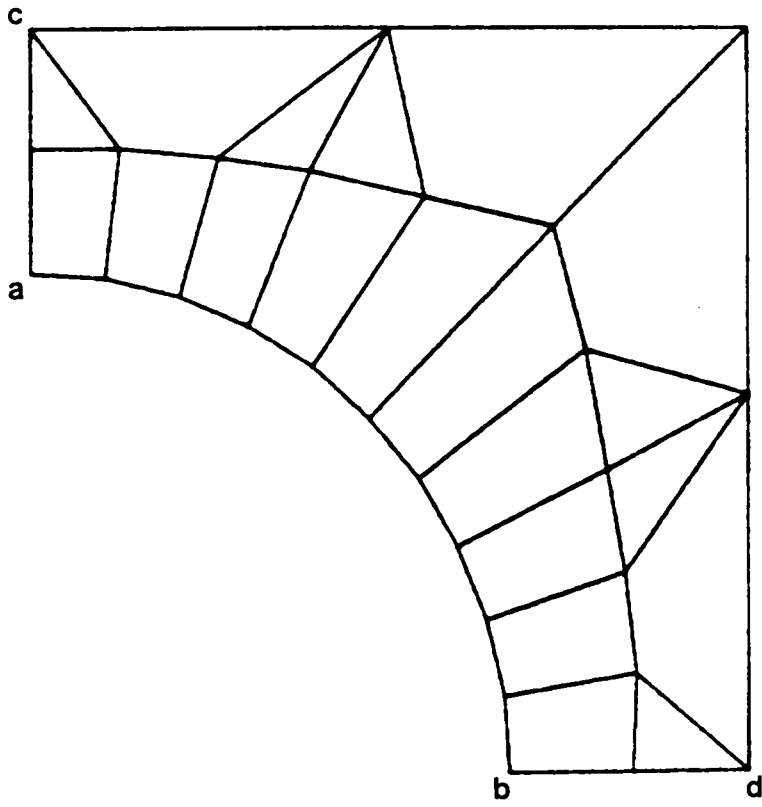


Figure B9. Subregion Model B1

APPENDIX C

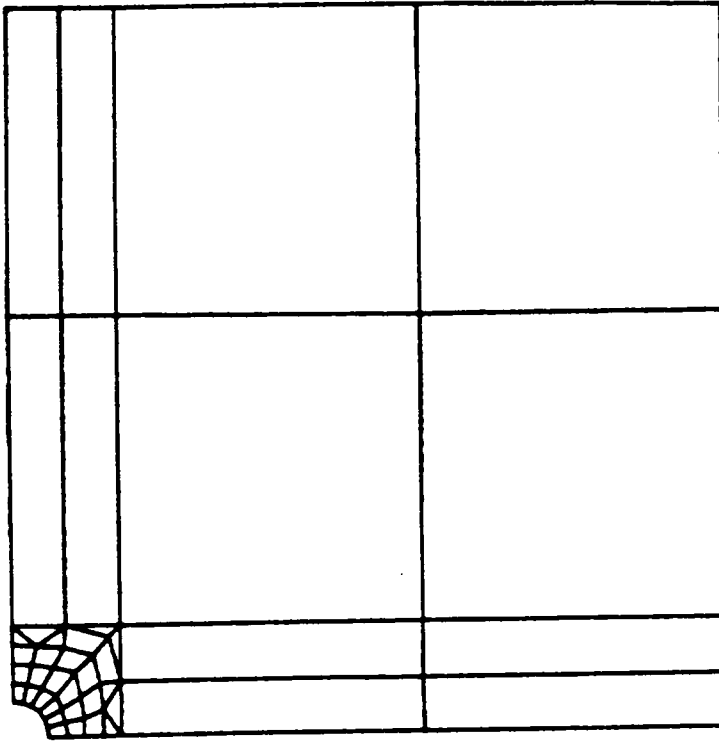


Figure C1. Mesh C2 for Direct Analysis of Subregion A2

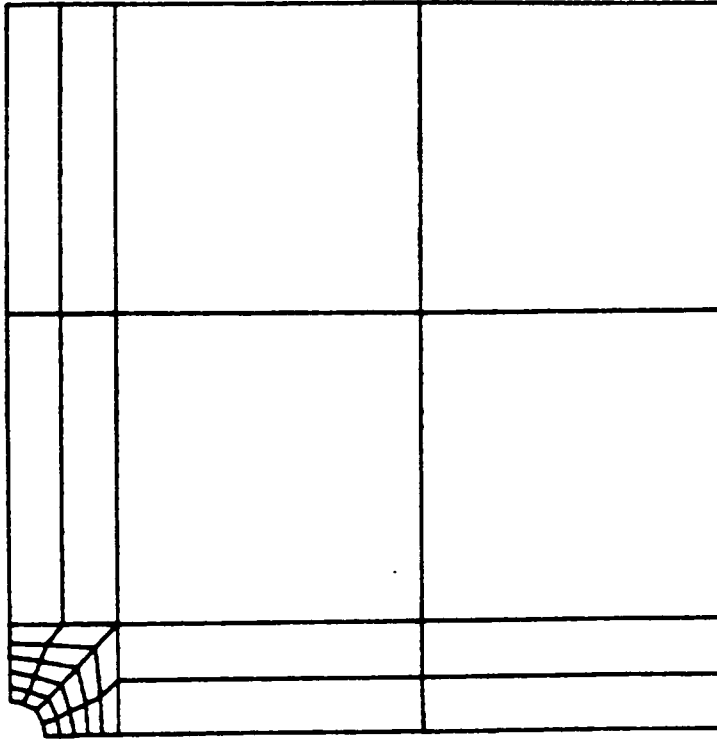


Figure C2. Mesh C3 for Direct Analysis of Subregion A3

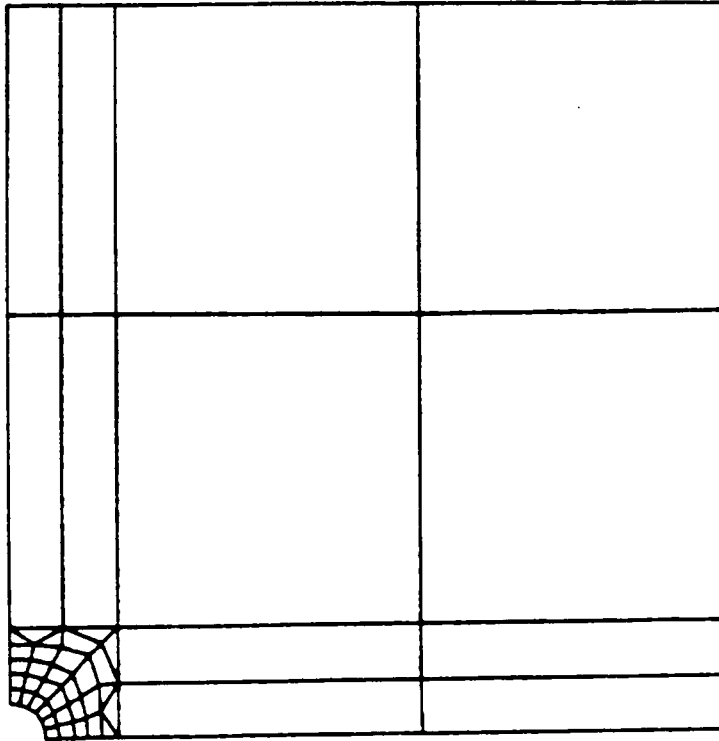


Figure C3. Mesh C4 for Direct Analysis of Subregion A4

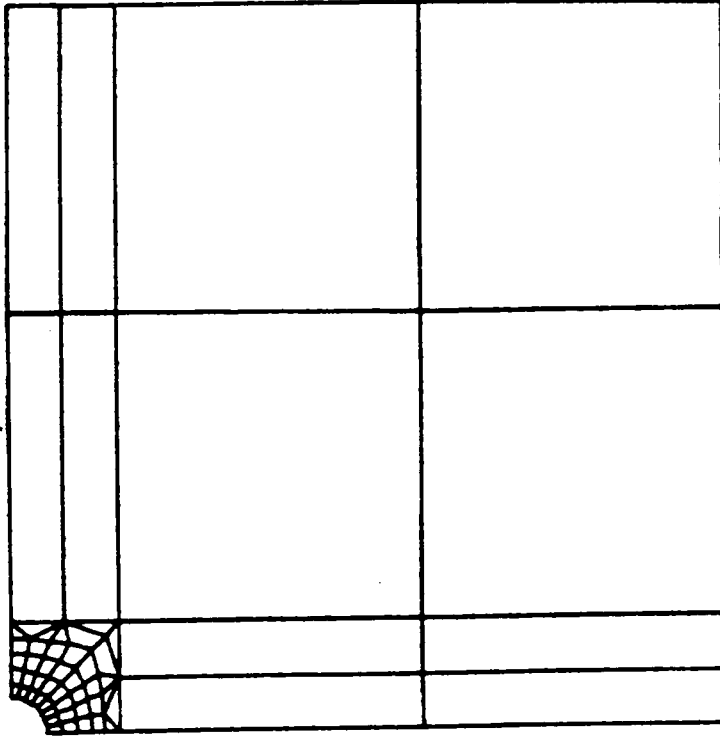


Figure C-1. Mesh C5 for Direct Analysis of Subregion A5



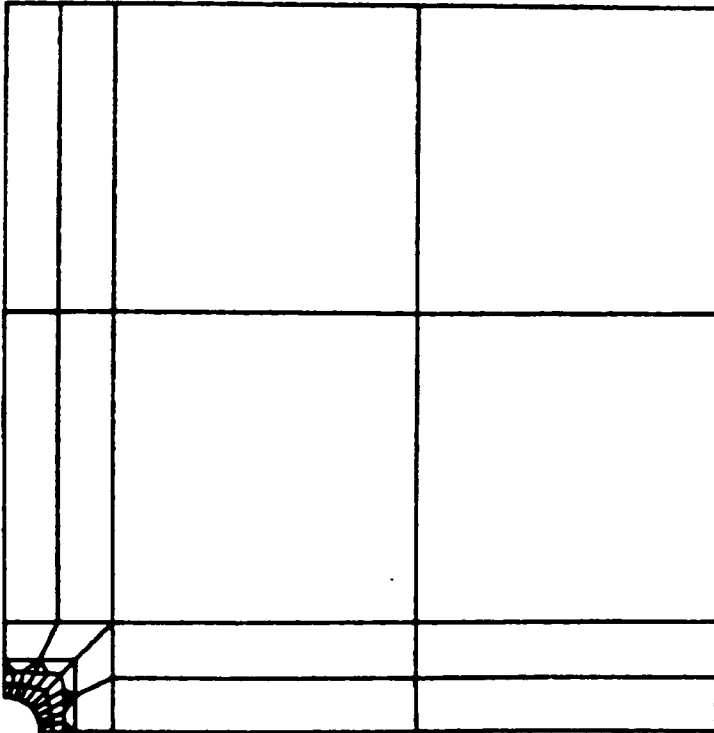


Figure C5. Mesh C6 for Direct Analysis of Subregion A6

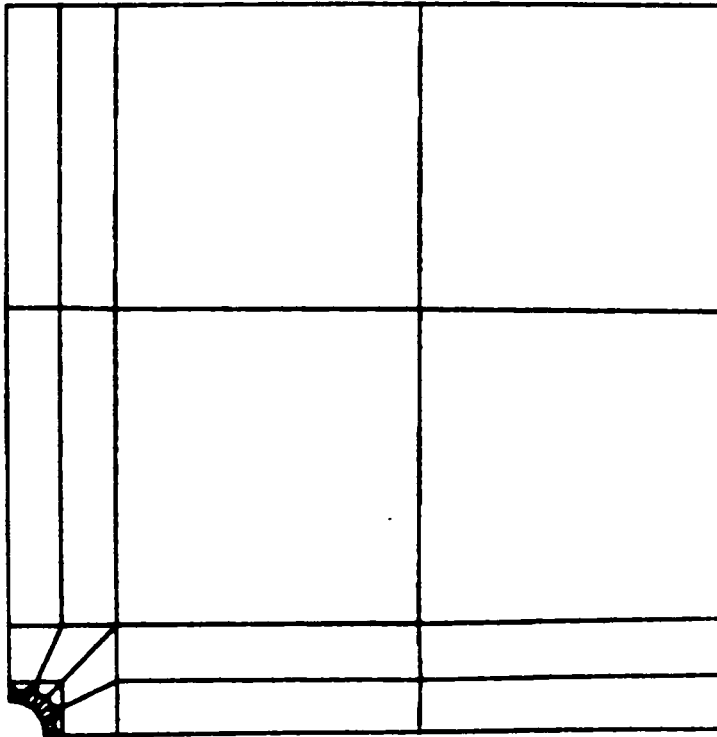


Figure C6. Mesh D1 for Direct Analysis of Subregion B1

## APPENDIX D

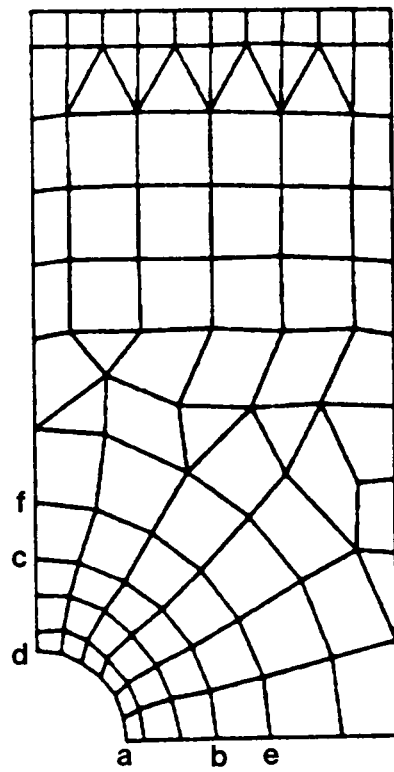


Figure D1. Parent Model AØ

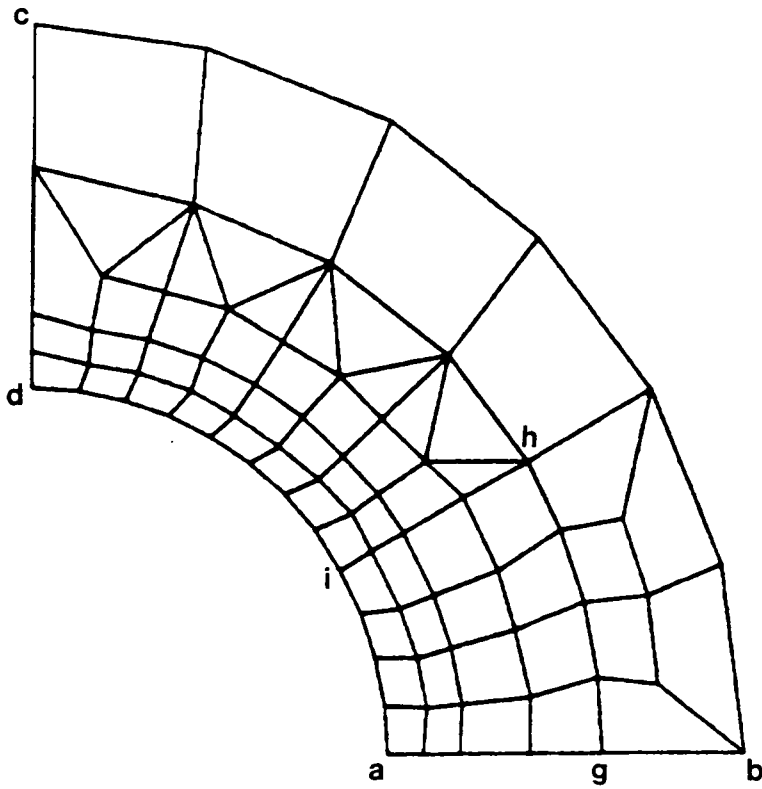


Figure D2. Subregion Model A1

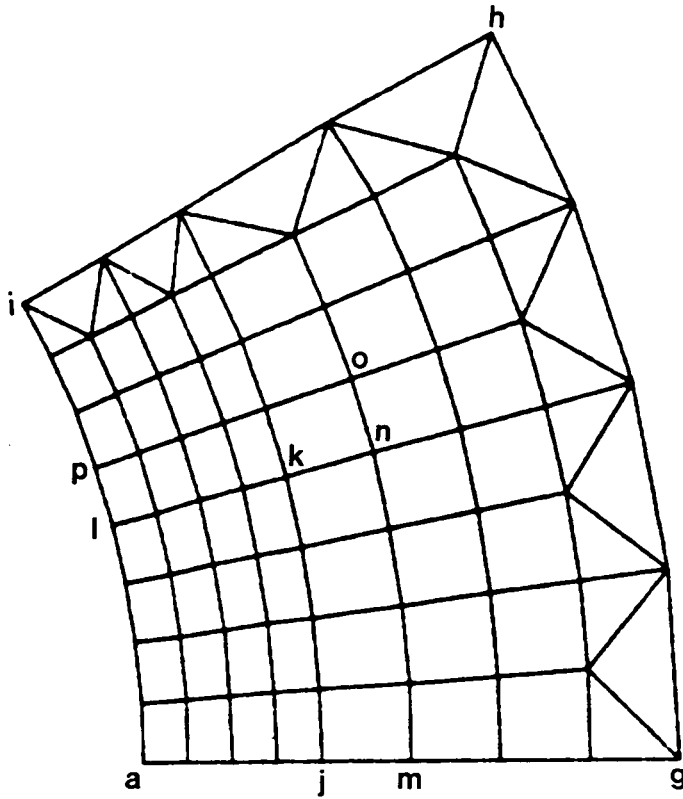


Figure D3. Subregion Model A2

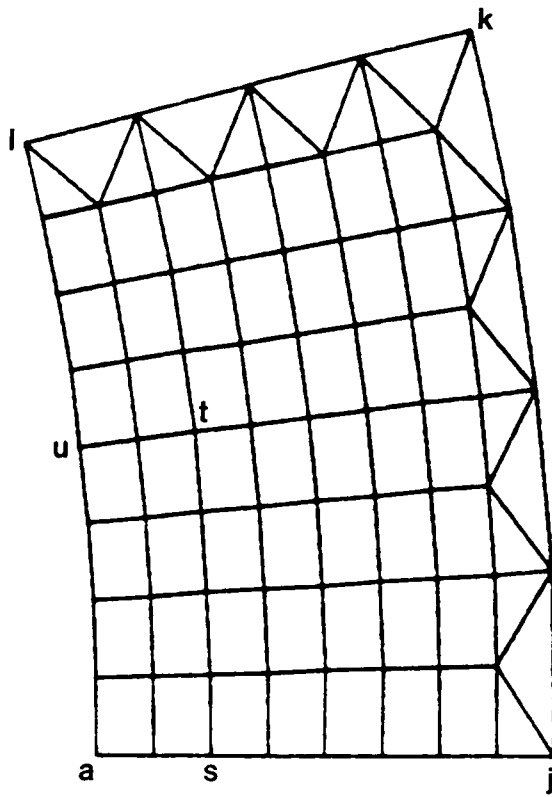


Figure D4. Subregion Model A3

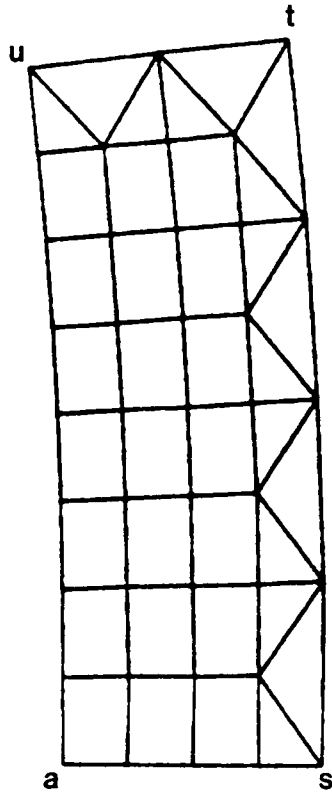


Figure D5. Subregion Model A4



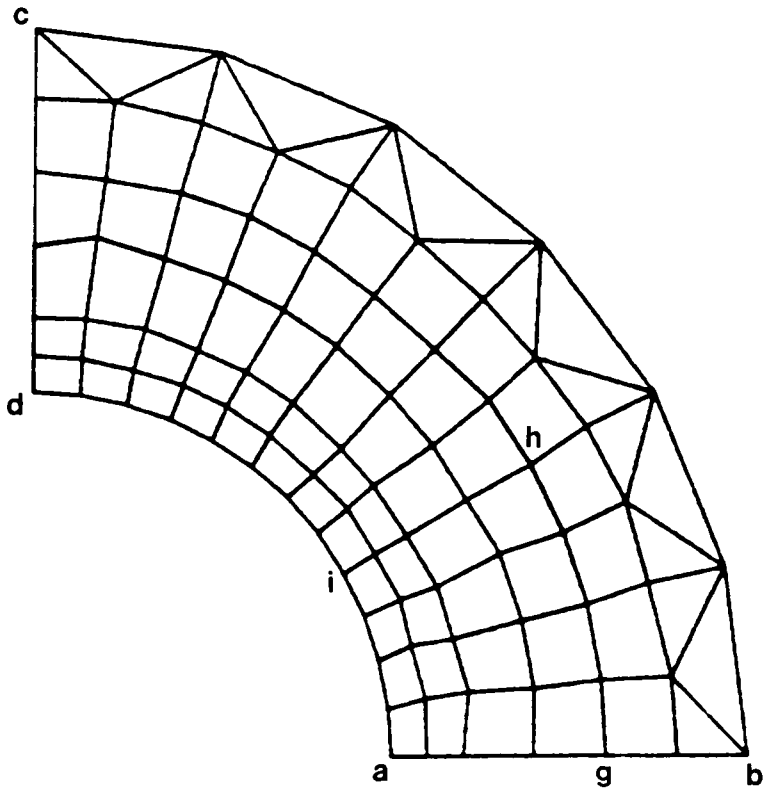


Figure D6. Subregion Model C1

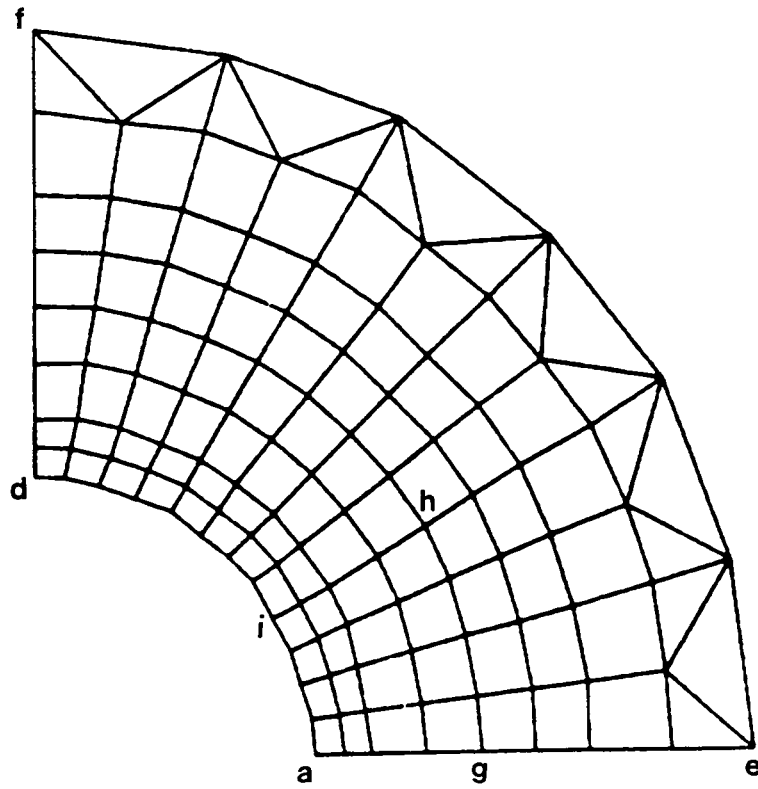


Figure D7. Subregion Model D1

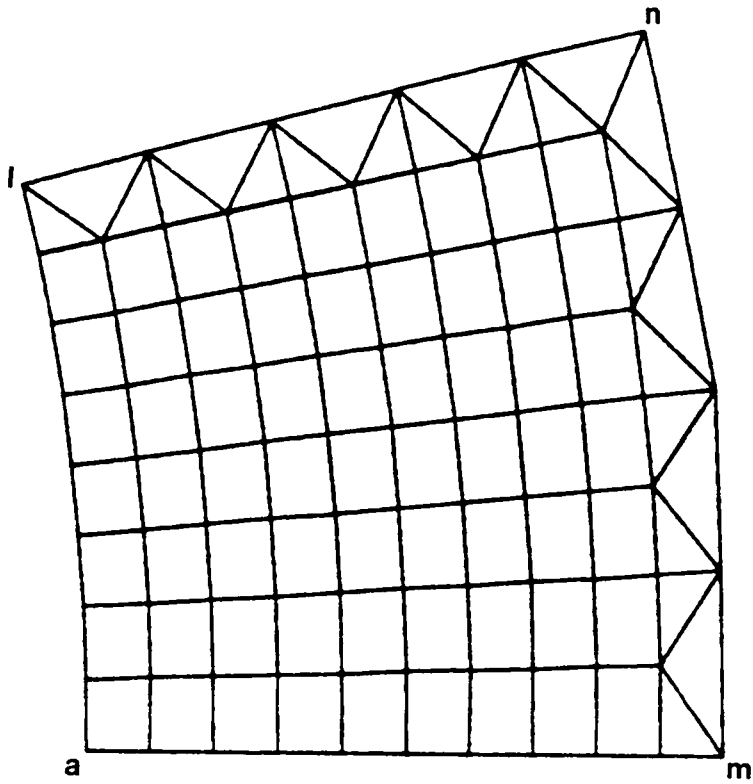


Figure D8. Subregion Model H3

**The vita has been removed from  
the scanned document**